Momentum Measurement in Magnetic Field

Momentum is determined by measurement of track curvature $\kappa = 1/\rho$ in B field:

Measure sagitta s of the track. For the momentum component transverse to B field:

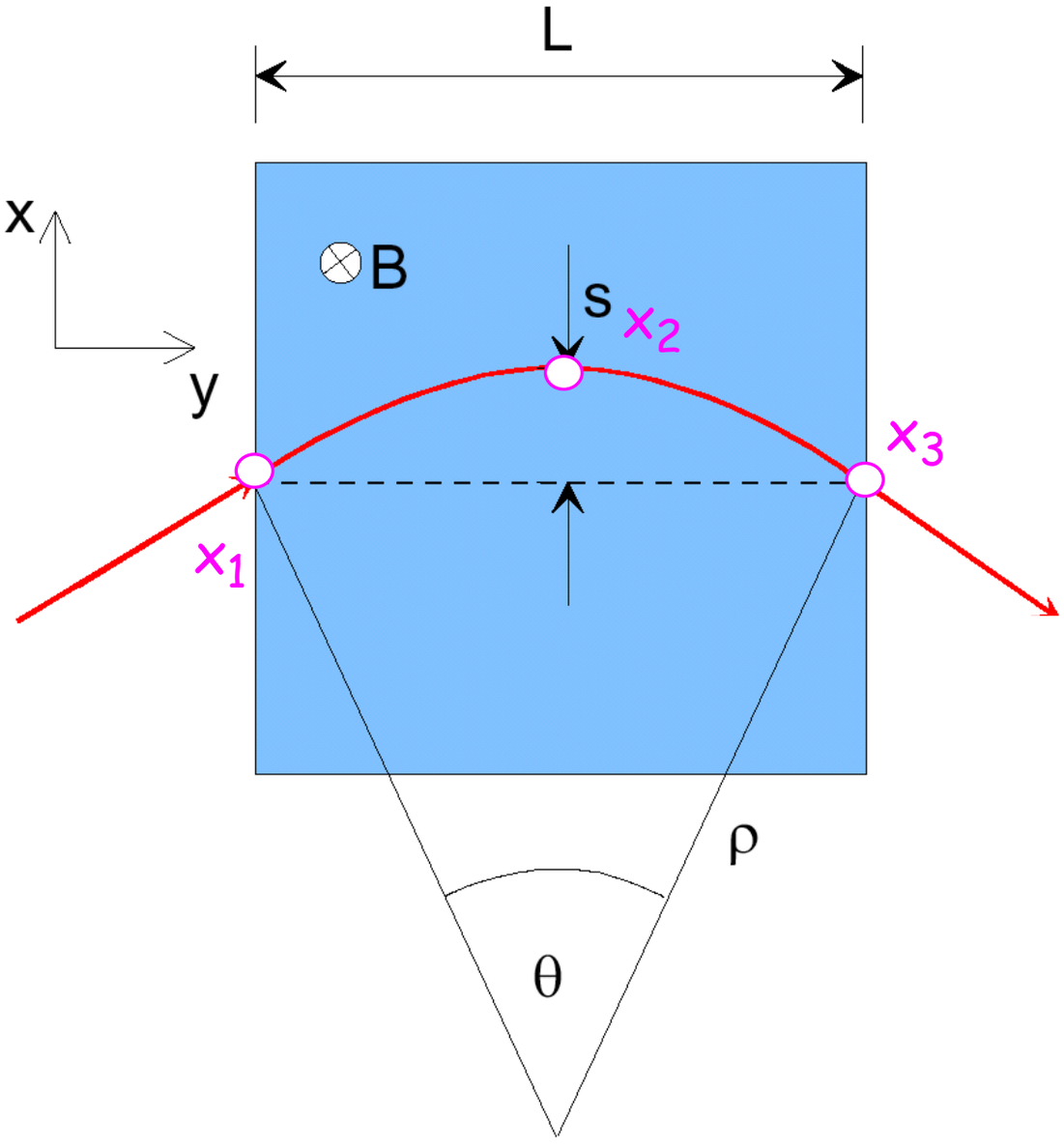

$$p_T = qB\rho$$

Units: $p_T[\mathrm{GeV}] = 0.3B[\mathrm{T}]\rho[\mathrm{m}]$

$$\frac{L/2}{\rho} = \sin\frac{\theta}{2} \approx \frac{\theta}{2} \text{ (for small } \theta) \Rightarrow \theta \approx \frac{L}{\rho} = \frac{0.3B \cdot L}{p_T}$$

$$s = \rho\left(1 - \cos\frac{\theta}{2}\right) \approx \rho\left(1 - \left(1 - \frac{1}{2}\frac{\theta^2}{4}\right)\right) = \rho\frac{\theta^2}{8} \approx \frac{0.3}{8}\frac{L^2 B}{p_T}$$

For the simple case of three measurements:

$$s = x_2 - (x_1 + x_3)/2 \Rightarrow ds = dx_2 - dx_1/2 - dx_3/2$$

with $\sigma_x \approx dx_i$ uncorrelated error of single measurement:

$$\sigma_s^2 = \sigma_x^2 + \frac{\sigma_x^2}{4} \cdot 2 = \frac{3}{2}\sigma_x^2$$

carsten.niebuhr@desy.de

Relative Momentum Error

For 3 points the relative momentum resolution is given by: $\frac{\sigma(p_T)}{p_T} = \frac{\sigma_s}{s} = \sqrt{\frac{3}{2}}\sigma_x \cdot \frac{8 p_T}{0.3 B L^2}$

- degrades linearly with transverse momentum
- improves linearly with increasing B field
- improves quadratically with radial extension of detector

In the case of N equidistant measurements according to Gluckstern [NIM 24 (1963) 381]:

$$\frac{\sigma(p_T)}{p_T} = \frac{\sigma(\kappa)}{\kappa} = \frac{\sigma_x \cdot p_T}{0.3 B L^2}\sqrt{\frac{720}{(N+4)}}$$

(for $N \geq 10$, curvature $\kappa = 1/\rho$)

Example: For $p_T = 1\text{GeV}$, $L = 1\text{m}$, $B = 1\text{T}$, $\sigma_x = 200\,\mu\text{m}$ and $N = 10$ one obtains:

$$\frac{\sigma(p_T)}{p_T} \approx 0.5\% \quad \text{for a sagitta} \quad s \approx 3.8\text{cm}$$

Important track detector parameter: $\frac{\sigma(p_T)}{p_T^2}$ (%/GeV)

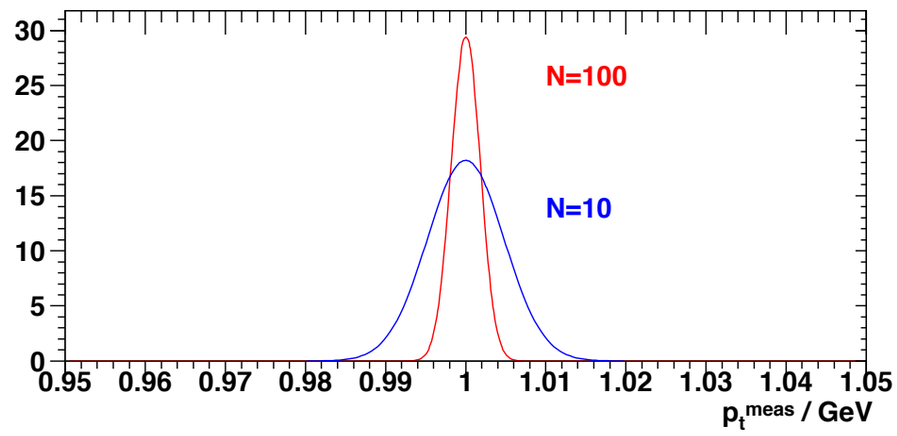

Measurement of Total Momentuum

In general one is interested in measuring the total momentum. The longitudinal component is derived from the measured polar angle θ with respect to the B-field axis. In the projection plane arc-length s versus z the trajectory is a straight line.

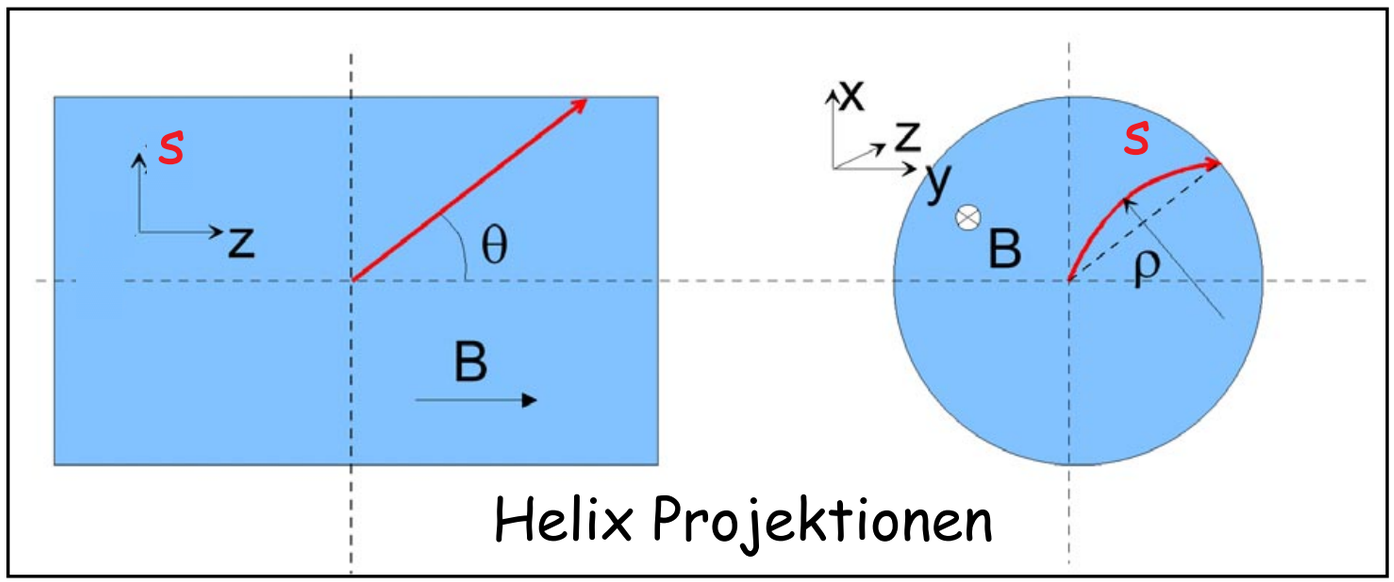

- in the case of N equidistant measurements with error :

$$\sigma_\theta^{Det} = \frac{\sigma(z)}{L}\sqrt{12\frac{N-1}{N(N+1)}}$$

- in most cases the contribution from the transverse component dominates

$$\left(\frac{\sigma(p)}{p}\right)^2 = \left(\frac{\sigma(p_T)}{p_T}\right)^2 + \cot^2(\theta\sigma_\theta) \simeq \left(\frac{\sigma(p_T)}{p_T}\right)^2$$

- all contributions discussed so-far result from the intrinsic detector resolution. In addition one has to consider the effect of multiple scattering.

Contributions from Multiple Scattering

The contribution to the momentum error from MS is given by:

$$\left.\frac{\sigma(p_T)}{p_T}\right|_{MS} = \frac{\sigma^{MS}(s)}{s} = \frac{\frac{L'}{\sqrt{3}}\frac{13.6\times10^{-3}}{p\beta}z\sqrt{\frac{L'}{X_0}}}{0.3BL^2z/(8p_T)} = \frac{0.2}{\beta B\sqrt{LX_0\sin\theta}}$$

with $L' = L/\sin\theta$ total path

$p_T = p\sin\theta$

for $\beta \to 1$ this part is momentum independent !

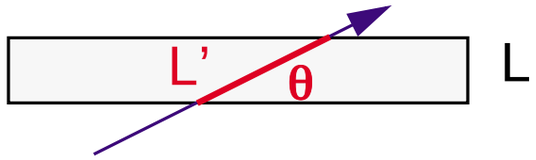

The combined total momentum error is:

$$\left(\frac{\sigma_p}{p}\right)^2 = \left(\sqrt{\frac{720}{N+4}}\frac{\sigma_x p\sin\theta}{0.3BL^2}\right)^2 + \left(\frac{0.2}{\beta B\sqrt{LX_0\sin\theta}}\right)^2 + (\cot\theta\sigma_\theta)^2$$

Example for momentum dependence of individual contributions

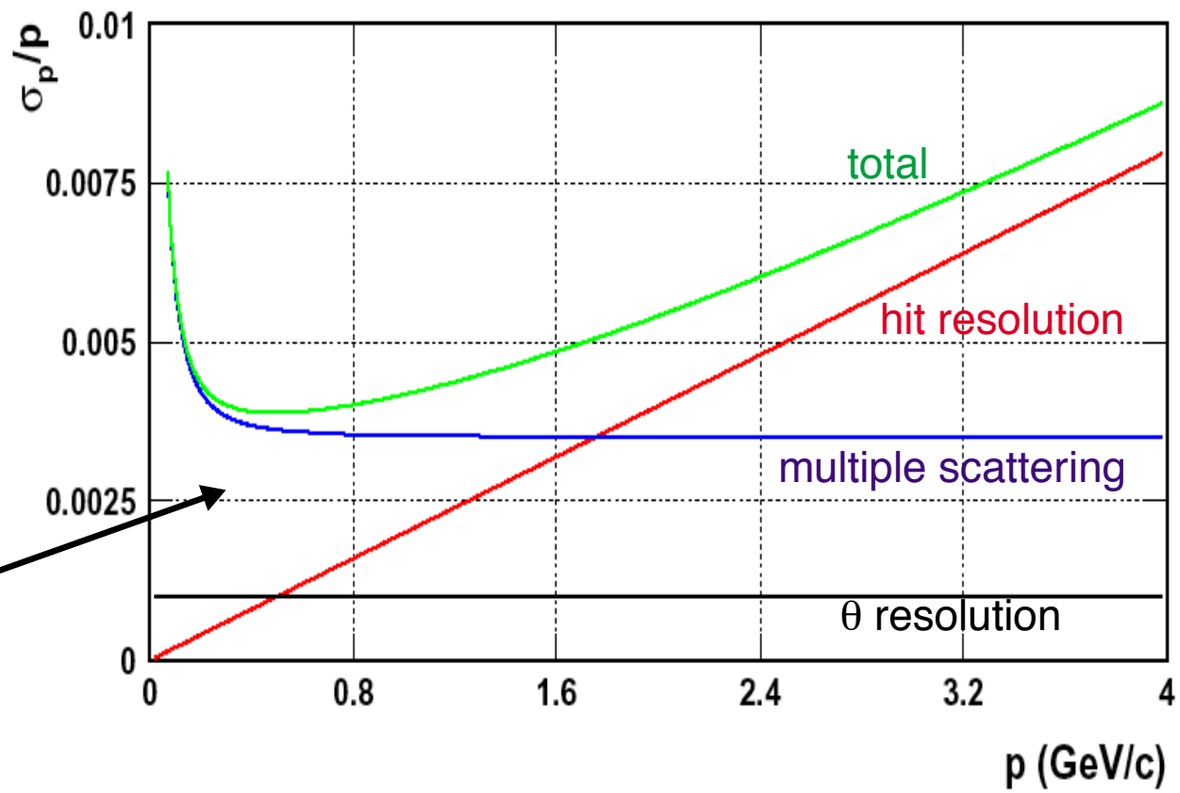

First Track Detectors

Until ≈ 1970:

- optical measurements using
  - bubble chambers
  - emulsions
  - spark chambers
- manual reconstruction
- can handle only very low data rates

BEBC bubble chamber

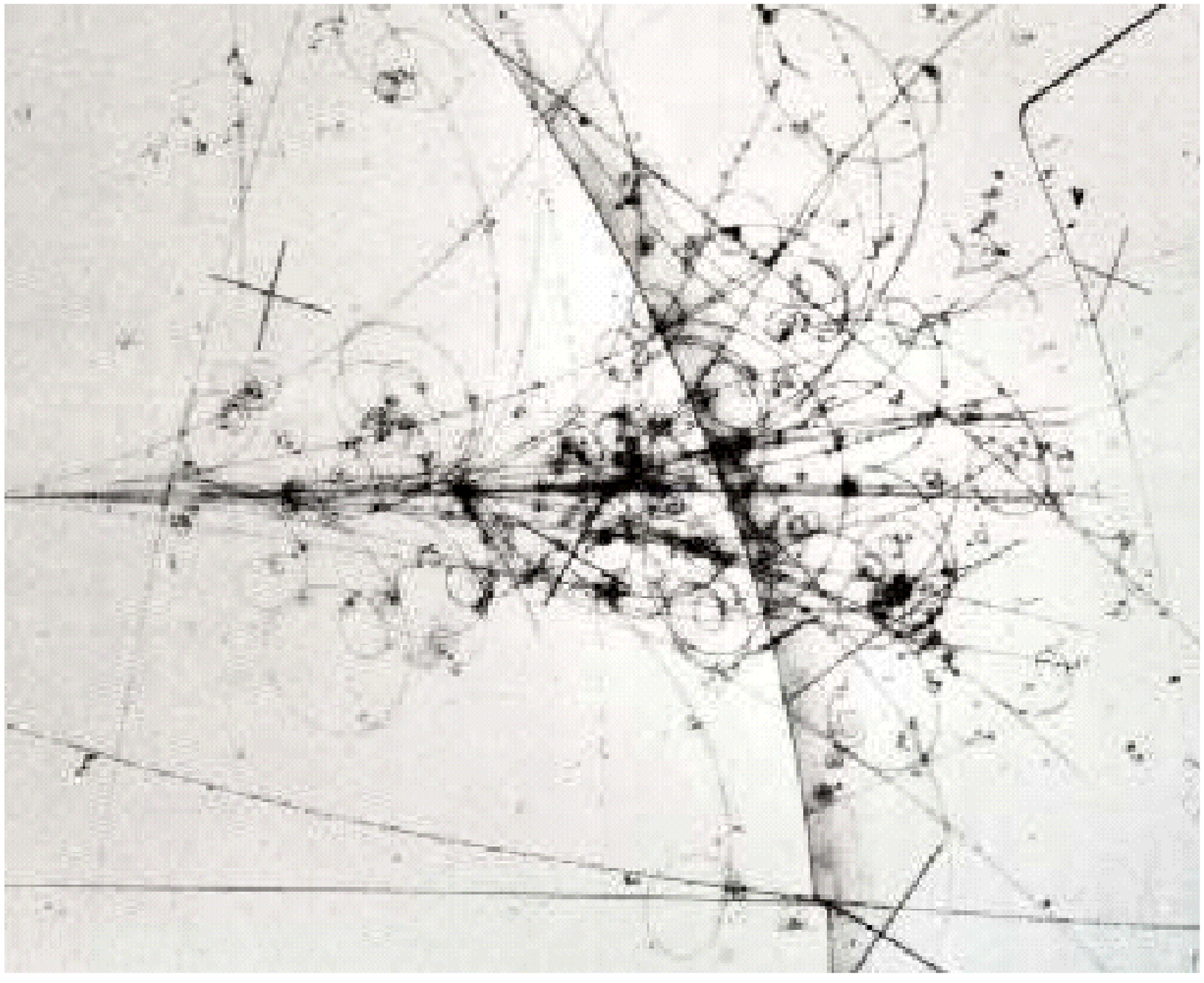

Gas Detectors

Criteria for optimal momentum resolution:

- many measurement points
- large detector volume
- very good single point resolution
- as little multiple scattering as possible

Gas detectors provide a good compromise and are used in most experiments. However:

- per cm in Argon only ca. 100 electron-ion pairs are produced by ionisation (see next page)
- this has to be compared with the noise of a typical amplifier of ≈1000 e-

⇒ a very efficient amplification mechanism is required

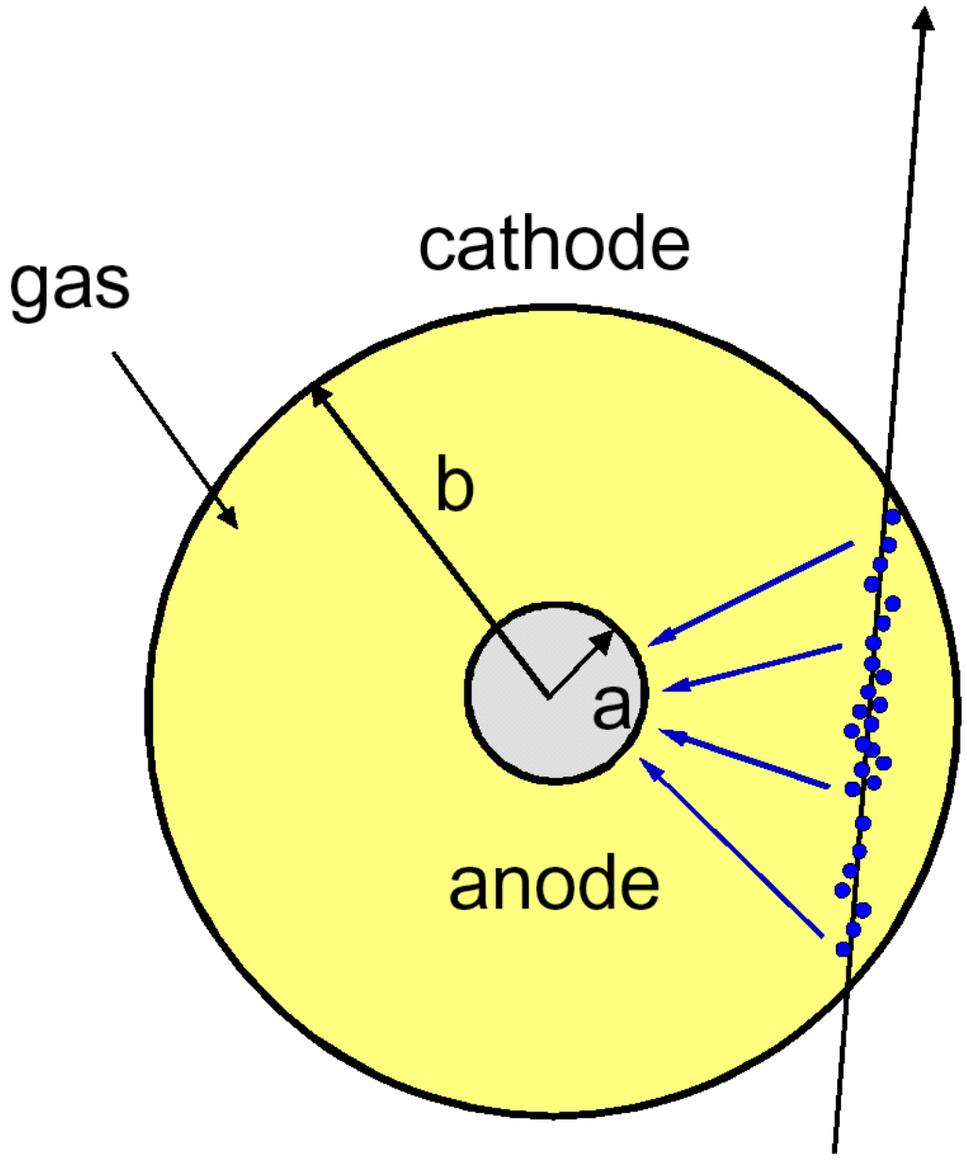

Primary and Total Ionisation Yield in Gases

Gas	Density ρ [g/cm^3]	I_0 [eV]	W [eV]	n_p [cm^{-1}]	n_T [cm^{-1}]
H_2	8.99 x 10^{-5}	15.4	37	5.2	9.2
He	1.78 x 10^{-4}	24.6	41	5.9	7.8
N_2	1.23 x 10^{-3}	15.5	35	10	56
O_2	1.43 x 10^{-3}	12.2	31	22	73
Ne	9.00 x 10^{-4}	21.6	36	12	39
Ar	1.78 x 10^{-3}	15.8	26	29	94
Kr	3.74 x 10^{-3}	14.0	24	22	192
Xe	5.89 x 10^{-3}	12.1	22	44	307
CO_2	1.98 x 10^{-3}	13.7	33	34	91
CH_4	7.17 x 10^{-4}	13.1	28	16	53
C_4H_{10}	2.67 x 10^{-3}	10.8	23	46	195

avg. ionisation pot. / shell elect.
average energy loss./ion pair
number primary electron-ion pairs
total number electron-ion pairs

@ STP

Total number of produced electron-ion pairs: $n_T = \frac{\Delta E}{W_i} = \frac{\frac{dE}{dx}\Delta x}{W_i}$ with

- ΔE = total energy loss in Δx and
- W_i = average energy loss per produced ion pair: $n_T \approx 2 \ldots 7 \cdot n_p$

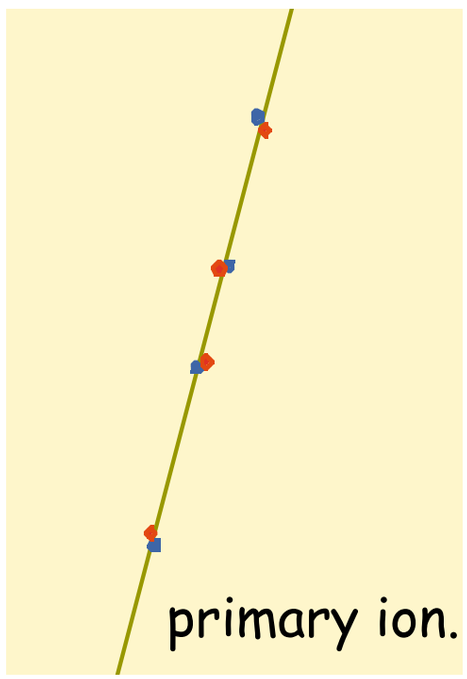

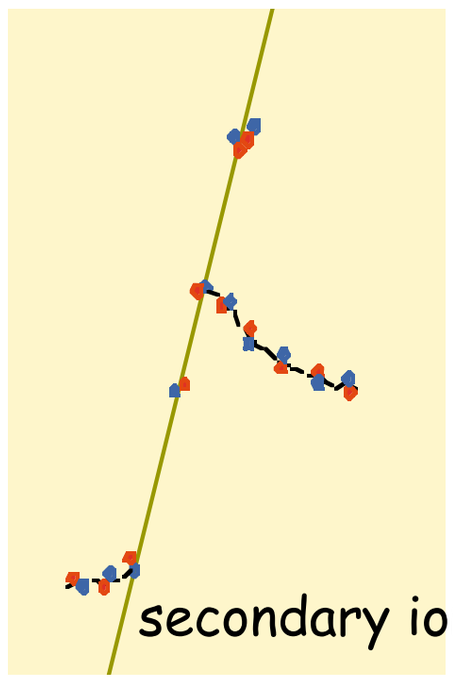

Signal Formation in a Condenser

Simple case of a condenser in a gas tight box:

- electric field $E = V_0 / d$
- capacity C
- accumulated charge $Q_0 = C V_0$
- number of produced electron-ion pairs N
- if RC >> t_{drift} ⇒ charge on condenser plates will be reduced by $N|q|$

⇒ resulting voltage pulse: V reduces by $\Delta V = N|q|/C$

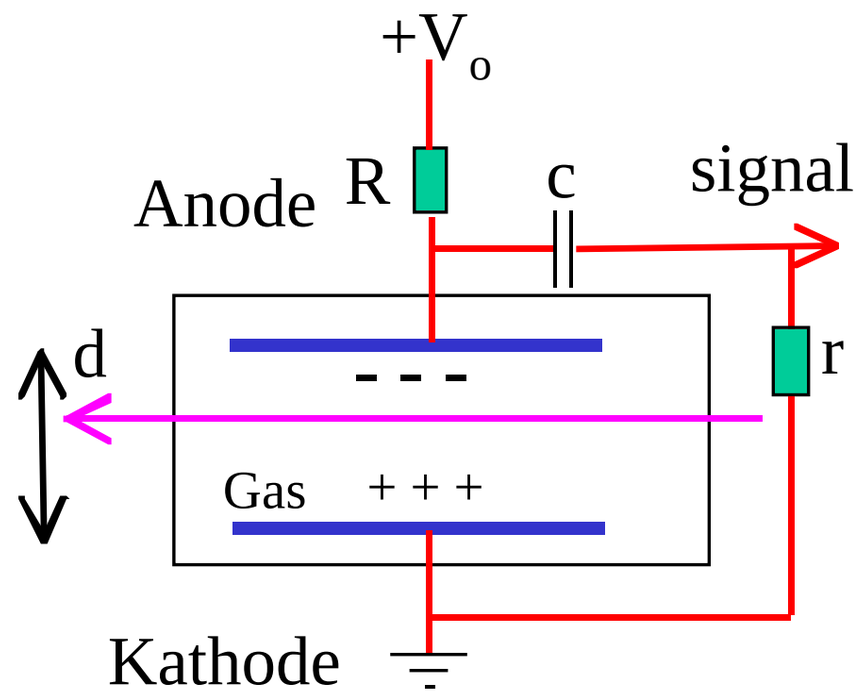

C = chamber capacity

c = pulse forming and coupling capacitor

R = resistor of power supply

r = pulse forming resistor

Example:

N ≈ 120 for Argon, C = 10 pF ⇒

$$\Delta V = \frac{120 \cdot e}{10pF} = \frac{120 \cdot 1.6 \times 10^{-16} C}{10 \times 10^{-9} F} \simeq 2\mu V$$

too small !

Gas Amplification

For cylindrical geometry:

$$E(r) \propto \frac{1}{r} \quad \text{and} \quad V(r) \propto \ln\frac{r}{a}$$

- the primary electrons drift towards the positive anode

- due to 1/r dependence the electric field close to very thin wires reaches values of E > kV/cm

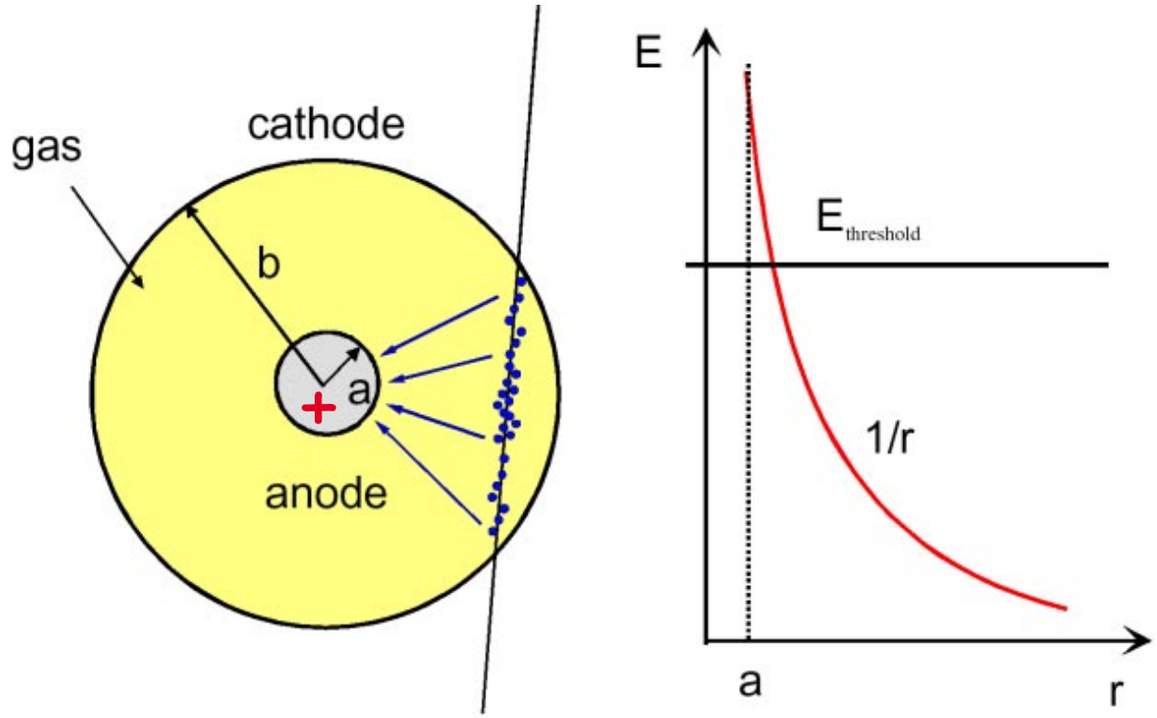

- ⇒ in between collisions with atoms electrons gain enough energy to ionize further gas molecules

- ⇒ exponential increase in number of electron-ion pairs very close (few μm) to the wire

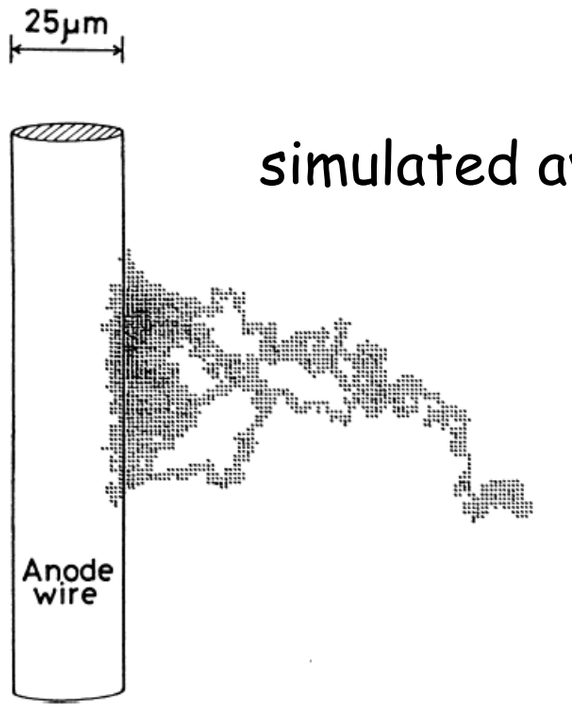

simulated avalanche

First Townsend Coefficient

Number of electron-ion pairs created per unit length in the avalanche per electron is given by the first Townsend coefficient α :

- relation to cross section for ionisation:

$$\alpha = \sigma_{ion} \cdot \frac{N_A}{V_{Mol}}$$

- number of produced ions: $n(x) = n_0 \cdot \exp(\alpha(E) \cdot x)$

- the gas gain is given by:

$$A = \frac{n}{n_0} = \exp\left[\int_a^{r_c} \alpha(r) dr\right]$$

with a anode diameter and r_c distance to wire where avalanche starts

- example: Argon and E = 100eV:
  $\sigma = 3 \times 10^{-16} cm^2 \quad \Rightarrow \alpha^{-1} \approx 1 \mu m$

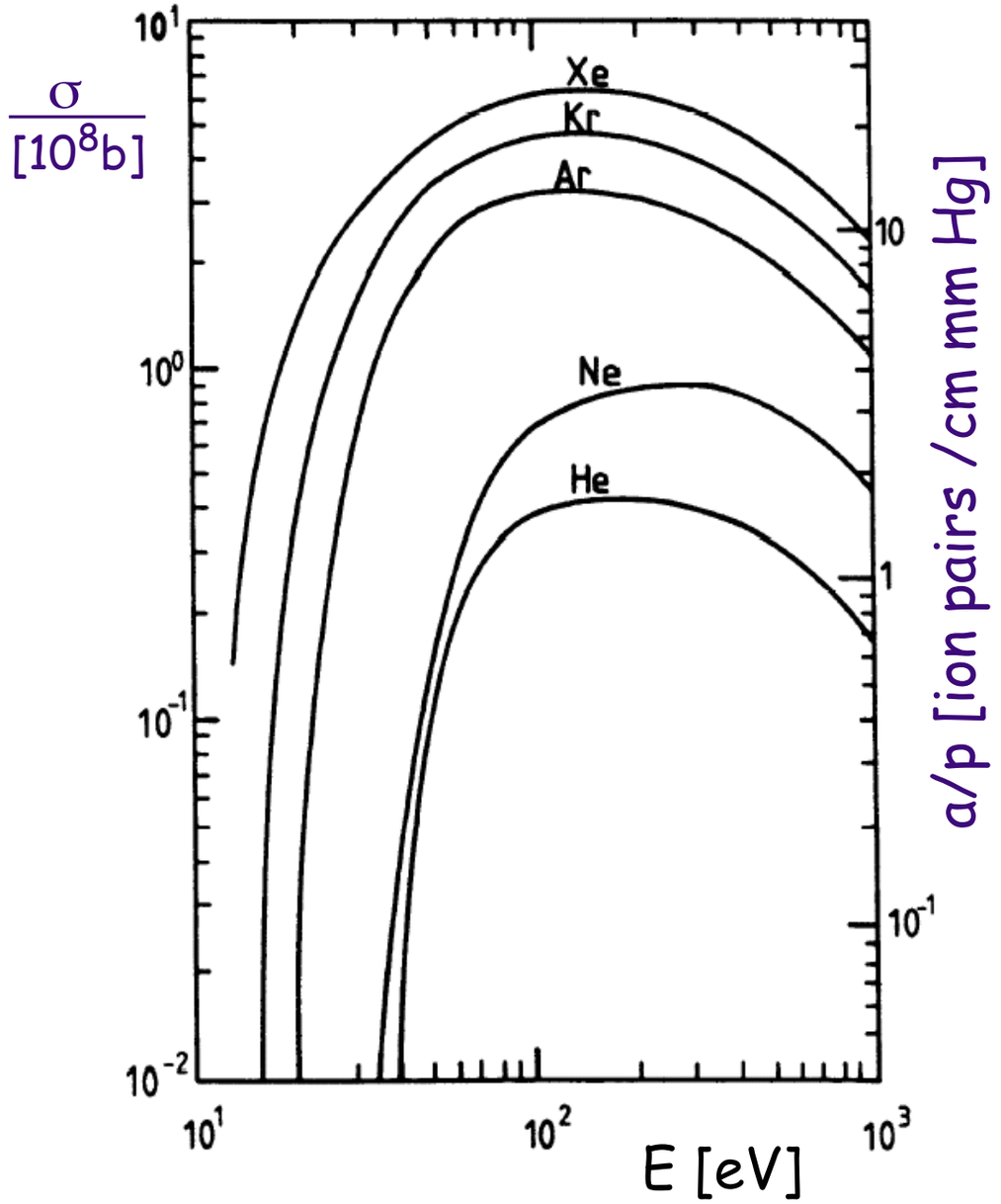

Raether limit: avalanche size limited to $A < \sim 10^8$ or $\alpha \cdot x < 20$

Second Townsend Coefficient

- In the avalanche many atoms are excited. When they return to their ground state UV photons are emitted.
- UV photons create more electrons through photo electric effect with gas atoms or when they hit the metallic electrodes
- The exponential growth of the gas amplification with increasing HV starts to get damped when the number of ionization processes by UV photons gets significant
  - start of the avalanche n_0 primary electrons
  - after amplification An_0
  - number of photo electrons $An_0\gamma$ with $\gamma \ll 1$ (2. Townsend coefficient)
  - which get amplified to $A^2n_0\gamma$ etc.
  - in total there are:

$$A_\gamma n_0 = n_0 A \sum_{n \geq 0} (A\gamma)^n = \frac{n_0 A}{1 - A\gamma}$$

where A_γ denotes the gas amplification including photons

- for $A\gamma \rightarrow 1$ the expression diverges, i.e. the signal no longer depends on the amount of primary ionization: Geiger Müller region

Pulse Formation in Cylindrical Chamber

In such a cylindrical geometry the following relations hold:

$$\phi(r) = \frac{CV_0}{2\pi\epsilon L}\ln\left(\frac{r}{a}\right) \qquad E(r) = \frac{CV_0}{2\pi\epsilon L}\frac{1}{r} \qquad C = \frac{2\pi\epsilon L}{\ln(b/a)}$$

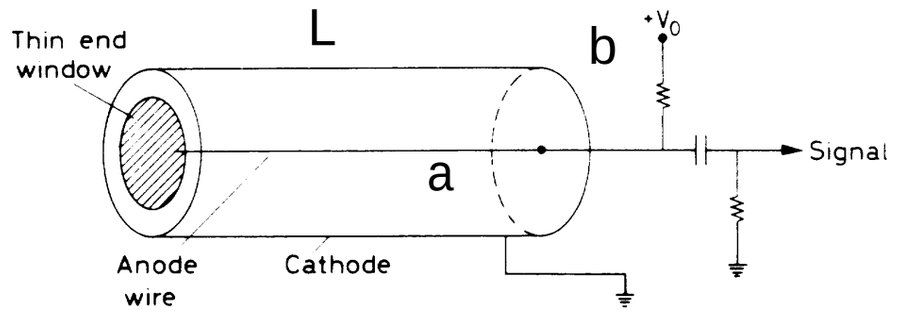

The stored electric energy is: $W = \frac{1}{2}CV_0^2$

When the charge q moves a distance dr this causes a change of potential energy by:

$$dW = q\frac{d\phi(r)}{dr}dr \equiv CV_0 dV \Rightarrow dV = \frac{q}{CV_0}\frac{d\phi(r)}{dr}dr$$

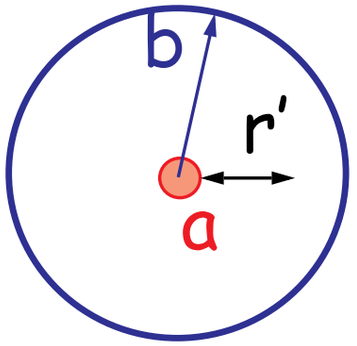

At the position r´ the electrons induce a voltage of:

$$\Delta V^- = \frac{-q}{CV_0}\int_{a+r'}^{a}\frac{d\phi(r)}{dr}dr = \frac{-q}{CV_0}\int_{a+r'}^{a}\frac{-CV_0}{2\pi\epsilon L}\frac{dr}{r} = \frac{-q}{2\pi\epsilon L}\ln\frac{a+r'}{a}$$

Similarly the voltage induced by the moving ions at the position r´ amounts to:

$$\Delta V^+ = \frac{+q}{CV_0}\int_{a+r'}^{b}\frac{d\phi(r)}{dr}dr = \frac{+q}{CV_0}\int_{a+r'}^{b}\frac{-CV_0}{2\pi\epsilon L}\frac{dr}{r} = \frac{-q}{2\pi\epsilon L}\ln\frac{b}{a+r'}$$

The resulting total voltage is given by : $\Delta V = \Delta V^- + \Delta V^+ = -q/C$

Contribution of Ions and Electrons to the Signal

The contribution of electrons and ions to the signal is very different in the case of gas amplification, since this occurs very close to the anode wire at a distance: $r' = k \cdot \lambda$

where *k* is the number of mean free path-lengths λ, which are required for avalanche formation.

As a consequence the drift path of the ions is much longer. For example in the case
b = 1cm, a = 10µm, r´= 2µm

$$\frac{\Delta V^+}{\Delta V^-} = \frac{\ln \frac{b}{a+r'}}{\ln \frac{a+r'}{a}} \approx \frac{\ln 10^3}{\ln 1.2} \approx 40$$

The time dependence in this case is given by (r´≈ 0): $V(t) = V^+(t) = -\frac{q}{2\pi\epsilon L} \ln \frac{r(t)}{a}$

The solution of the problem is to find the relation $r(t)$

The mobility is given by: $\mu \equiv \frac{v_{drift}}{E(r)} = \frac{1}{E(r)} \frac{dr}{dt}$

For cylindrical geometry: $\frac{dr}{dt} = \mu E(t) = \mu \frac{CV_0}{2\pi\epsilon L} \frac{1}{r} \Rightarrow r dr = \mu \frac{CV_0}{2\pi\epsilon L} dt$

Time Evolution of the Signal

Integration of $rdr = \mu \frac{CV_0}{2\pi\epsilon L} dt$ yields:

$$\int_{r(0)=a}^{r(t)} rdr = \mu \frac{CV_0}{2\pi\epsilon L} \int_0^t dt \Rightarrow r(t) = \left(a^2 + \frac{\mu C V_0}{\pi\epsilon L} t \right)^{1/2}$$

$$V(t) = \frac{-q}{2\pi\epsilon L} \ln \frac{r(t)}{a} = \frac{-q}{4\pi\epsilon L} \ln \left(1 + \frac{\mu C V_0}{\pi\epsilon L a^2} t \right) = \frac{-q}{4\pi\epsilon L} \ln \left(1 + \frac{t}{t_0} \right) \quad \text{with} \quad t_0 = \frac{a^2 \ln(b/a)}{2\mu V_0}$$

The total drift time T follows from $r(T) = b$

$$T = \frac{t_0}{a^2}(b^2 - a^2) \approx \frac{b^2}{a^2} t_0$$

Example:

$\mu = 1.5 cm^2 s^{-1} V^{-1}$, V = 1500V, a = 10µm, b = 1cm and $t_0 = 1.5 \times 10^{-9}$ s

$\Rightarrow$ T = 1.5×10^{-3} s

Usually it is necessary to differentiate the signal (which makes it shorter) by the electronics to reduce the dead time.

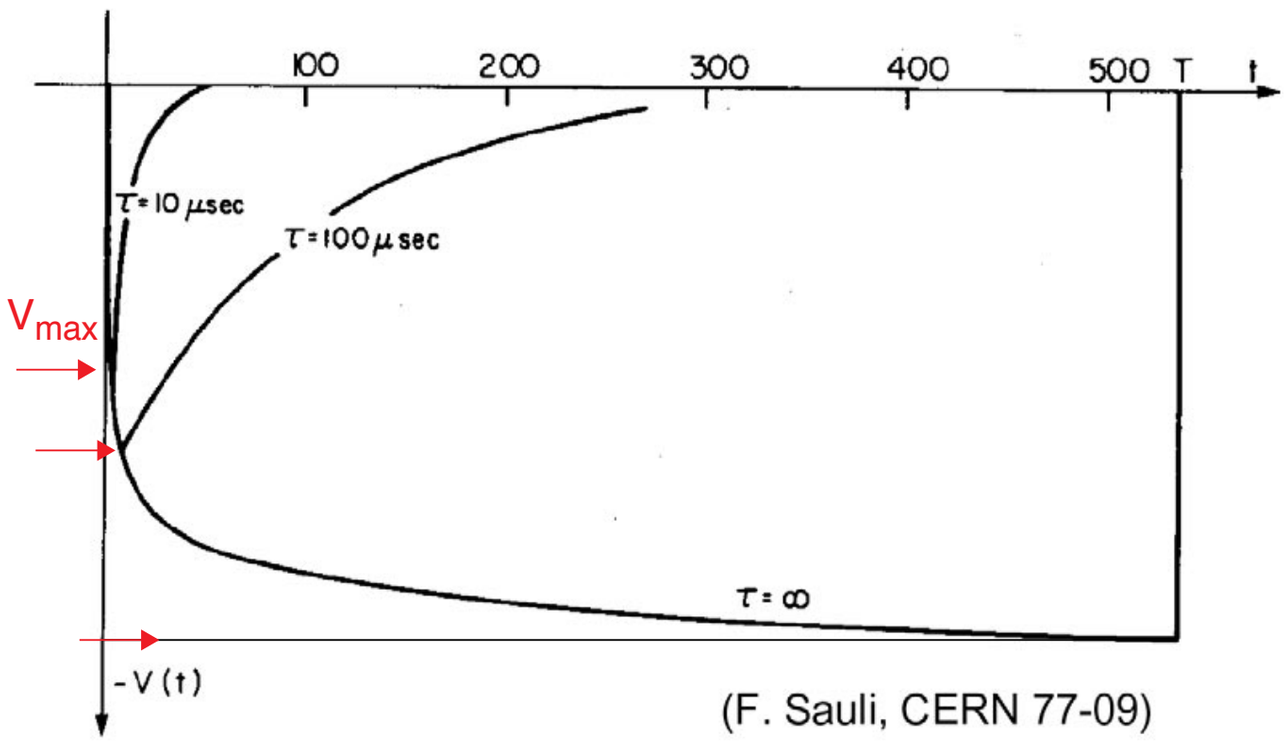

(F. Sauli, CERN 77-09)

Considerations on the Choice of Gas

In principal avalanche formation occurs in every gas.
However the gas should have properties which lead to:

- low operation voltage
- stable operation also at high gas gain
- good rate capability
- sufficient longevity
- fast recovery

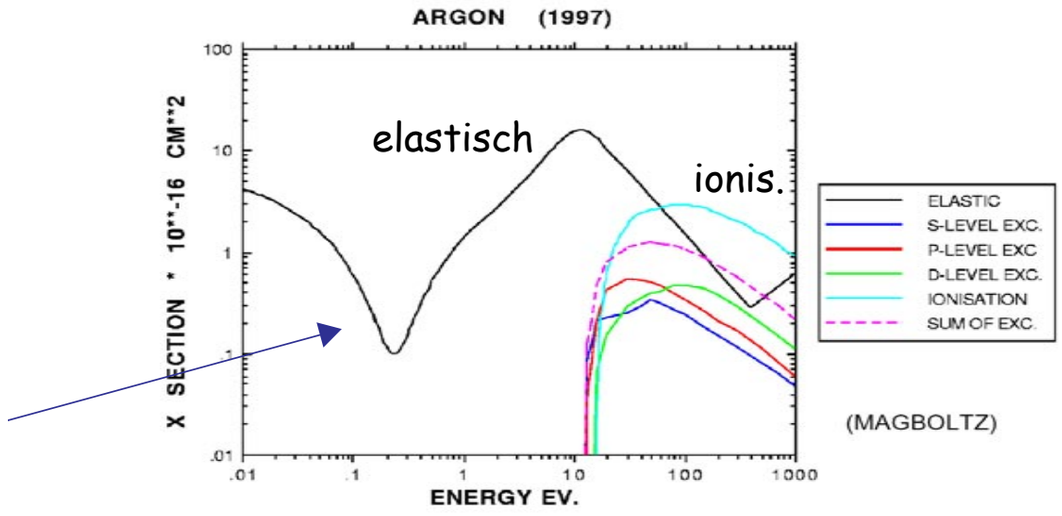

The main component of a chamber gas usually is a noble gas, since it is mono-atomic and the electrons mainly experience elastic collisions with little energy transfer. This enables gas gain already at low voltages. For price reasons the choice in most cases is Argon.

Stable operation in most cases requires the presence of additives.
In the avalanche Ar atoms get excited, which emit UV photons when they return to their ground state (E>11.6 eV). When these photons reach the cathode made from Al or Cu (≈ 7.7 eV excitation potential) electrons are liberated by the photo electric effect which drift back to the anode and create another avalanche.
This would lead to „breakdown“ already at relatively low voltages for a detector with pure Ar.

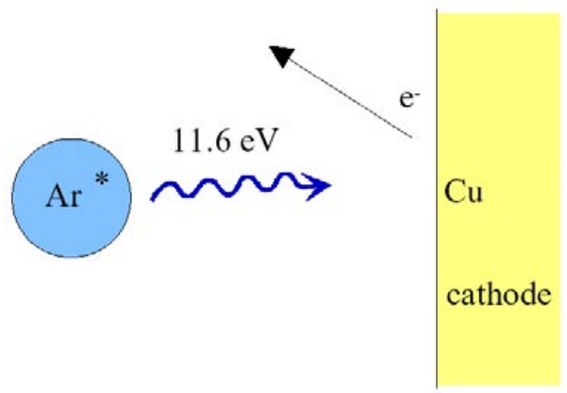

Additives to the Chamber Gas: Quencher

The solve this problem one usually adds a poly-atomic component to the gas.

- these gases have many non-radiative vibrational and rotational states over a wide range of energies
- the molecules easily absorb the UV photons in the range ≈100-200 nm
- they de-excite by collisions or dissociation
- because $\tau_{emission} >> \tau_{collision}$ the UV photons are very efficiently eliminated or quenched

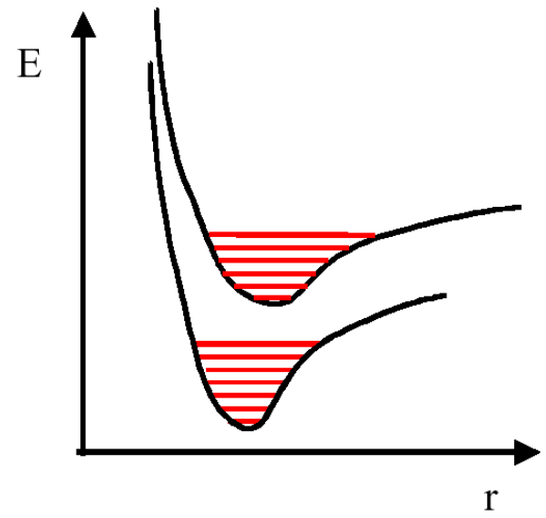

Typically hydrocarbon components are being used:

- Methan CH_4
- Ethan C_2H_6
- Isobutane iC_4H_{10}
- or alcohol vapours

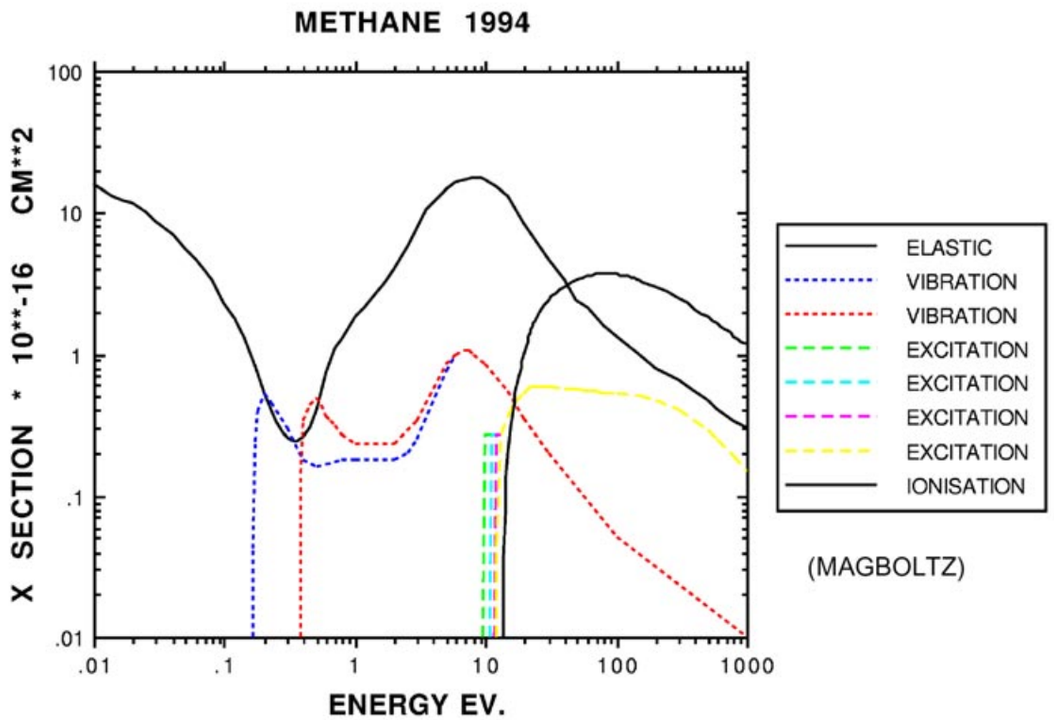

Drift and Diffusion in Gases

In a field free region:
Due to multiple collisions electron-ion pairs assume a thermal energy distribution. According to the law of equal partition the average energy at room temperature is given by:

$$\epsilon_T = \frac{3}{2}kT \approx 0.035\ eV$$

- they follow a Maxwell-Boltzmann distribution: $F(\varepsilon) = const \cdot \sqrt{\varepsilon} \cdot \exp\left(-\varepsilon/kT\right)$
- a point-like charge distribution will diffuse due to multiple scattering into the neighboring space:

  $\frac{dN}{N} = \frac{1}{\sqrt{4\pi Dt}} \exp\left(-\frac{x^2}{4Dt}\right) dx$ is the fraction of charge located in dx at the distance x at the time t
- D is the so-called diffusion coefficient
- linear diffusion: $\sigma_x = \sqrt{2Dt}$
- volume diffusion: $\sigma_{vol} = \sqrt{3}\sigma_x = \sqrt{6Dt}$
- mean free path of diffusion: $\lambda(\varepsilon) = \frac{1}{N\sigma(\varepsilon)}$

  where $N = N_0\rho/A$ is the number of molecules/volume

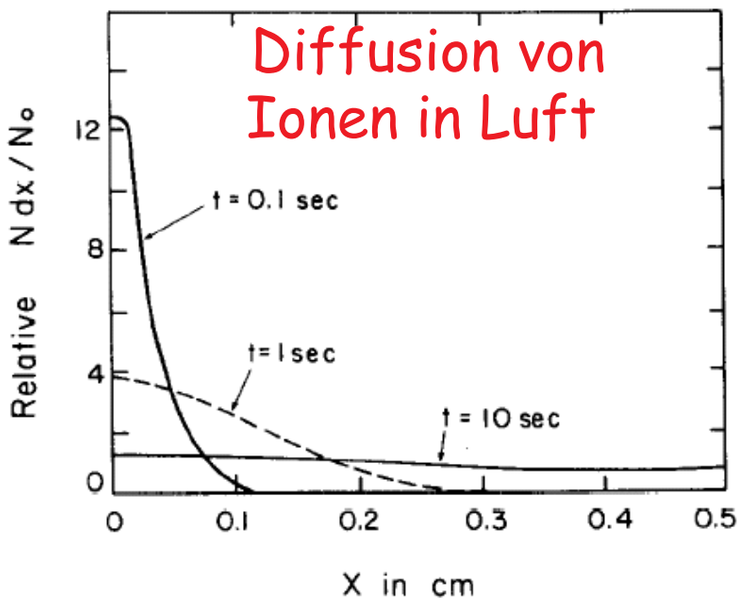

Motion of Charge Carriers in electric Field

In an electric field a directional drift parallel to the field direction is superimposed on the irregular motion of diffusion. Definition of drift velocity:

$$\vec{v}_{\text{drift}} = \mu(E) \cdot \vec{E} \cdot \frac{p_0}{p}$$ with:

- $\mu(E)$ energy dependent mobility of charge carriers
- $\vec{E}$ electric field
- $\frac{p_0}{p}$ normalized pressure (to STP)

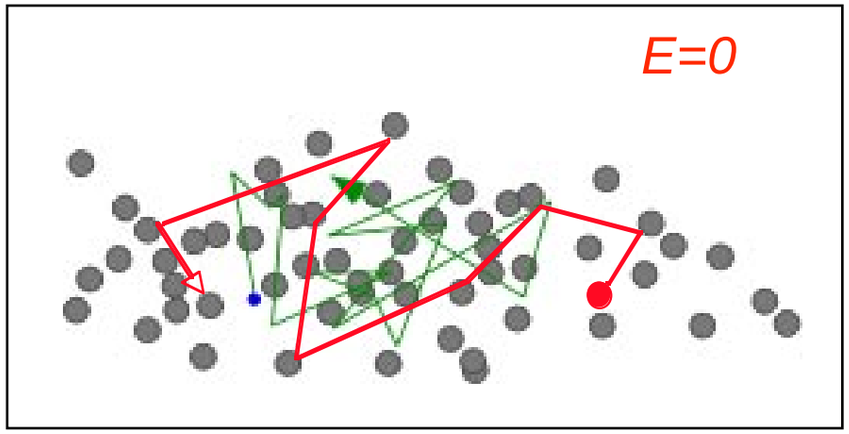

Figures taken from F. Sauli, CERN

Valid under the assumption:

- no recombination
- no attachment

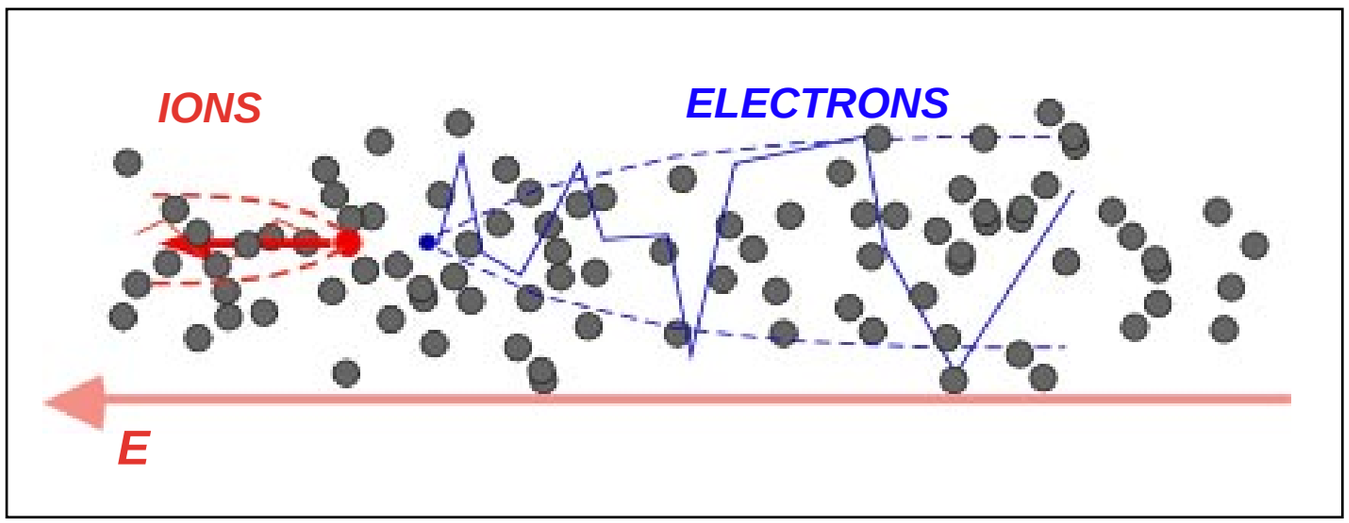

Impact of Diffusion on Position Resolution

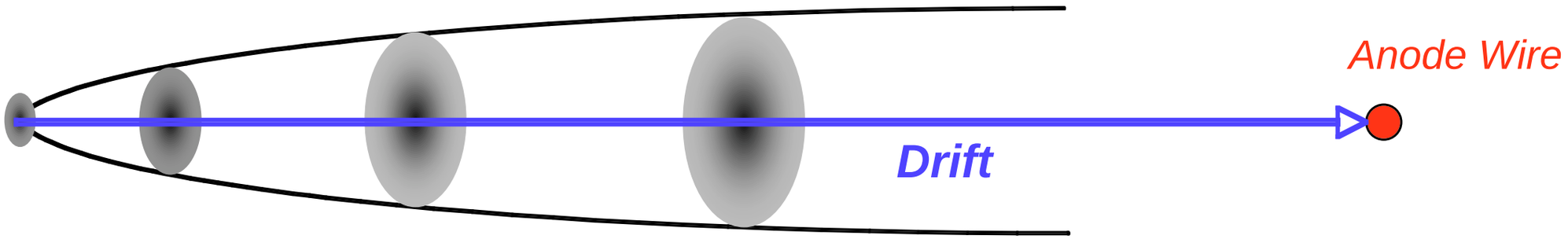

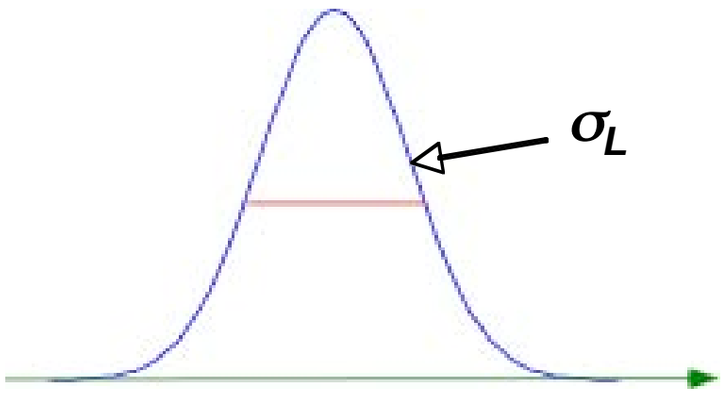

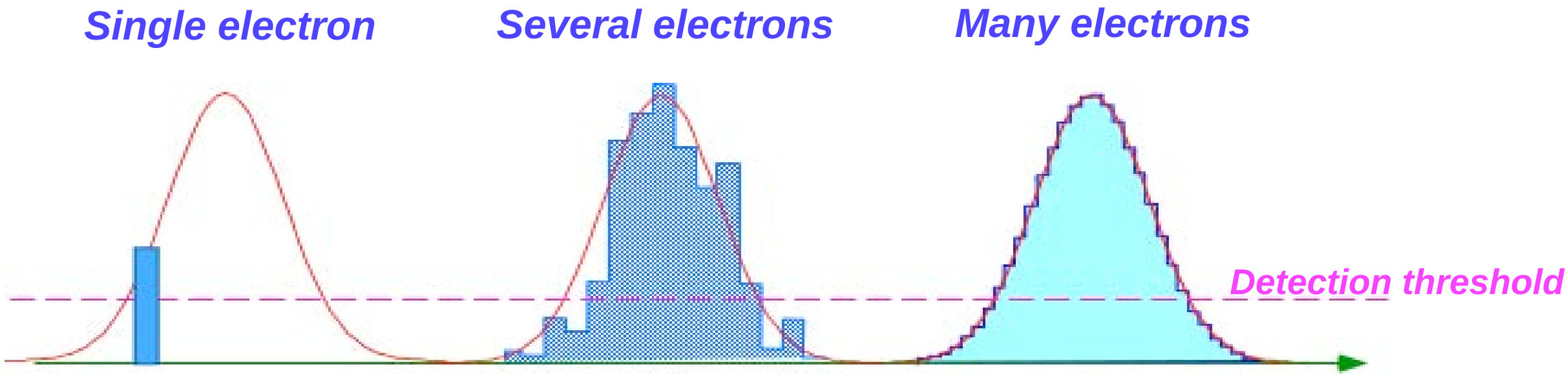

Slide taken from F. Sauli, CERN

carsten.niebuhr@desy.de

Recombination and Attachment

Recombination:

Ions and electrons created in the primary ionization process recombine before they are detected. This leads to an effective decrease of the density of positive ions n^+:

$$\frac{dn^+}{dt} = \alpha\, n^+ n^-$$ with recombination coefficient α

Values of α for O_2 or CO_2 are up to 10^{-6} (10^{-7}) $cm^{-3}\ s^{-1}$ in the case of recombination with negative ions (electrons)

Electron attachment:

For poly-atomic gases (no noble gases !) low energy electrons (≈ eV) can get attached to the molecule after a collision

- p_a probability per collision
- n_s number of collisions per time
- $t_a = 1/(p_a n_s)$ mean time until attachment

–> necessity for gas cleaning !

Anlagerungswahrscheinlichkeit pro Stoß

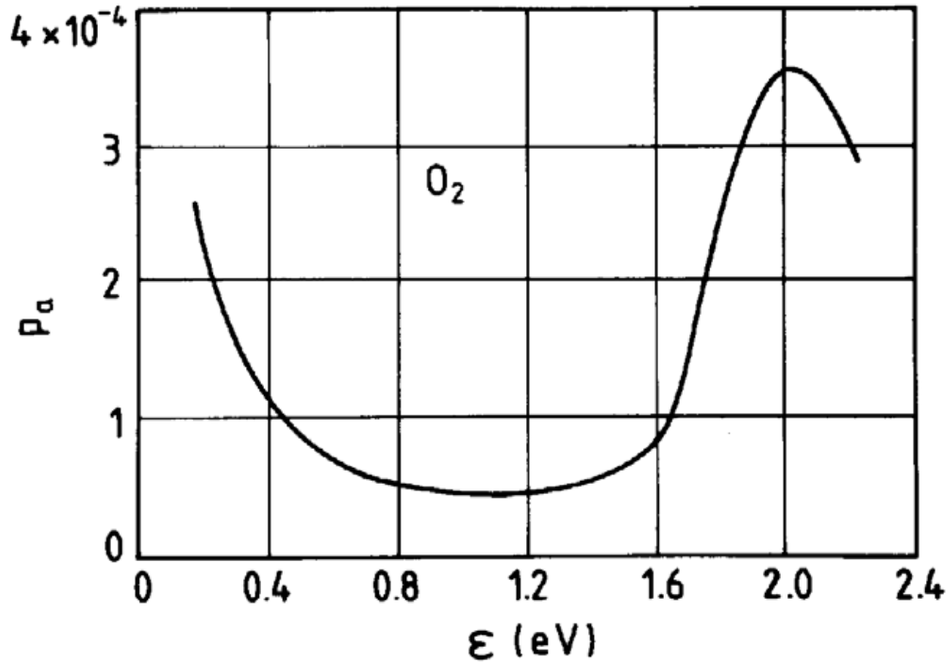

Elektronegative Gase (ohne E-Feld):

Gas	p_a	$n_s[s^{-1}]$	t_a [ns]
CO_2	6.2×10^{-9}	2.2×10^{11}	7.1×10^5
O_2	2.5×10^{-5}	2.1×10^{11}	190
H_2O	2.5×10^{-5}	2.8×10^{11}	140
Cl^-_2	4.8×10^{-4}	4.5×10^{11}	5

Ion- and Electron-Drift for several Gases

- mean free path
- diffusion coefficient
- mobility

von Ionen für einige Gase bei Normalbedinungen:

Gas	A	$\lambda_{Ion}[\mathrm{cm}]$	$D_{Ion}[\mathrm{cm}^2/\mathrm{s}]$	$\mu_{Ion}\left[\frac{\mathrm{cm/s}}{\mathrm{V/cm}}\right]$
H_2	2.02	1.8×10^{-5}	0.34	13.0
He	4.00	2.8×10^{-5}	0.26	10.2
Ar	39.95	1.0×10^{-5}	0.04	1.7
O_2	32.00	1.0×10^{-5}	0.06	2.2
H_2O	18.02	1.0×10^{-5}	0.02	0.7

- mobility of electrons is ≈10^3 times larger compared to ions
- mean free path of electrons $\lambda_e \sim 6 \times \lambda_{ion}$

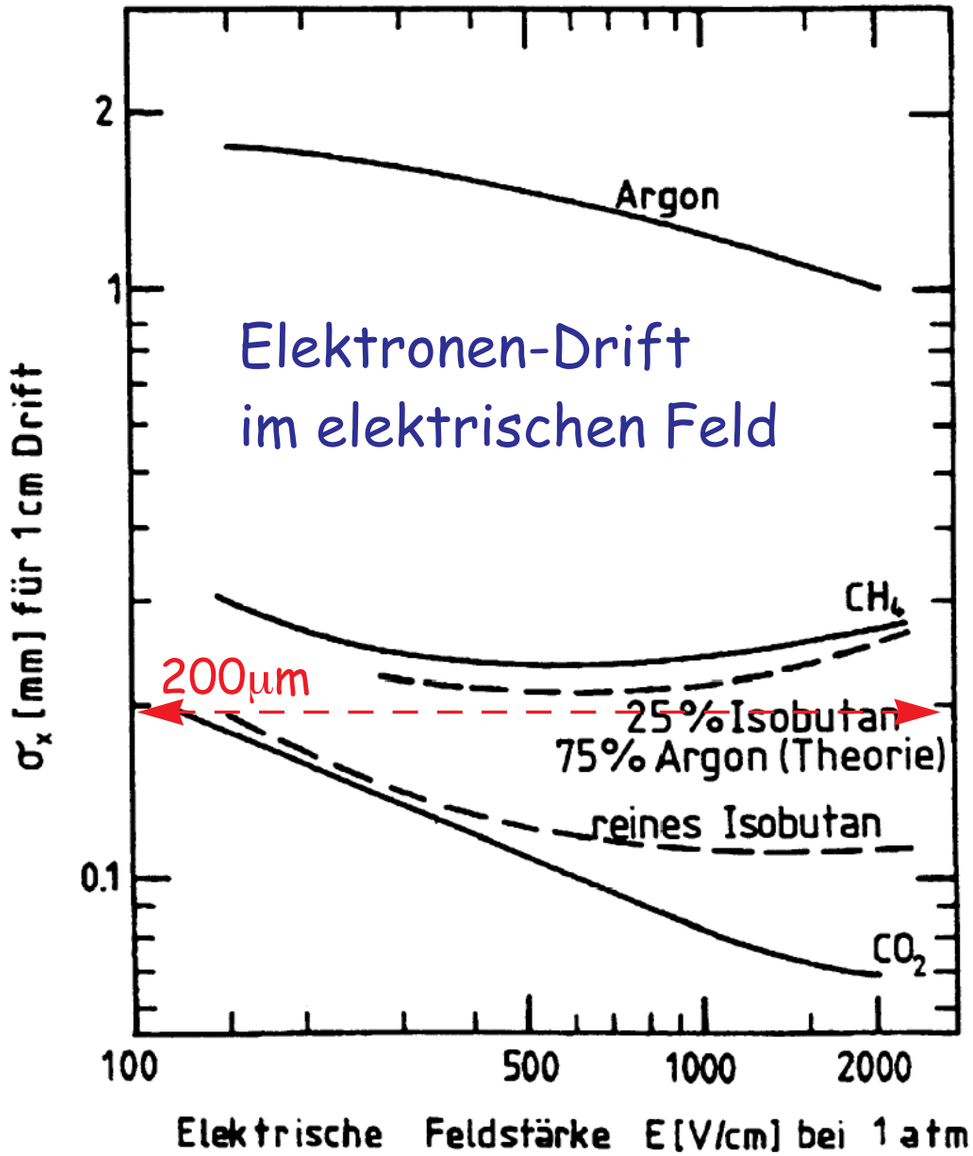

Transverse extension of an electron swarm after 1cm drift as a function of the applied electric field strength.

Ramsauer Effect

Due to their larger mean free path between collisions electrons can gain much more energy between collisions in the electric field than ions.

Drift velocity $\vec{v}_{\text{drift}} = \frac{e}{m} \cdot \vec{E} \cdot \tau(\vec{E}, \varepsilon)$, where the time τ between the collisions depends on the collision cross section.

Wavelengths of electrons in eV range roughly correspond to dimensions of molecules in noble gases
⇒ quantum mechanical interference effects lead to a strong variation of cross section σ with electron energy.

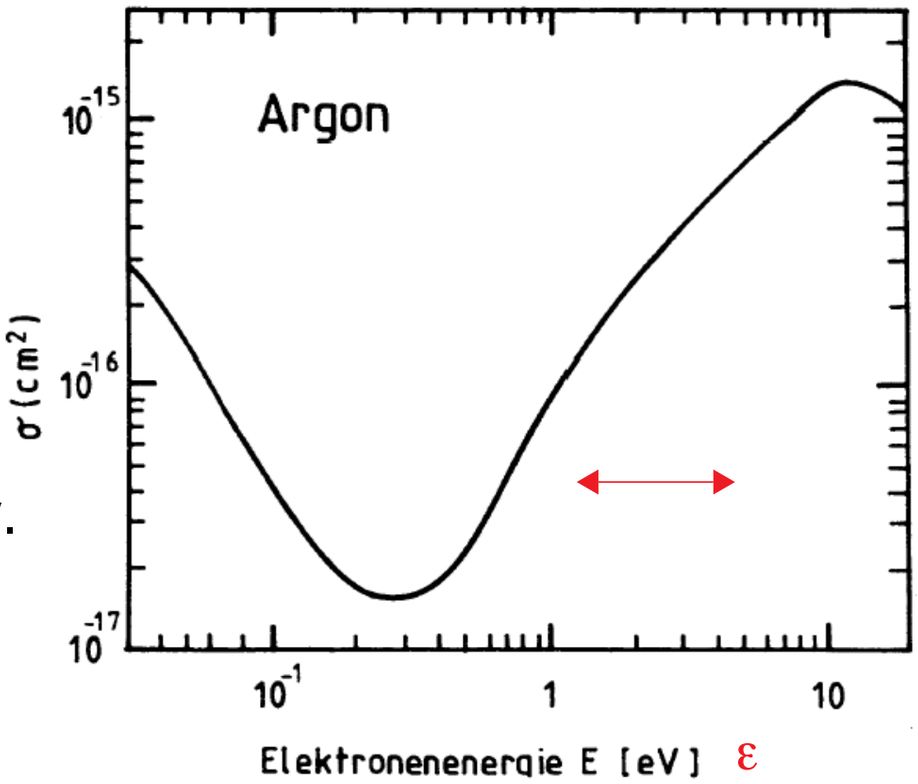

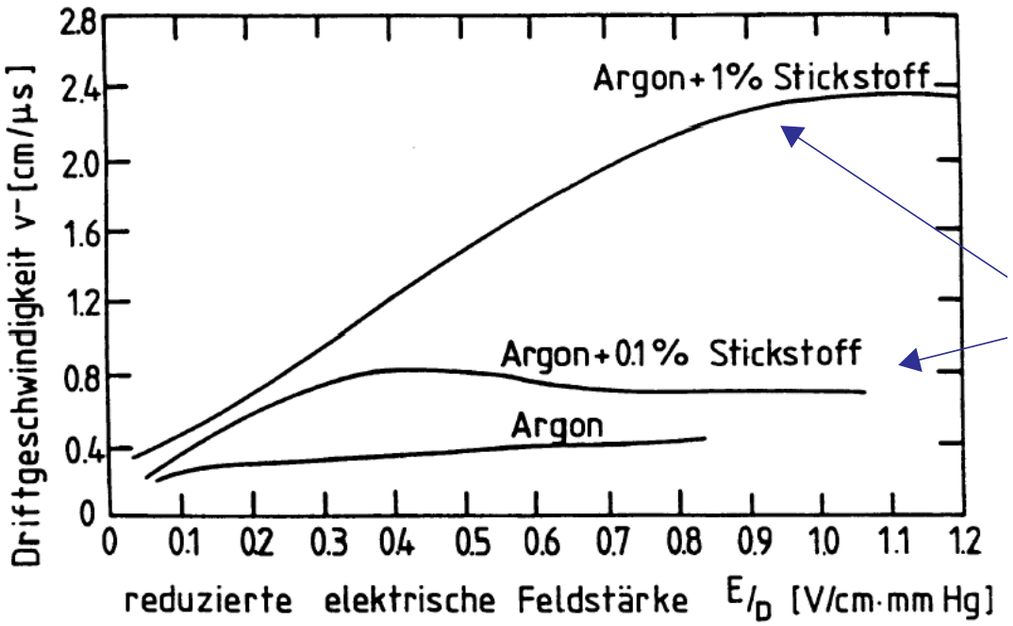

As a consequence already tiny impurities which lead to a small shift in the mean energy ε can cause a drastic change of the drift velocity of gases.

⇒ necessity of gas cleaning

v_{drift} vs E-Field for various Argon-Mixtures

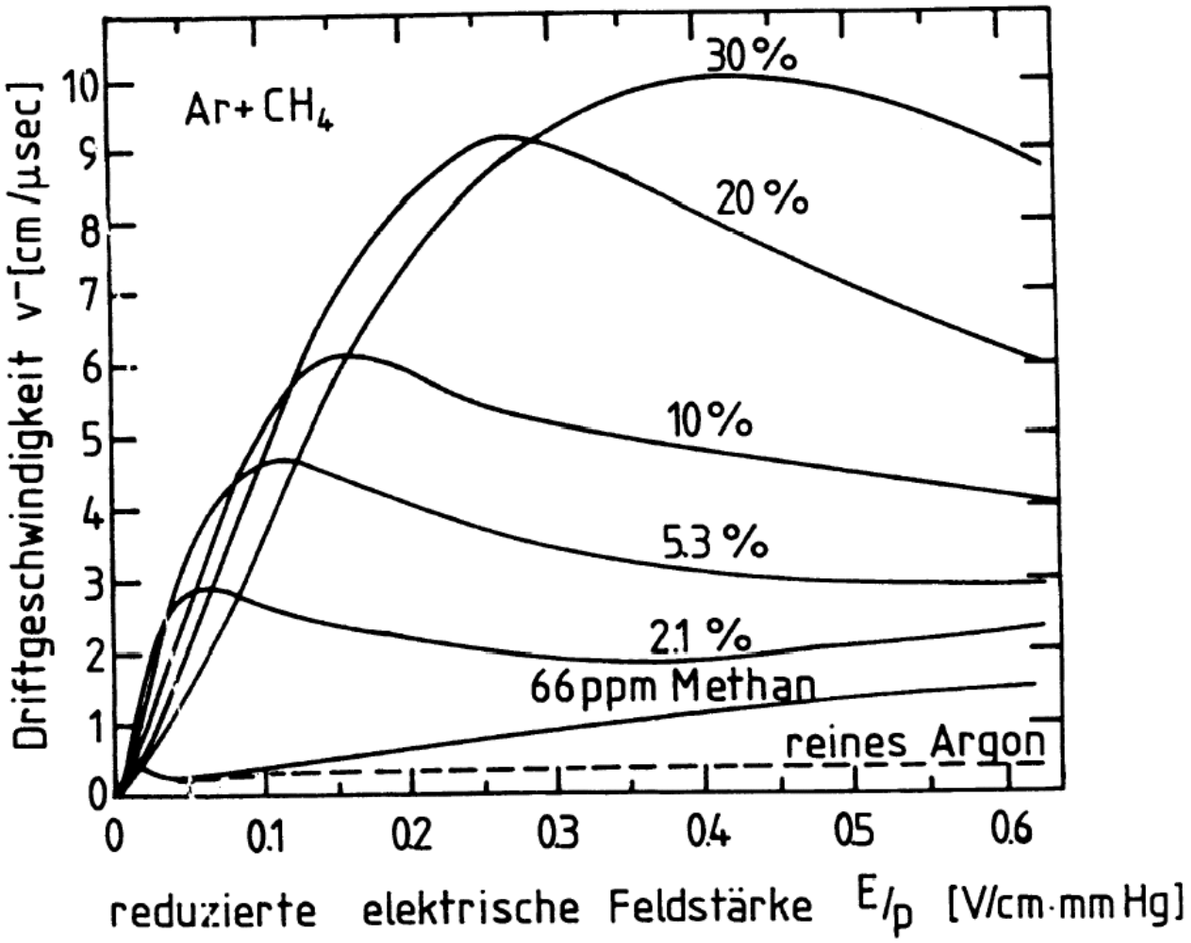

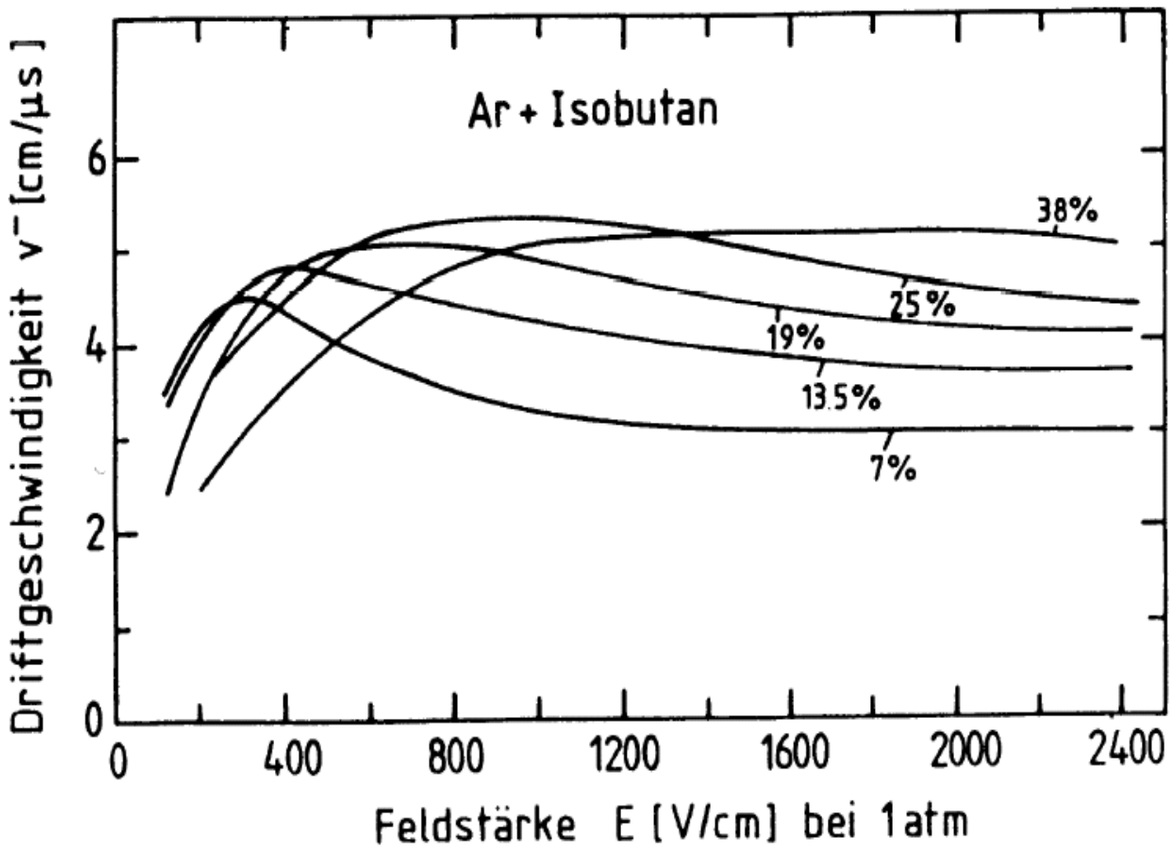

- details in the energy dependence of the cross section (Ramsauer minimum) lead to a characteristic maximum in the dependence on the electric field
- for stable operation one often tries to operate at the maximum: $\frac{dv_{\mathrm{drift}}}{dE} = 0$
- typical values for drift velocities are: v_{drift} ≈ 2-10 cm/µs = 20-100 µm/ns

Drift in E- und B-Fields: Langevin Equation

The presence of magnetic field drastically modifies the drift properties of electrons. The equation of motion: $m\ddot{\vec{x}} = q\vec{E} + q \cdot \vec{v} \times \vec{B} + m\vec{A}(t)$, where $m\vec{A}(t)$ represents a time dependent stochastic force, which results from the collisions with the gas molecules. In the time average this force can be described by a frictional force which is proportional to the velocity $-m\vec{v}/\tau$, where τ is the mean time between collisions. Integration yields:

$$\vec{v}_{\mathrm{drift}} = \frac{\mu}{1+\omega^2\tau^2}\left(\vec{E} + \frac{\vec{E}\times\vec{B}}{B}\omega\tau + \frac{(\vec{E}\cdot\vec{B})\cdot\vec{B}}{B^2}\omega^2\tau^2\right)$$ for the stationary case.

$\mu = e \cdot \tau/m$ mobility of charge carriers

$\omega = e \cdot B/m$ cyclotron frequency

For the frequently realized case $\vec{E} \perp \vec{B}$:

- modulus of drift velocity:

$$|\vec{v}_{\mathrm{drift}}| = \frac{\mu E}{\sqrt{1+\omega^2\tau^2}}$$

- Lorentzangle α between drift direction and direction of the magnetic field:

$$\alpha \approx v_{drift}\frac{B}{E} \quad \text{for} \quad \alpha \ll 1$$

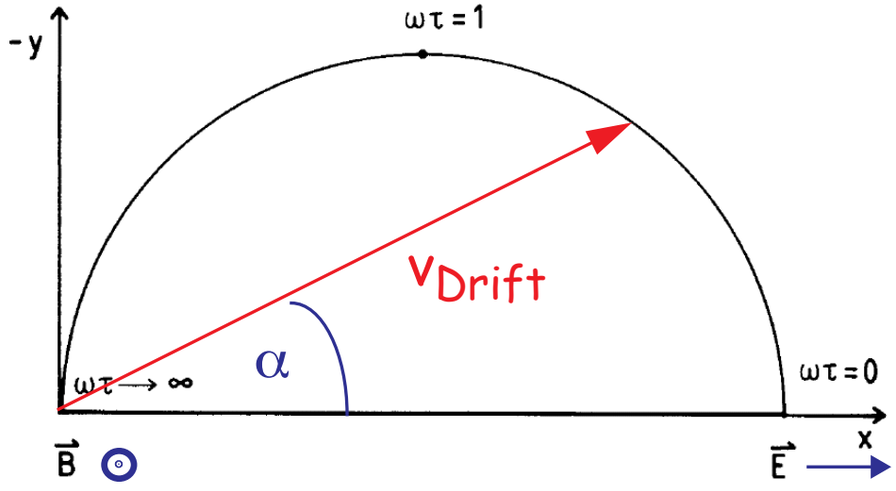

$$\tan\alpha = \omega\tau = \frac{1}{\sqrt{\frac{1}{\nu^2_{Drift}}\frac{E^2}{B^2} - 1}}$$

B-Field Dependence of v_{drift} and α

Example: Argon (67.2%) Isobutane (30.3%) Methylal (2.5%)

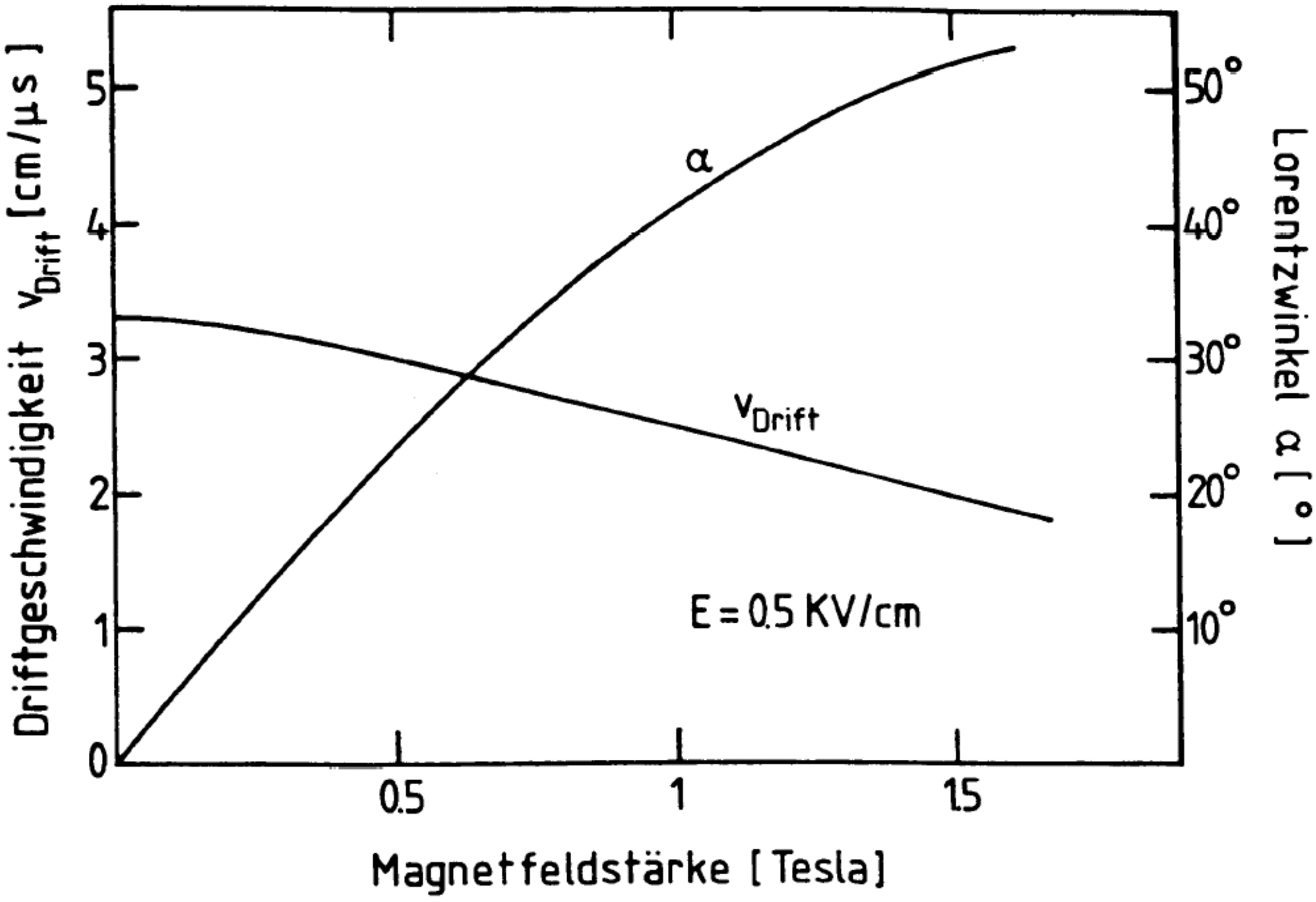

Diffusion in Electric and Magnetic Fields

The magnetic field also reduces the diffusion coefficient of electrons transversely to the direction of the magnetic field.

For $\vec{B} = (0, 0, B_z)$ i.e. $\vec{E} \| \vec{B}$ the diffusion coefficient gets modified to:

$$D_z = D$$

$$D_x = D_y = \frac{D}{1 + \omega^2 \tau^2}$$

This effected is for instance exploited in a TPC, in order to reduce the effect of transverse diffusion during the long drift time.

Transverse diffusion σ (μm) for a drift of 15 cm in different Ar/CH_4 mixtures

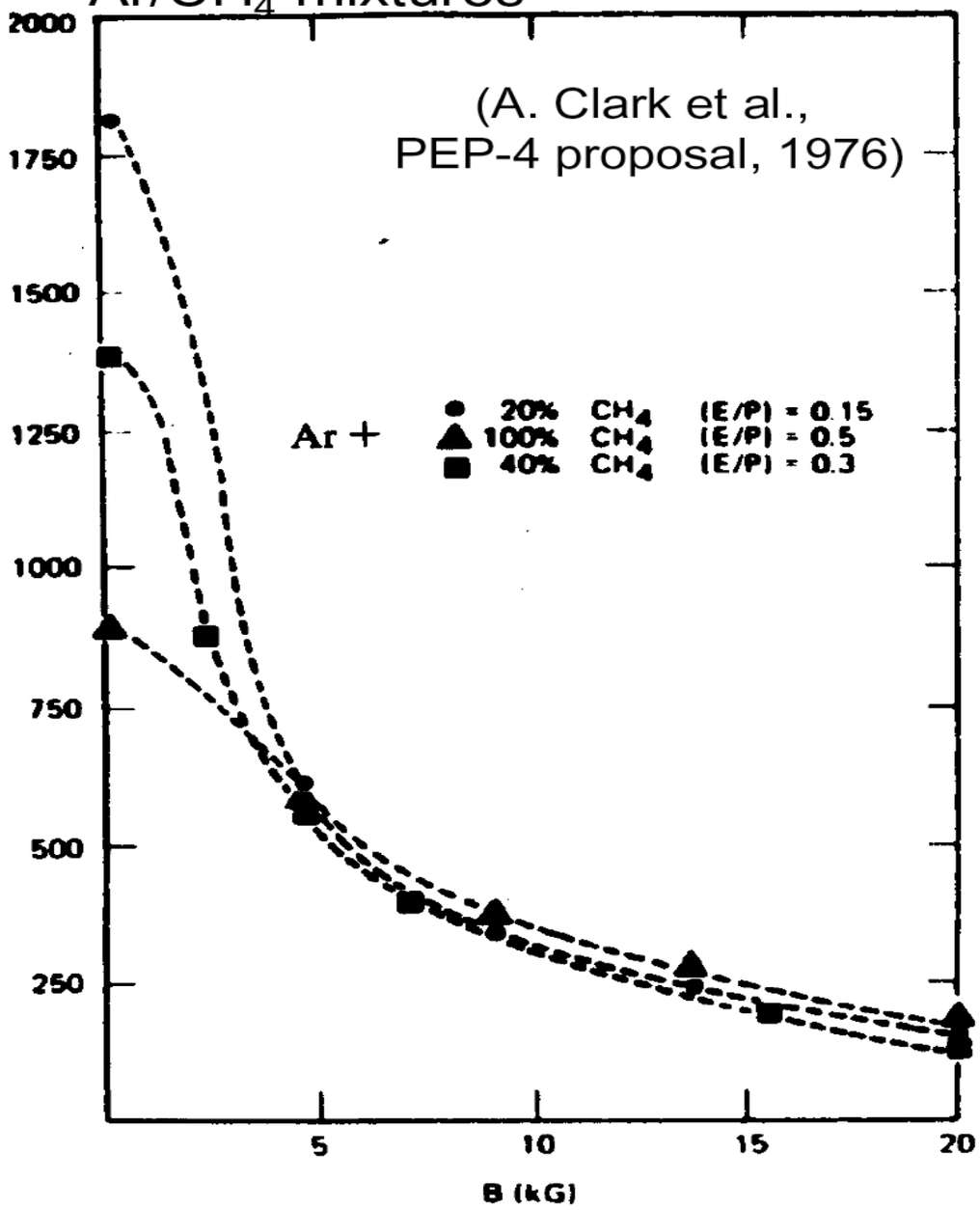

Avalanche Formation

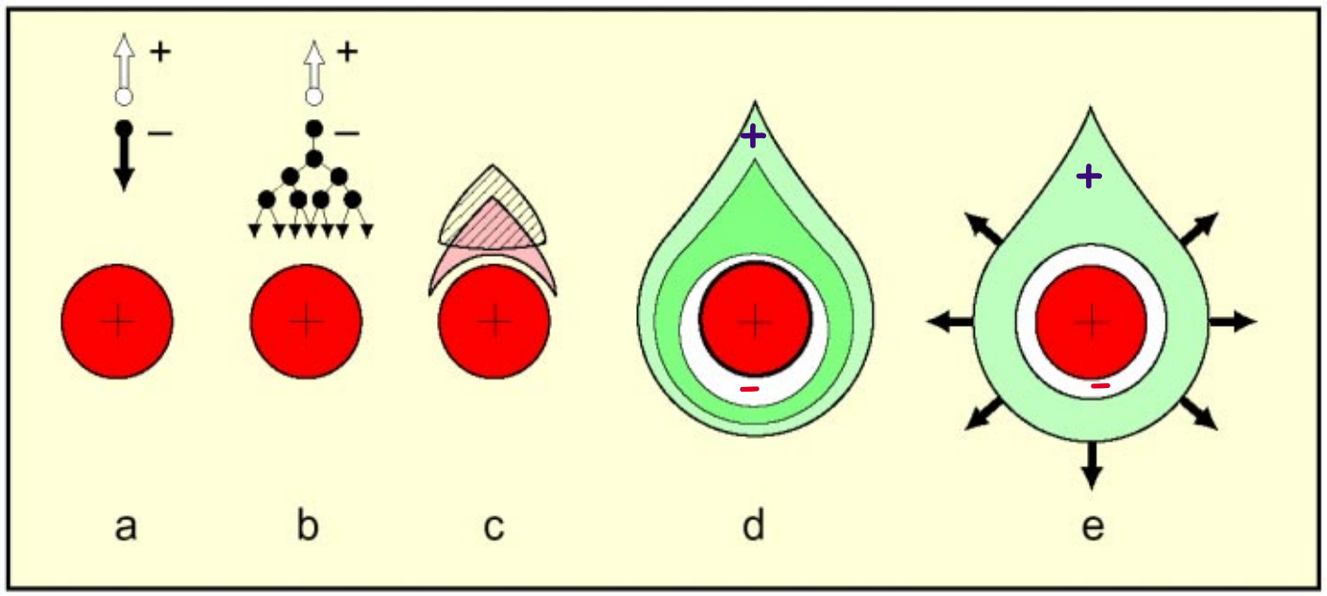

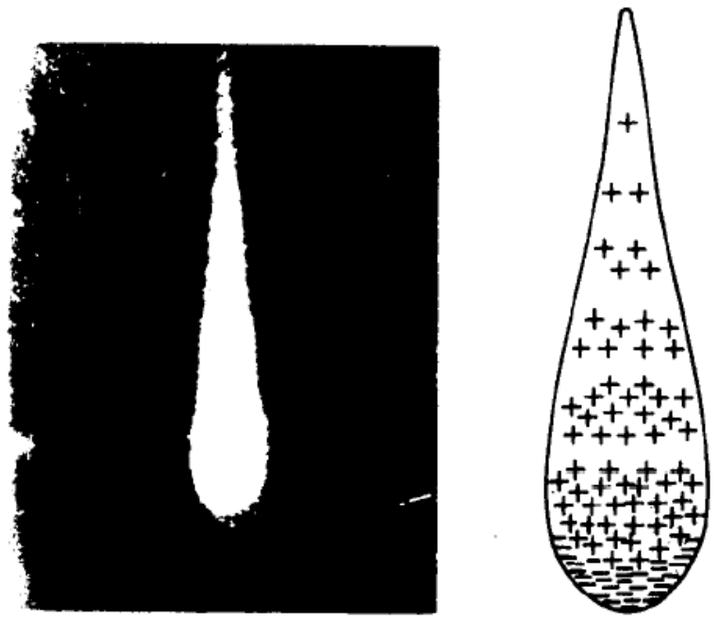

picture taken with cloud chamber

- due to transverse diffusion a droplet like avalanche develops around the anode
- electrons are collected very fast (≈ 1 ns)
  mobility of electrons ≈1000 times larger than for ions
- the cloud of positive ions remains and slowly drifts towards the cathode

Modes of Operation of Gas Detectors

- Ionisation chamber:
  complete charge collection, but no charge amplification.

- Proportional counter:
  above threshold voltage multiplication starts. Detected signal proportional to original ionization → energy measurement (dE/dx) possible. Secondary avalanches have to be quenched. Gain $\approx 10^4$-10^5

- Region of limited proportionality:
  or streamer mode: strong photo emission→ secundary avalanches. Needs efficient quencher or pulsed HV. Gain upto $\approx 10^9$, hence simple electronics sufficient.

- Geiger-Müller counter:
  massive photo emission. Full length of anode wire affected. Stop discharge by HV break down. Strong quenchers needed.

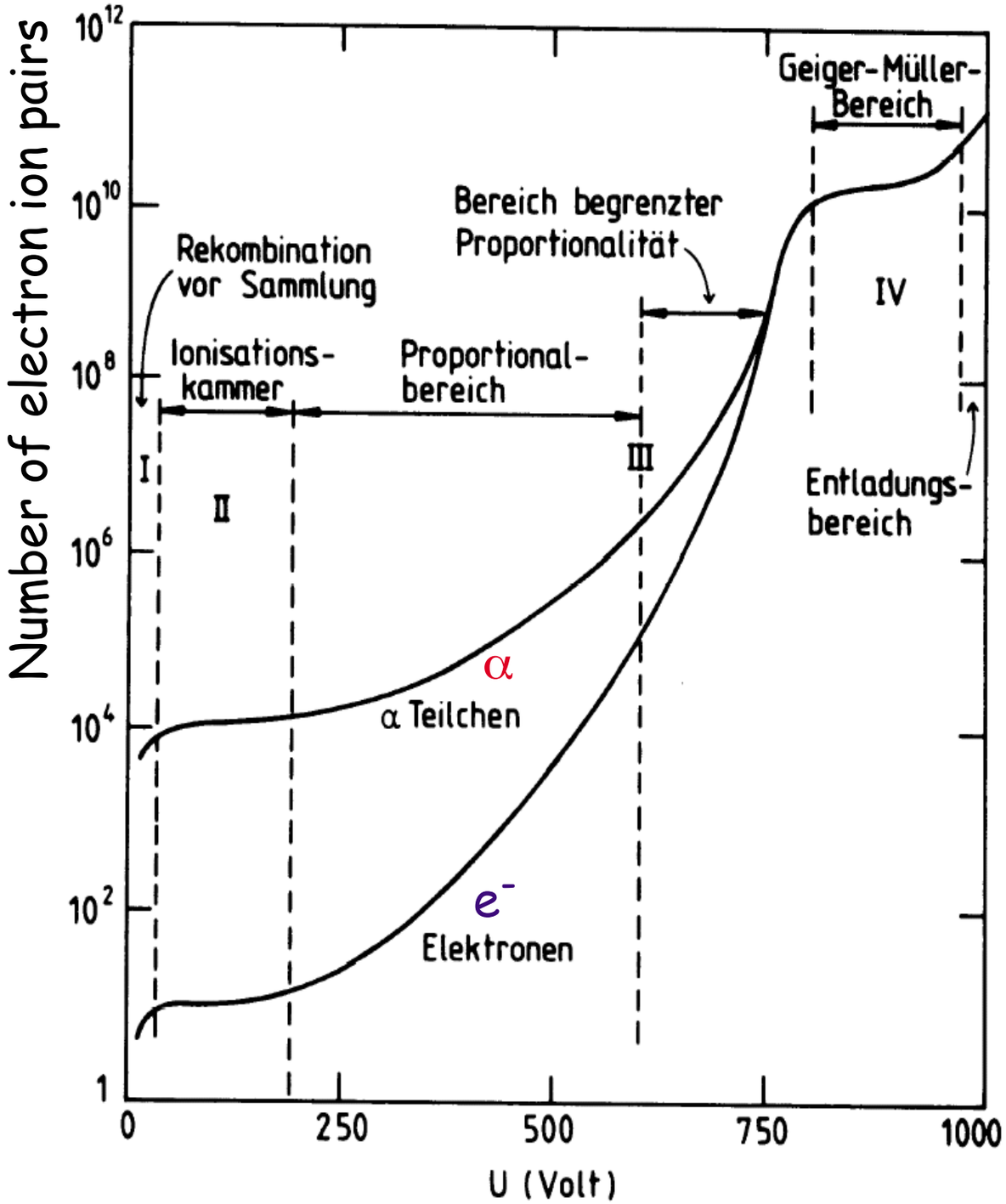

Family Tree of Gaseous Detectors

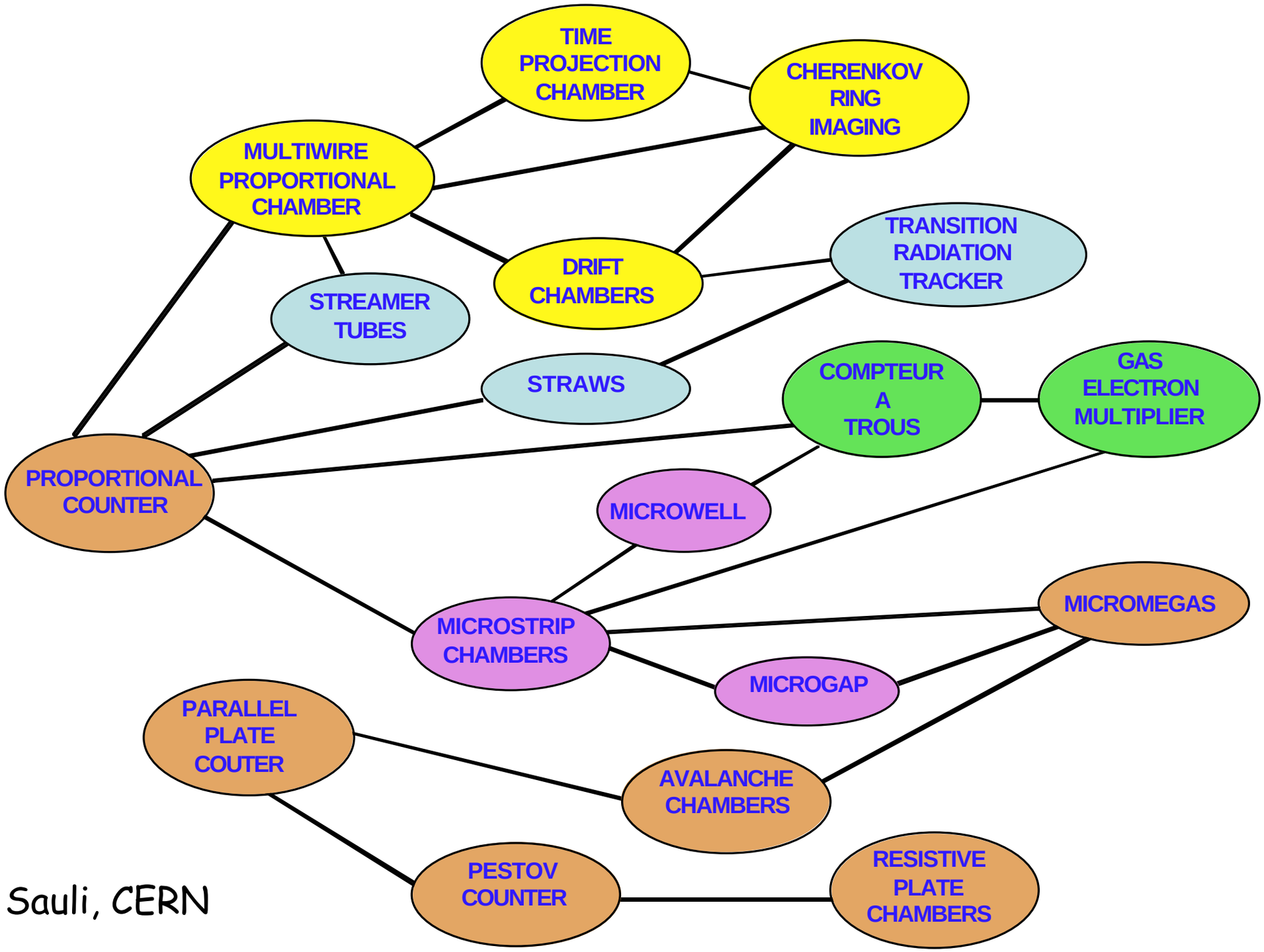

Fabio Sauli, CERN

Multi Wire Proportional Chamber

Generalize principal of proportional tube to large area detector.

Multi Wire Proportional Chamber: MWPC

George Charpak 1968

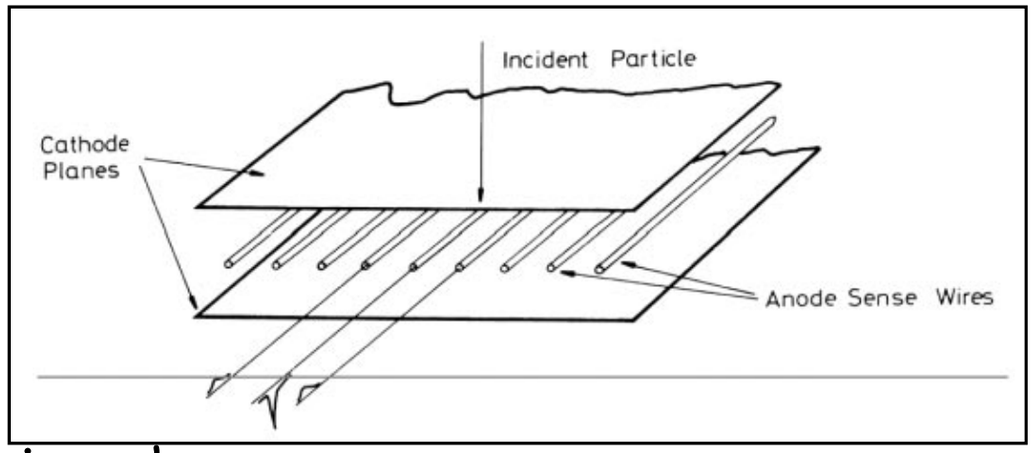

- anode wires act as independent detectors

- capacitive coupling of negative signal from anode wire where avalanche is formed to neighbours is small compared to pulse, which is generated by ions drifting towards cathode

- furthermore development in electronics: possibility to read many channels in parallel → 10^6 tracks per second

  ⇒ Breakthrough in detector development

Nobelprize for physics 1992

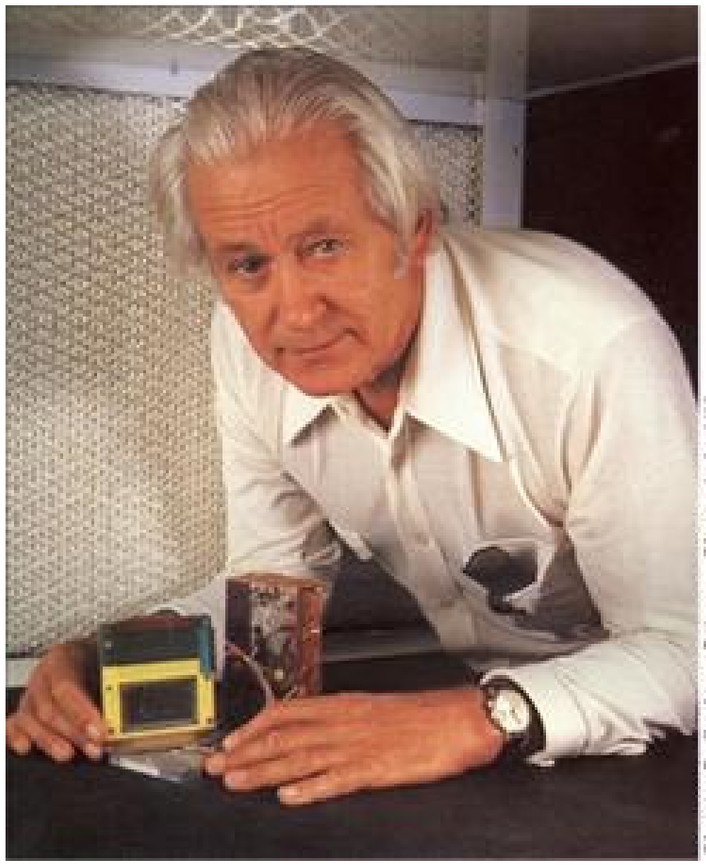

MWPC

Use of gold plated tungsten wires with diameter 15-30μm as anode wires. Chamber walls made from glas fiber material (rigid, low mass). Thin metal foil acting as cathode (typically d≈50μm). Typical dimensions: d = 2mm, L = 4mm.

Electrostatic potential in a planar MWPC given by:

$$V(x,y) = -\frac{q}{4\pi\varepsilon_0}\ln\left\{4\left[\sin^2\left(\frac{\pi x}{d}\right) + \sinh^2\left(\frac{\pi y}{d}\right)\right]\right\}$$

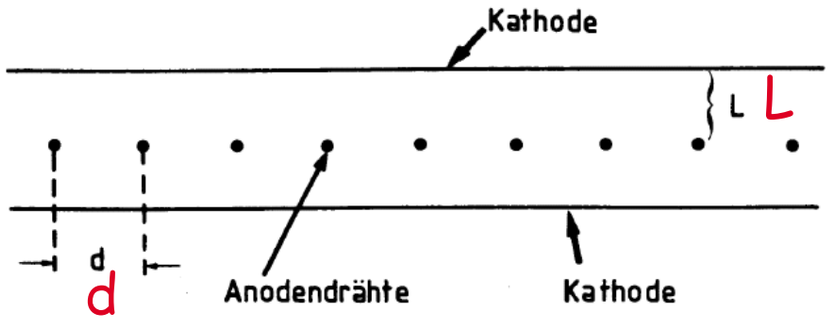

resolution $\sigma = d/\sqrt{12}$

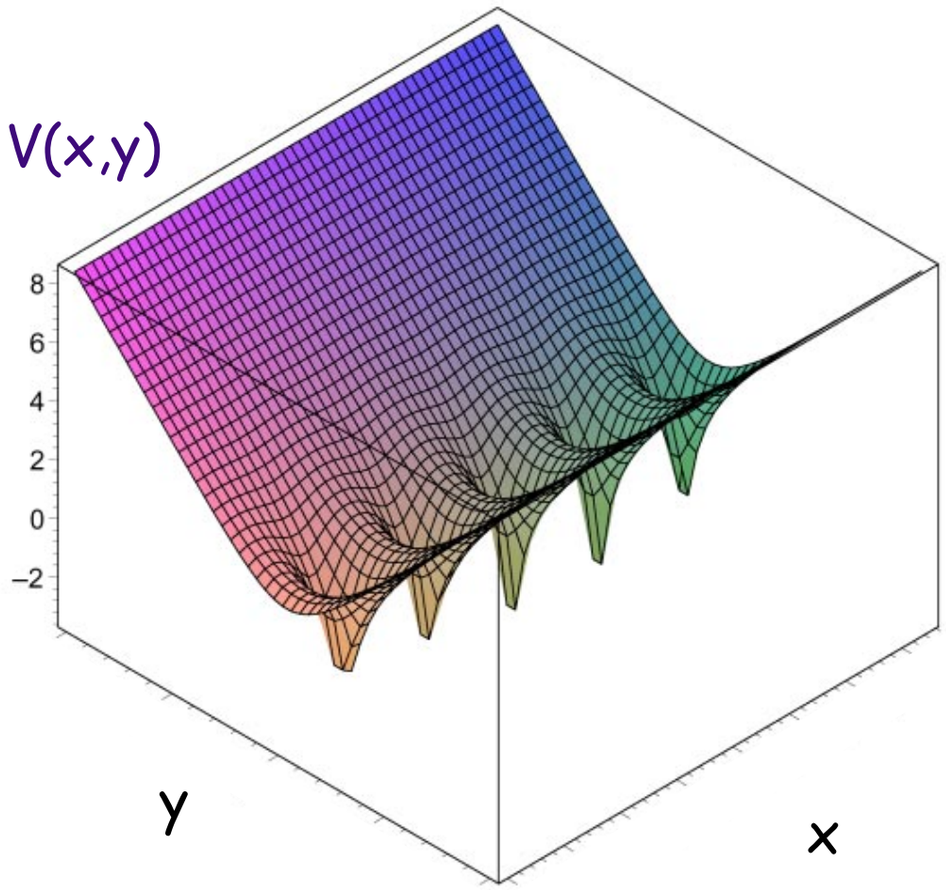

electric field lines

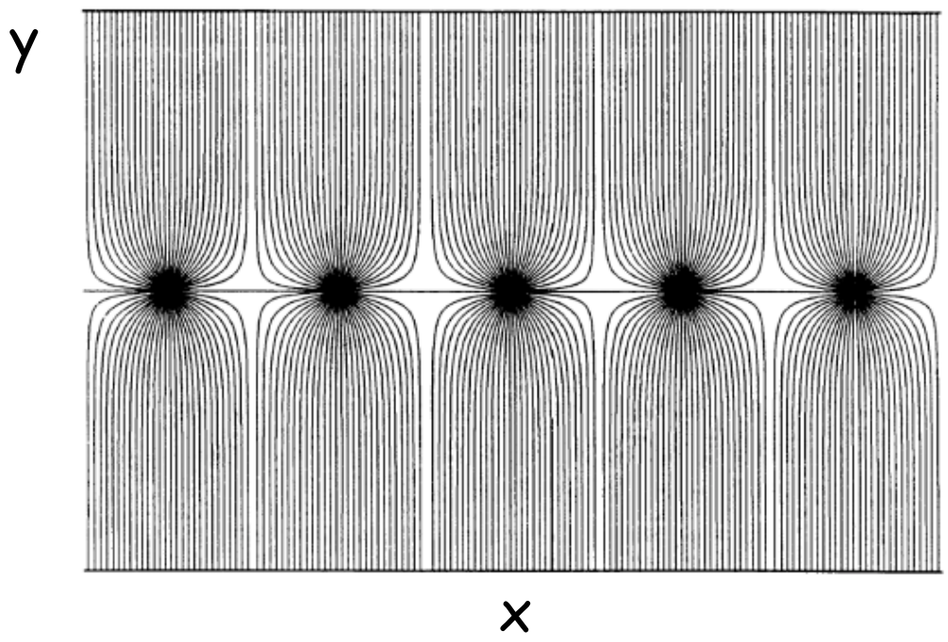

Signals in a MWPC

Using suitable electronics the avalanches caused by single ionization cluster can be made visible with an oscilloscope

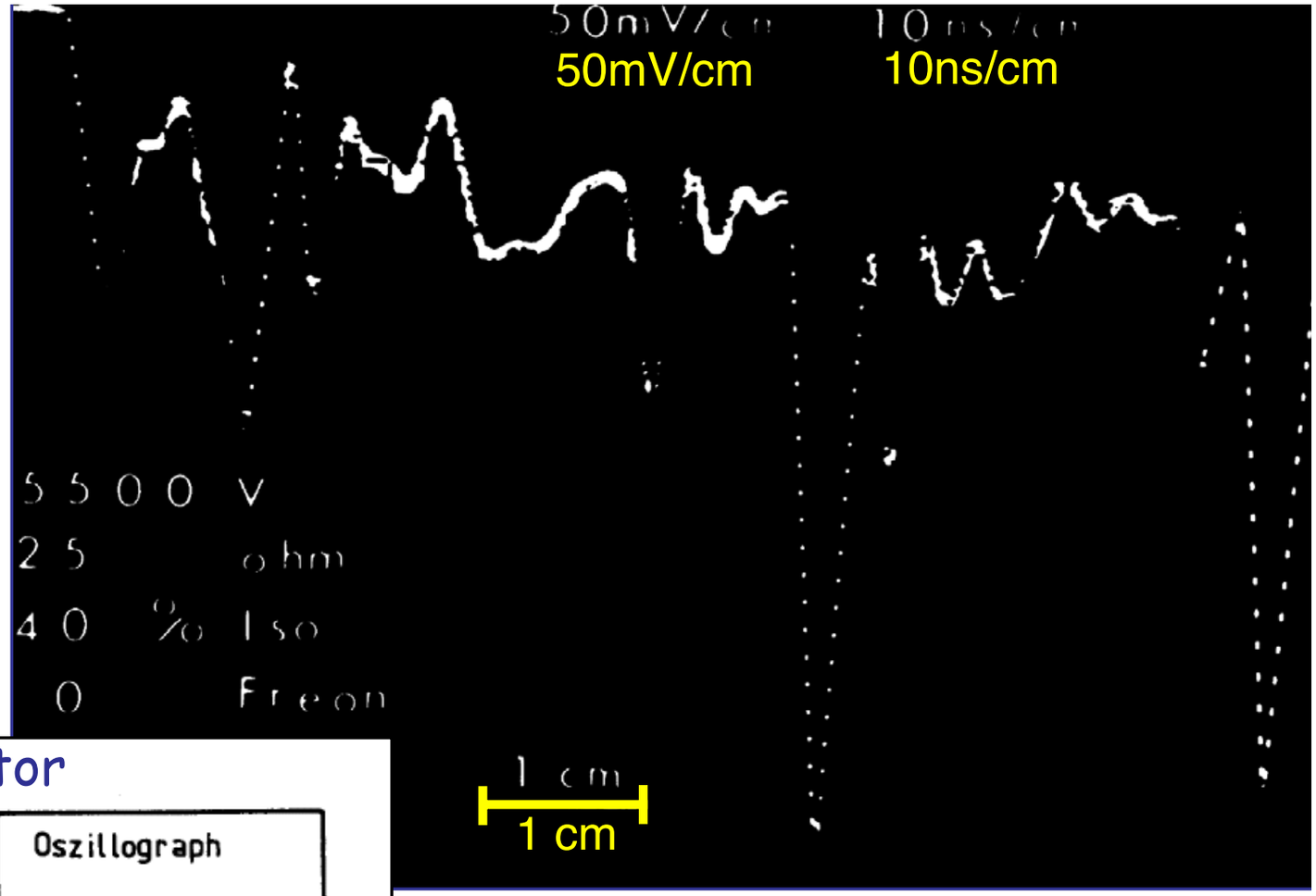

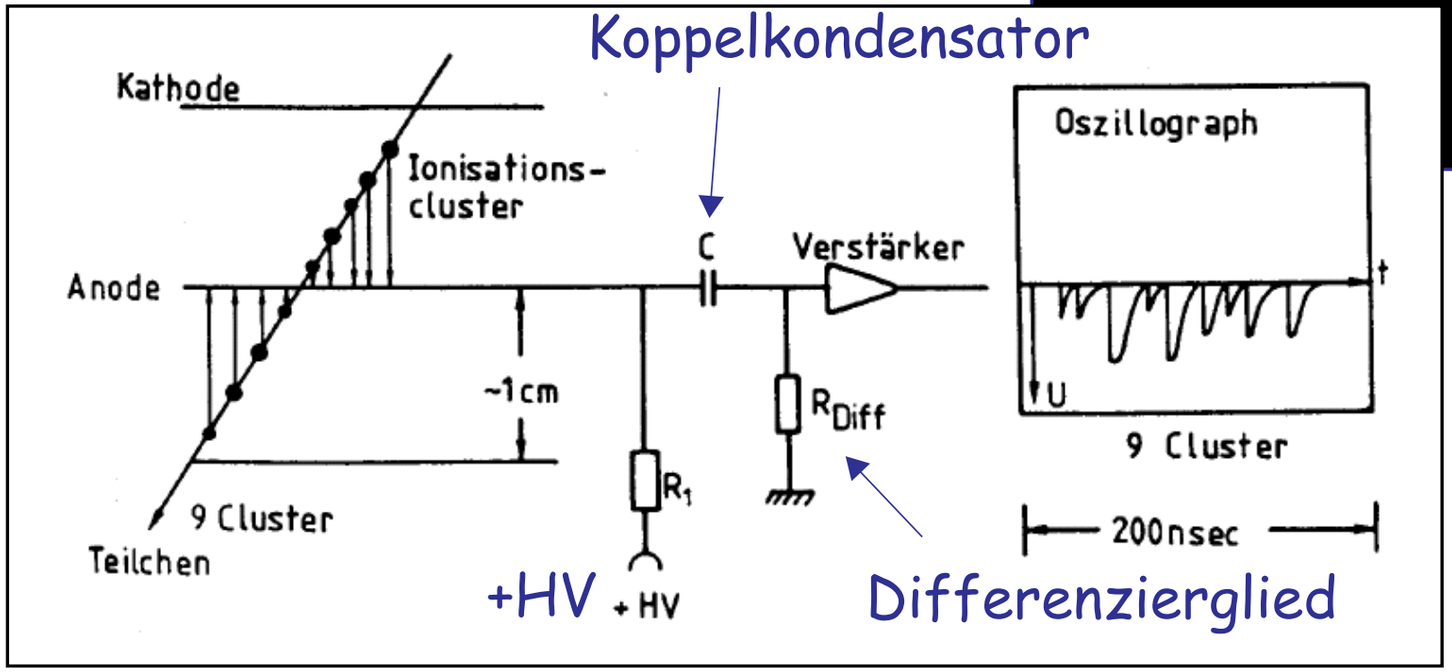

Plateau Curve

Readout of MWPCs is typical digital, i.e. all signals surpassing a given threshold are recorded.

The detection efficiency then depends on:

- applied high voltage
- threshold value
- selected duration of time window

=> chose HV so, that ≈ all signals are above threshold. i.e. $\varepsilon \approx 100\%$, but no continuos discharge anywhere in the detector

Ionisationen/cm 1/λ Dicke für 99% Effizienz: 4.6λ

	Encounters/cm	t_{99}(mm)	Free electrons/cm
He	5	9.2	16
Ne	12	3.8	42
Ar	25	1.8	103
Xe	46	1.0	340
CH_4	27	1.7	62
CO_2	35	1.3	107
C_2H_6	43	1.1	113

The actual choice of parameters depends on:

- level of noise
- sensitivity of electronics
- required time resolution

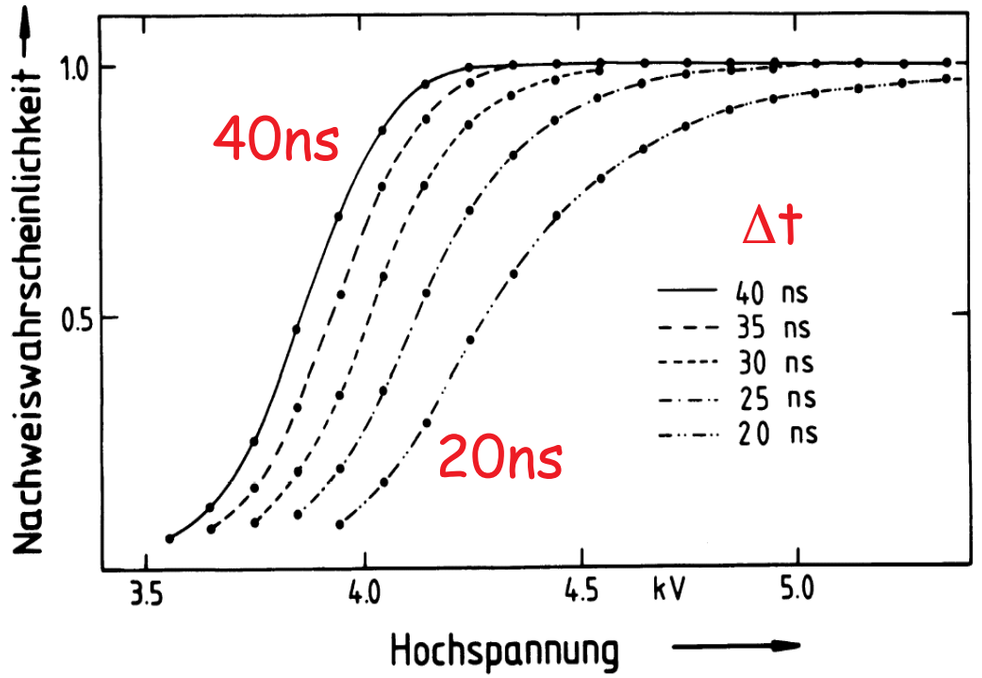

Mechanical Considerations

- Requirements on mechanical tolerances for stable operation are quite high
  - the gas gain M depends on variations of anode diameter a and gap size L

    $\frac{\Delta M}{M} \approx 3\frac{\Delta a}{a}$ resp. $\frac{\Delta M}{M} \approx 12\frac{\Delta L}{L}$ => effective shortening of plateau due to gap variations

- For digital readout the resolution perpendicular to wire directions is: $\sigma(x) = d/\sqrt{12}$

- Wire length and wire spacing can only be changed within certain limits

- Wire sagging is caused by forces acting perpendicular to the wires
  - electrostatic deflection
  - gravitation
- Range of stability: $\frac{d}{l} \geq 1.5 \times 10^{-3} V[kV]\sqrt{\frac{20}{T[g]}}$ with wire length l, high voltage V and wire tension T

  longer wires have to be mechanically supported (fixed), which however causes local inefficiencies

Pros and Cons of MWPCs

- Advantages
  - relatively easy to equip large areas
  - planar and cylindrical geometries can be realized
  - simple coordinate reconstruction using digital readout
  - good rate capability
  - operation in magnetic field without problem (small drift distances)
  - fast signal (t≈20-50 ns)

    => can be used for triggering

- Disadvantages
  - limited position resolution $\sigma(x) = d/\sqrt{12}$

    i.e. typically ≈ 0.5-1 mm
  - large tracking volumes need a large number of readout channels
  - => not suited for optimal momentum resolution
  - for very high rates gain loss due to space charge effects

Principal of a Driftchamber

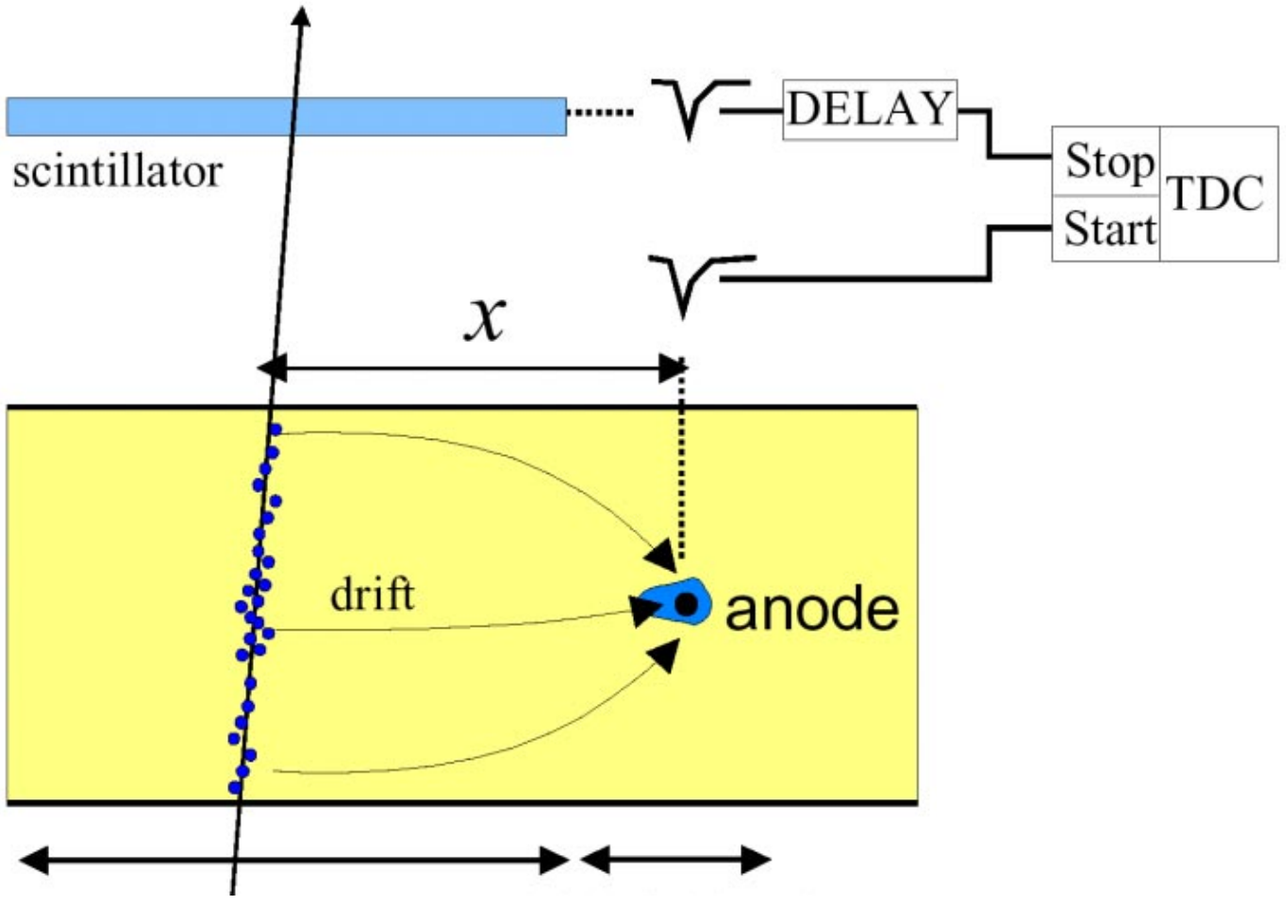

E-field small — drift region

E-field large — gas gain

TDC: Time to Digital Converter

Measure arrival time t_1 of electrons at anode wire relative to reference t_0.

- external definition of time reference t_0 (here by fast scintillator signal)
- x-coordinate given by:

$$x = \int_{t_0}^{t_1} v_D(t)\,dt$$

- if drift velocity v_D constant over full drift distance: $x = v_D(t_1 - t_0) = v_D \Delta t$
- advantage of drift chambers: much larger sensitive volume per read out channel

carsten.niebuhr@desy.de

First Drift Chamber Phys. Inst. Heidelberg 1971

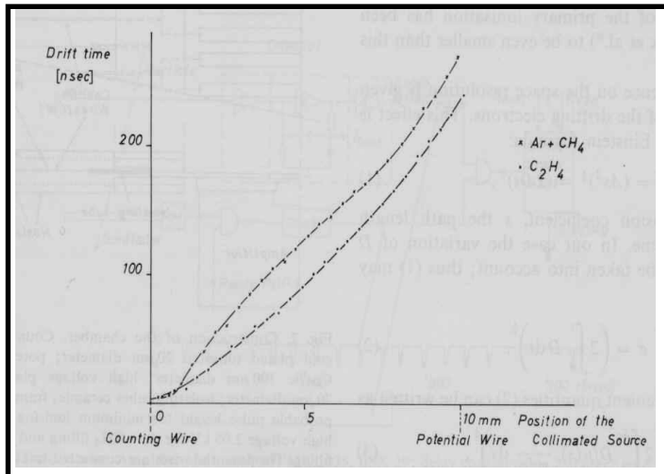

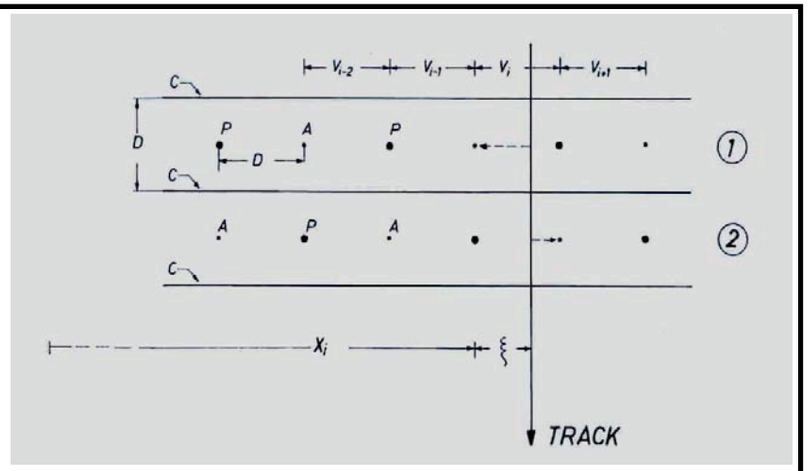

THE MULTIWIRE DRIFT CHAMBER
A NEW TYPE OF PROPORTIONAL WIRE CHAMBER*

A. H. WALENTA, J. HEINTZE and B. SCHÜRLEIN

I. Physikalisches Institut der Universität Heidelberg, Heidelberg, Germany

Received 27 November 1970

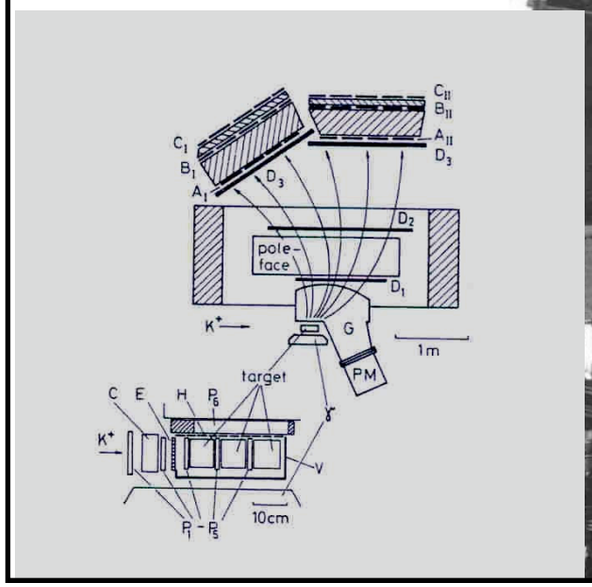

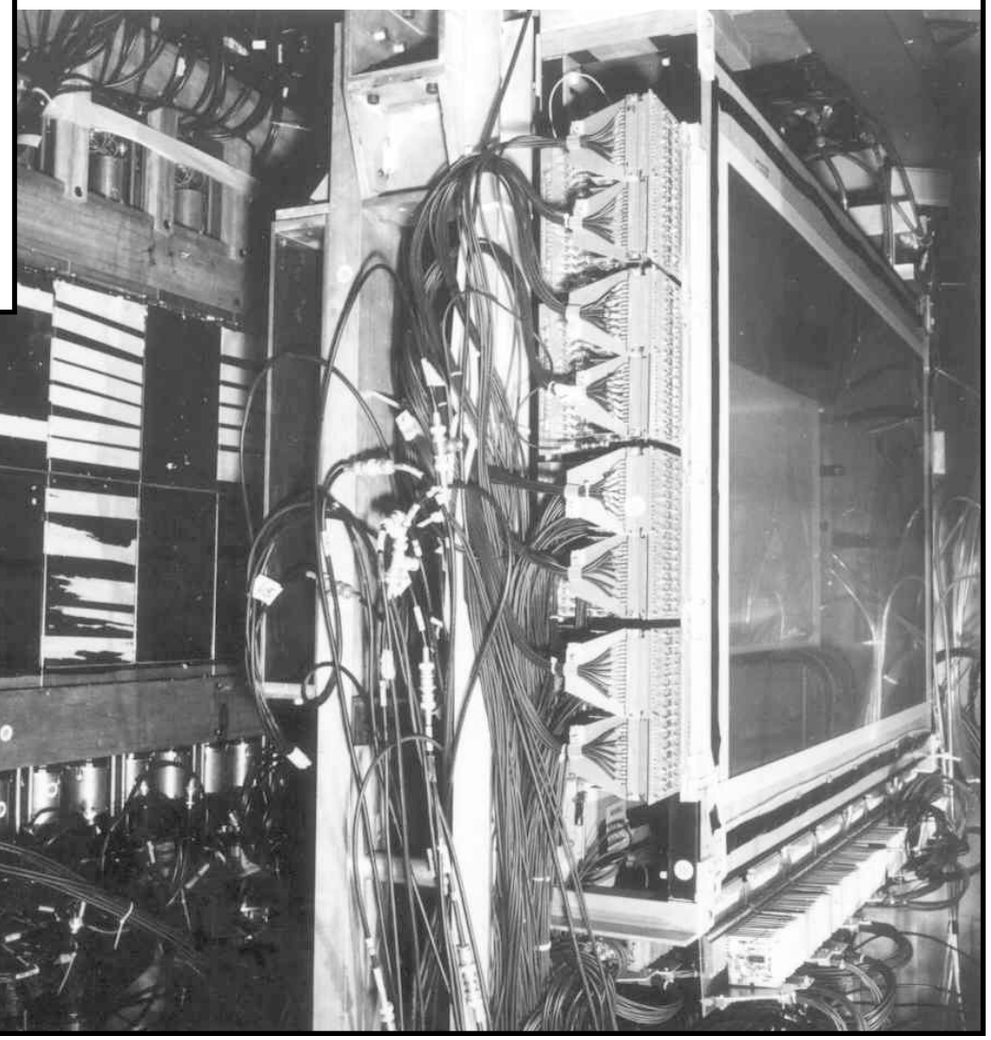

Signal Readout

Since the number of channels in a drift chamber usually does not exceed a few thousands, one can afford more complex readout electronics

In most cases not only time, but also pulse shape is measured.
Advantages:

- better time determination
- measurement of dE/dx possible -> particle identification

Very often so called Flash Analog Digital Converter (FADC) are used

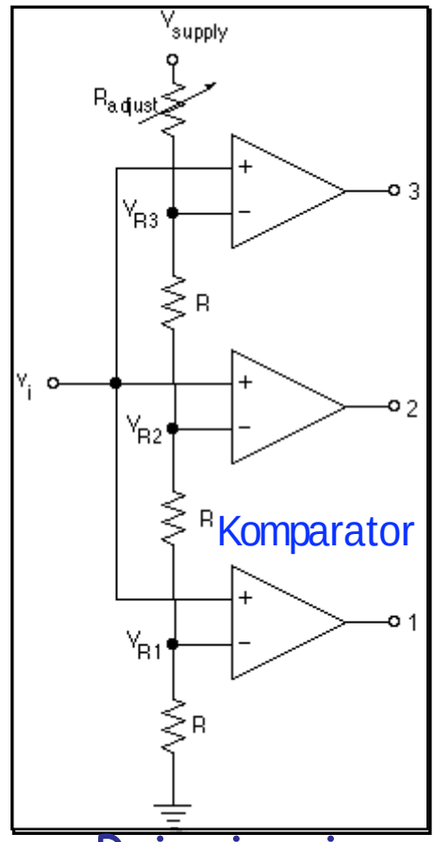

Prinzip eines 4-Bit FADC

Pulsdigitalisierung

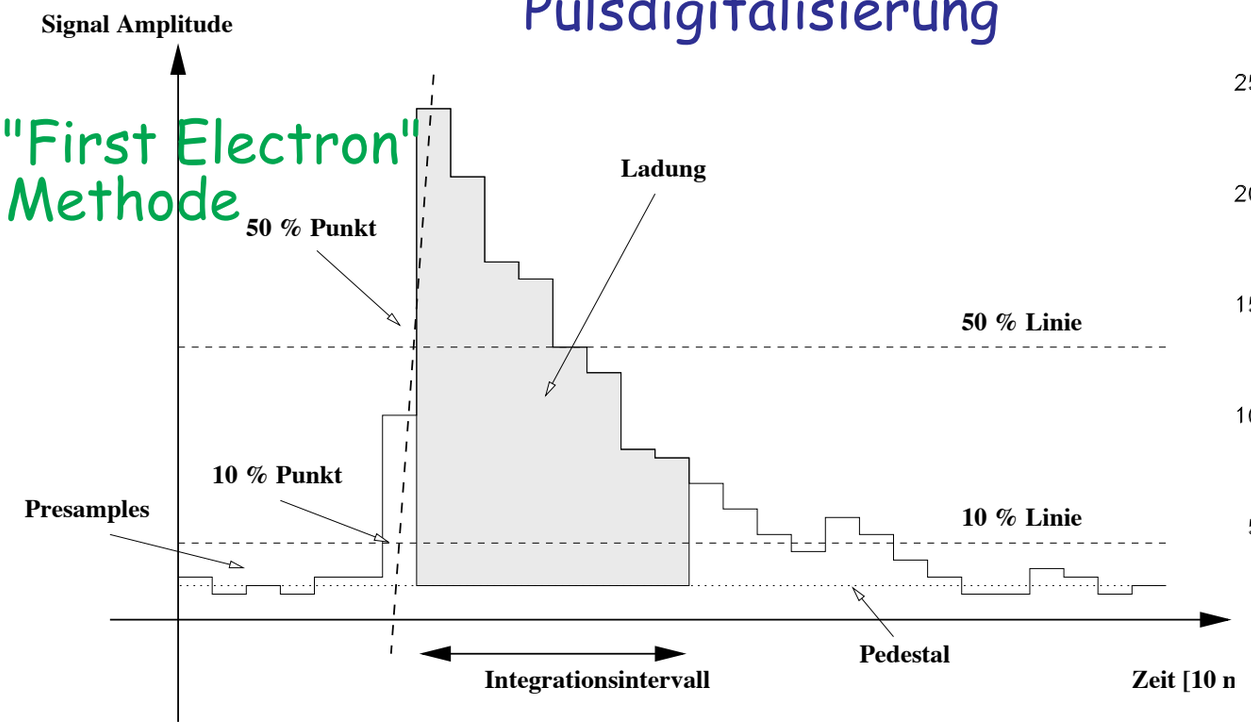

Nichtlineare Kennlinie

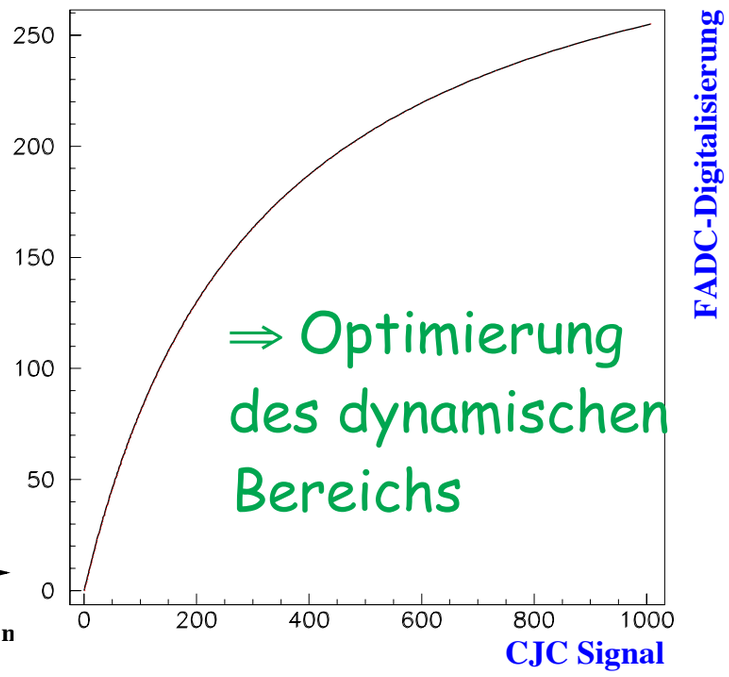

⇒ Optimierung des dynamischen Bereichs

Examples for Planar Cell Geometries

Geometrie

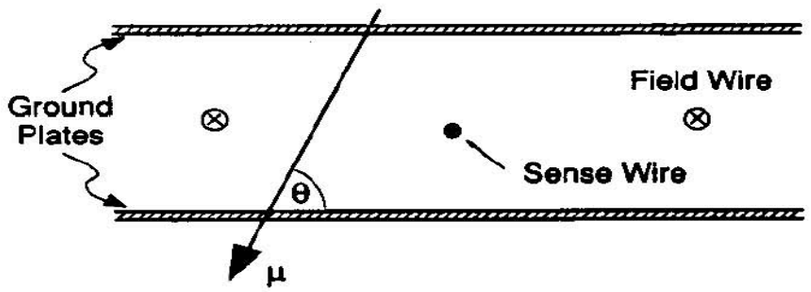

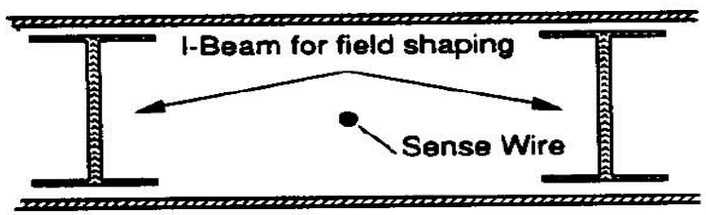

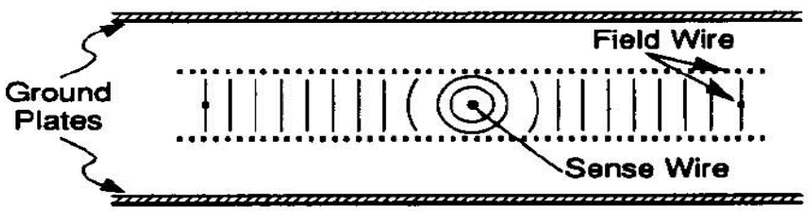

Zellgrösse kann sehr gross gewählt werden

Feldlinienverlauf

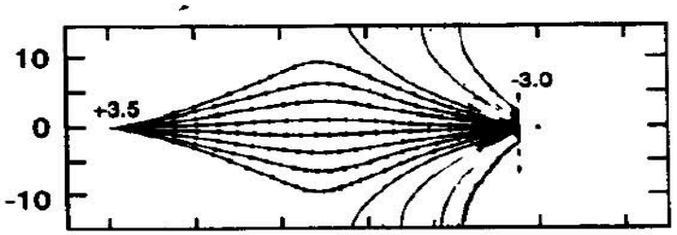

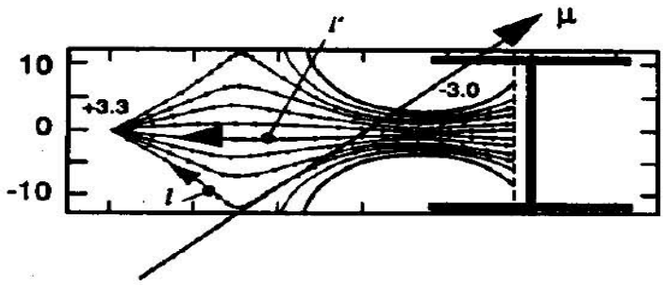

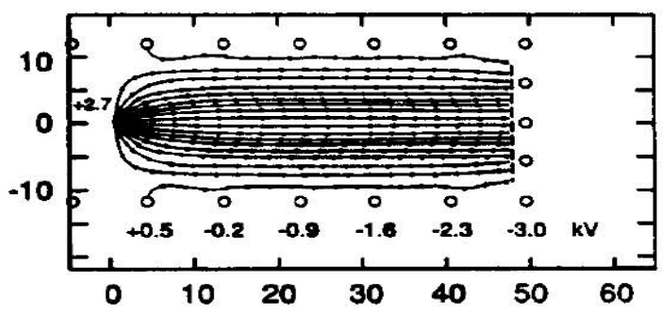

E-Feld

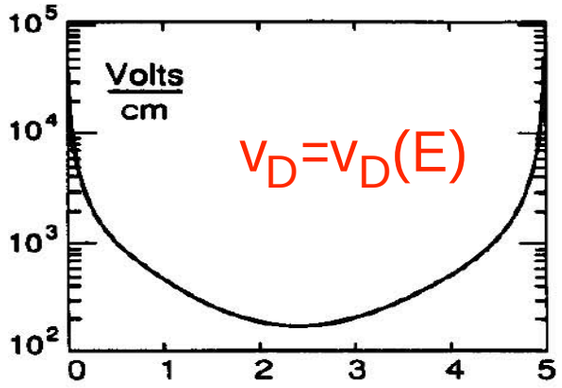

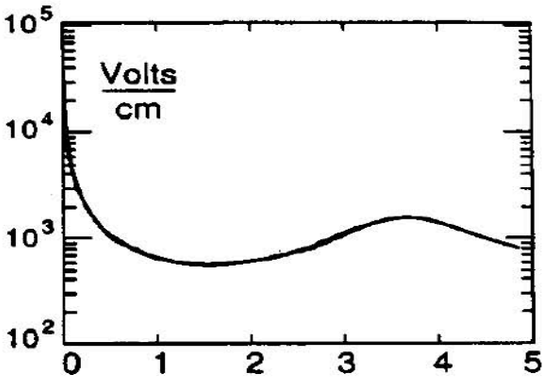

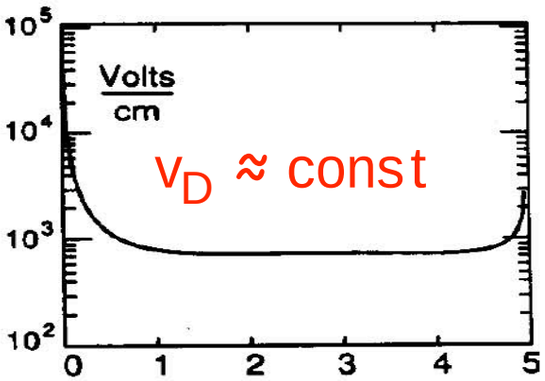

Field Shaping

By suitable choice of geometry and potential of field forming wires one can reach constant E-field within the drift region and therefore constant drift velocity !

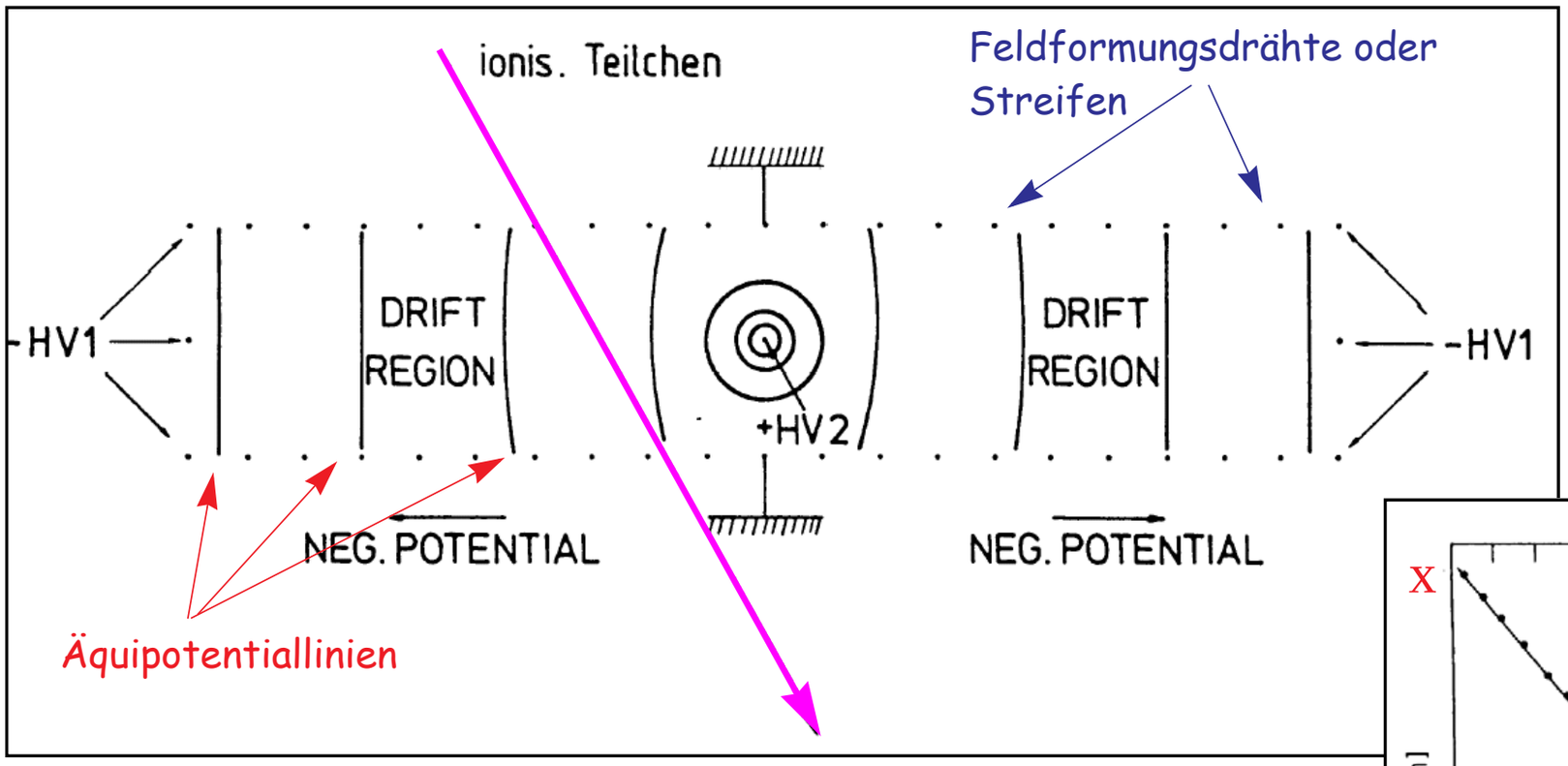

Space - drift time relation

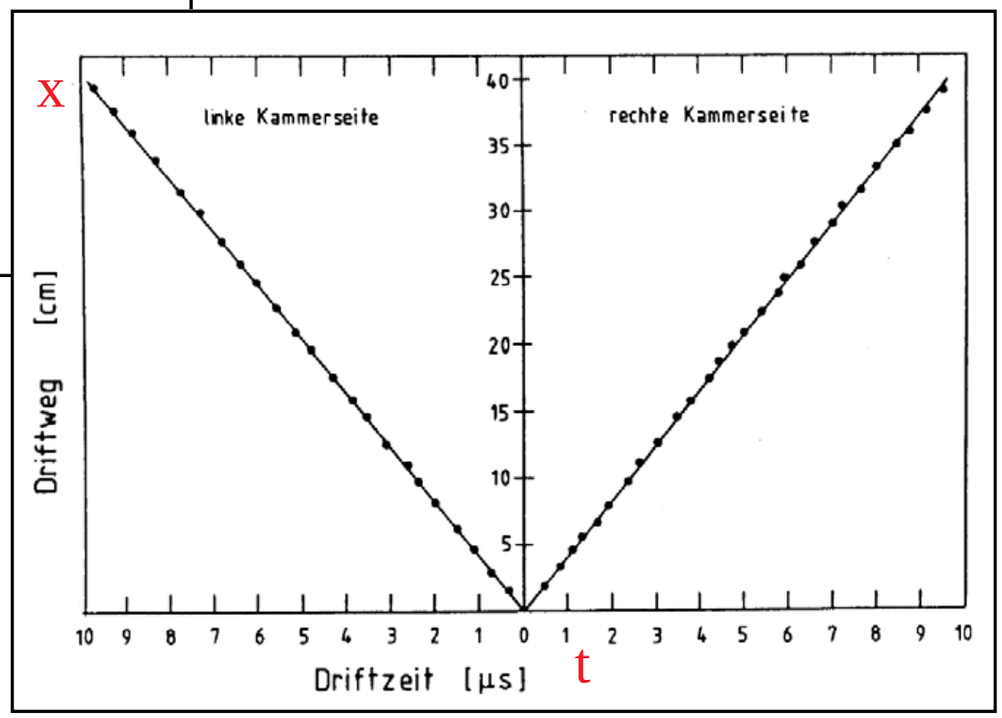

Problem: for a single hit one can not determine on which side of the sense wire the particle passed

=> left-right ambiguity

Examples of Cylindrical Diftchamber Geometries

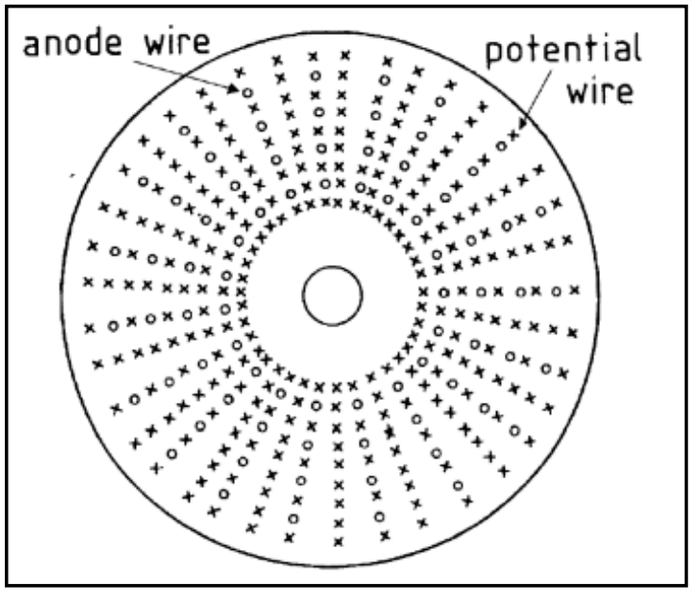

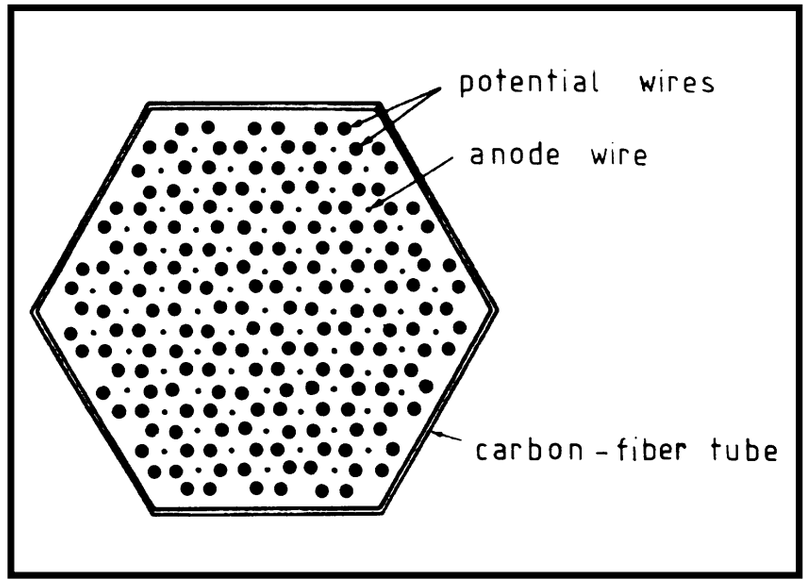

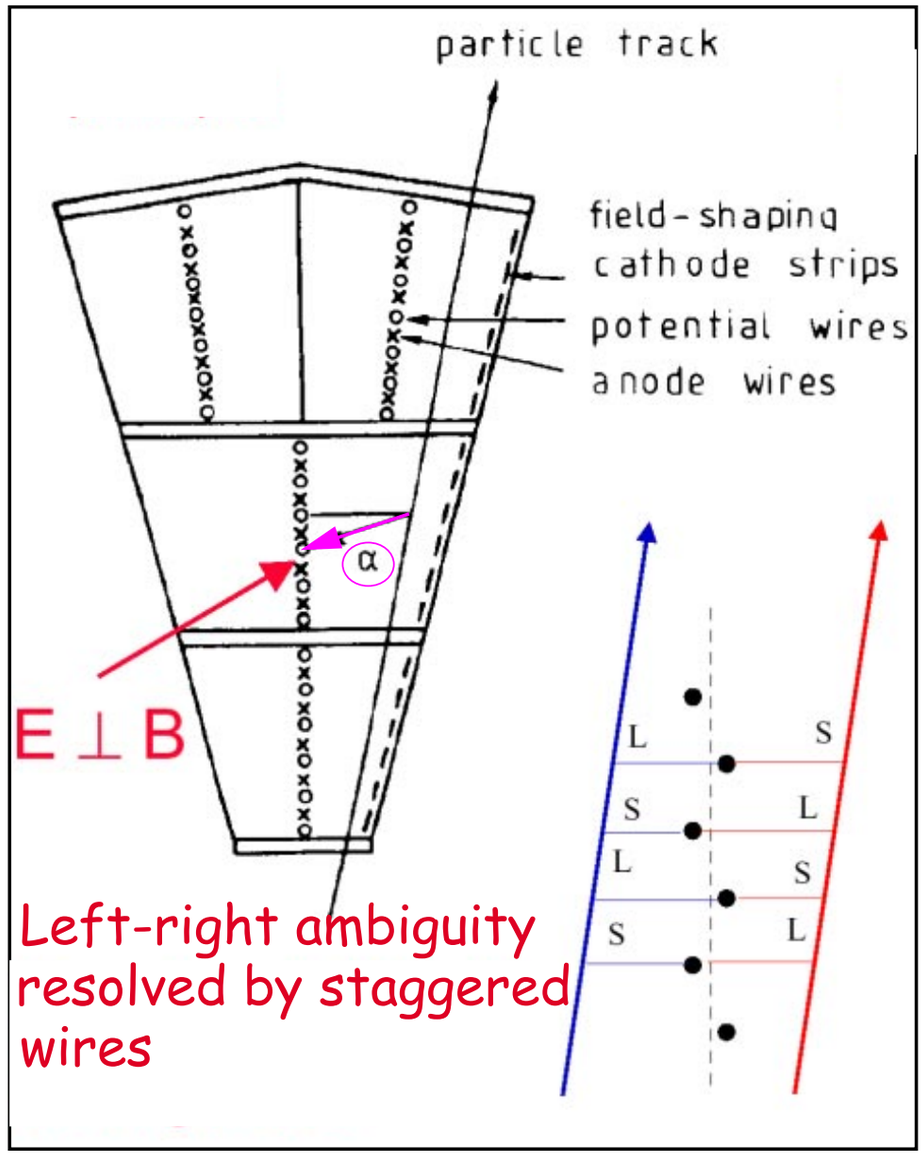

cell of a "jet"-driftchamber

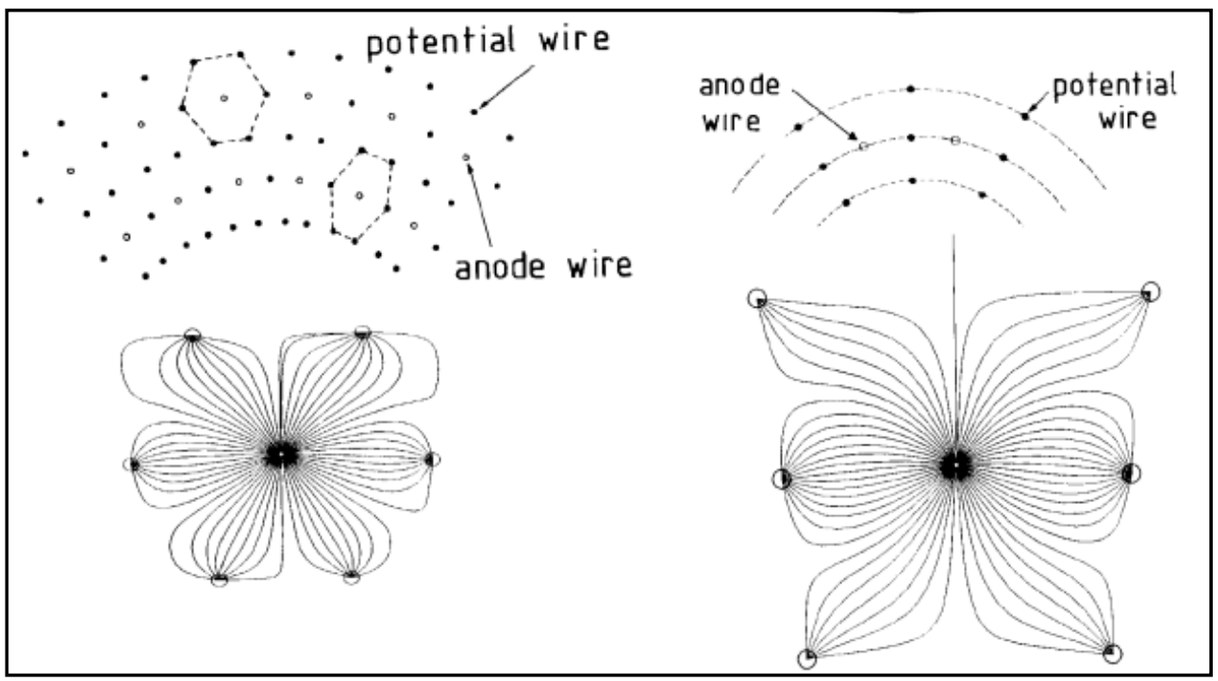

Lorentzangle and Isochrones

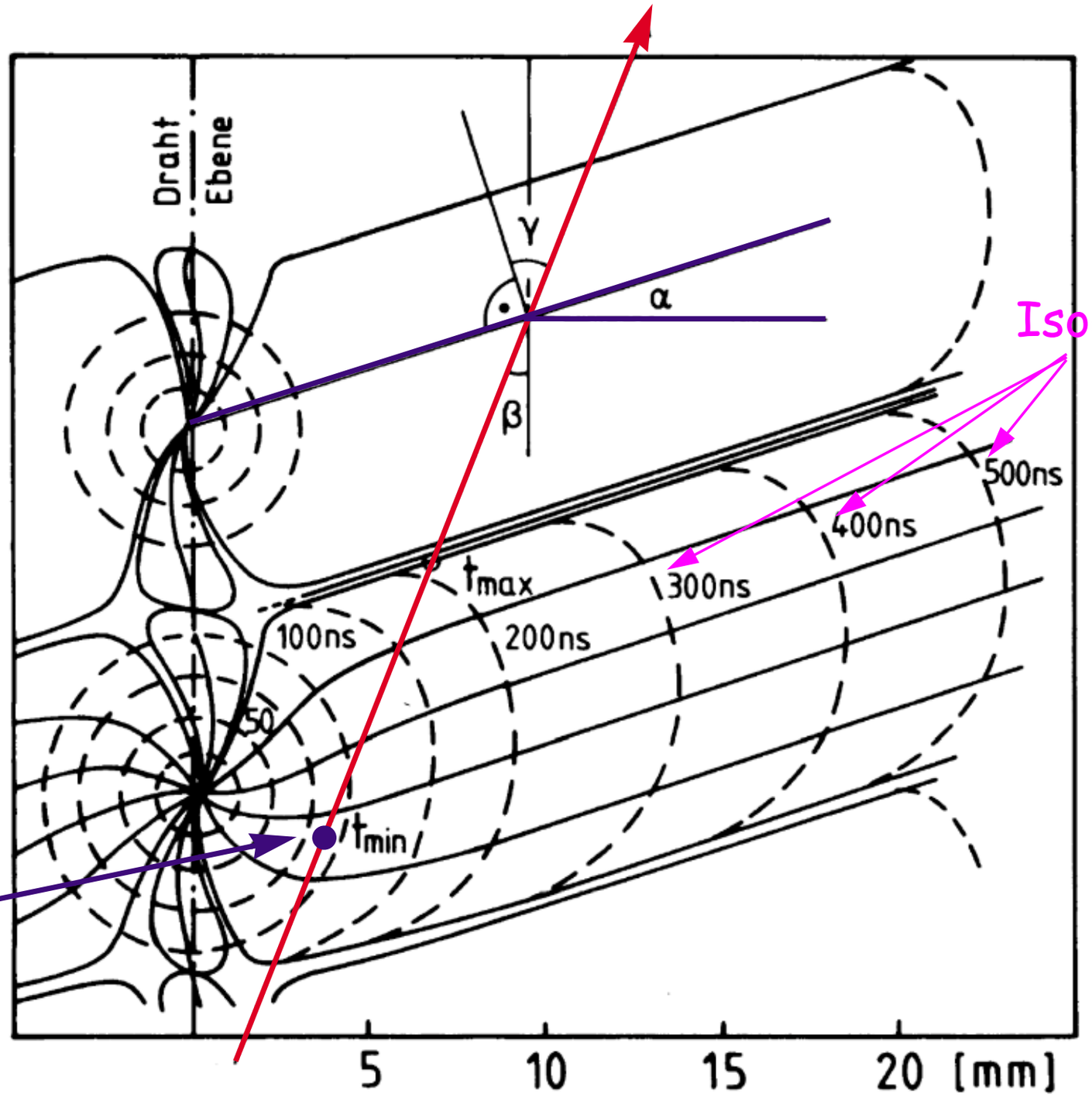

Intrinsic Position Resolution

The intrinsic position resolution is influenced by three effects:

- statistics of primary ionisation: point of origin of primary cluster varies by ≈100μm

- diffusion of electron cloud during it's drift to anode
  - $\sigma = \frac{1}{\sqrt{n}}\sqrt{\frac{2Dx}{\mu E}}$
  - Lorentz effect

- limitations in time resolution of whole chain of electronic signal processing
  - cabel
  - pulse shaping
  - definition of time refernce t_0 etc

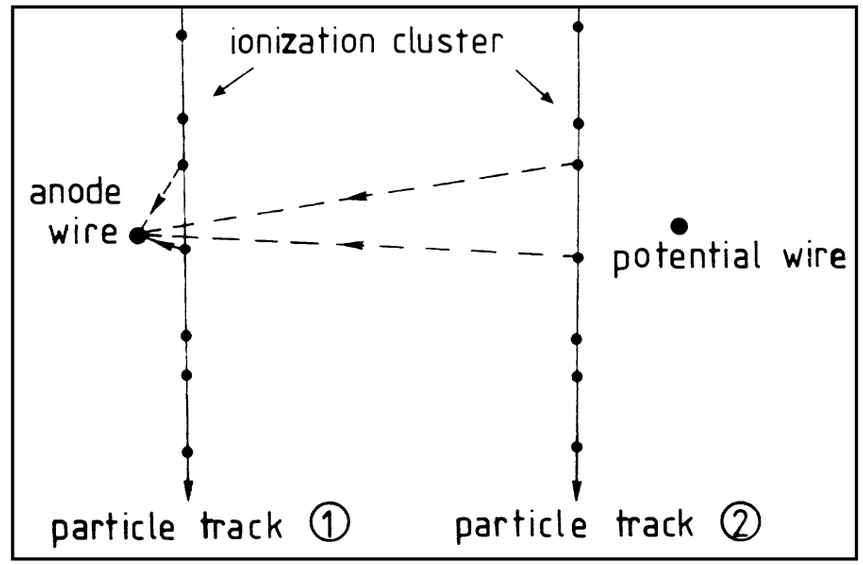

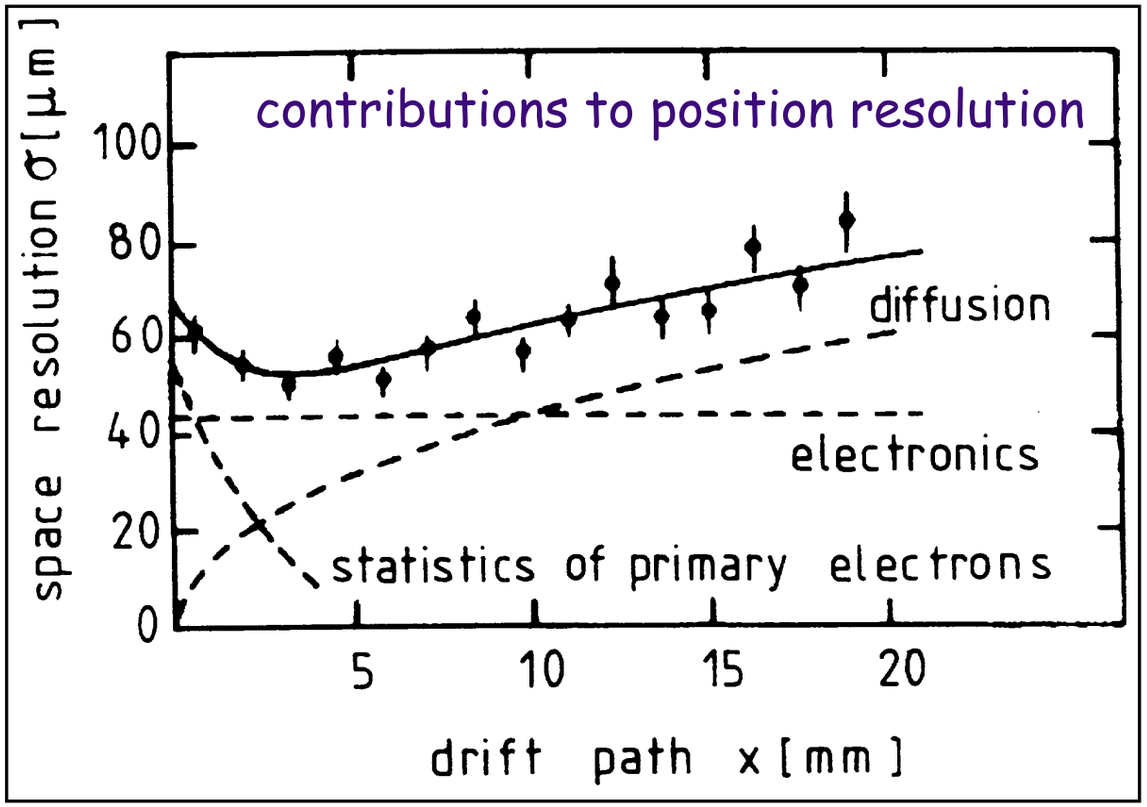

Drift Chambers during Construction

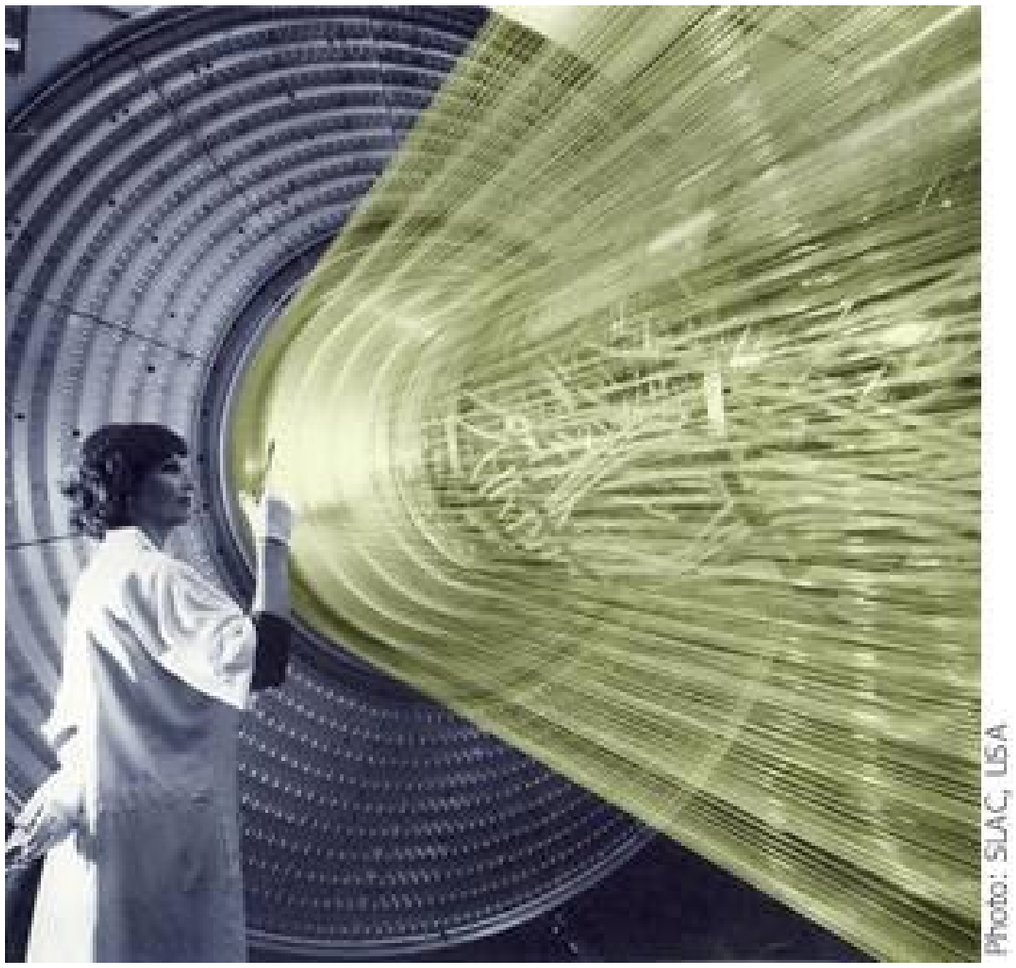

H1 Central Jet Chamber

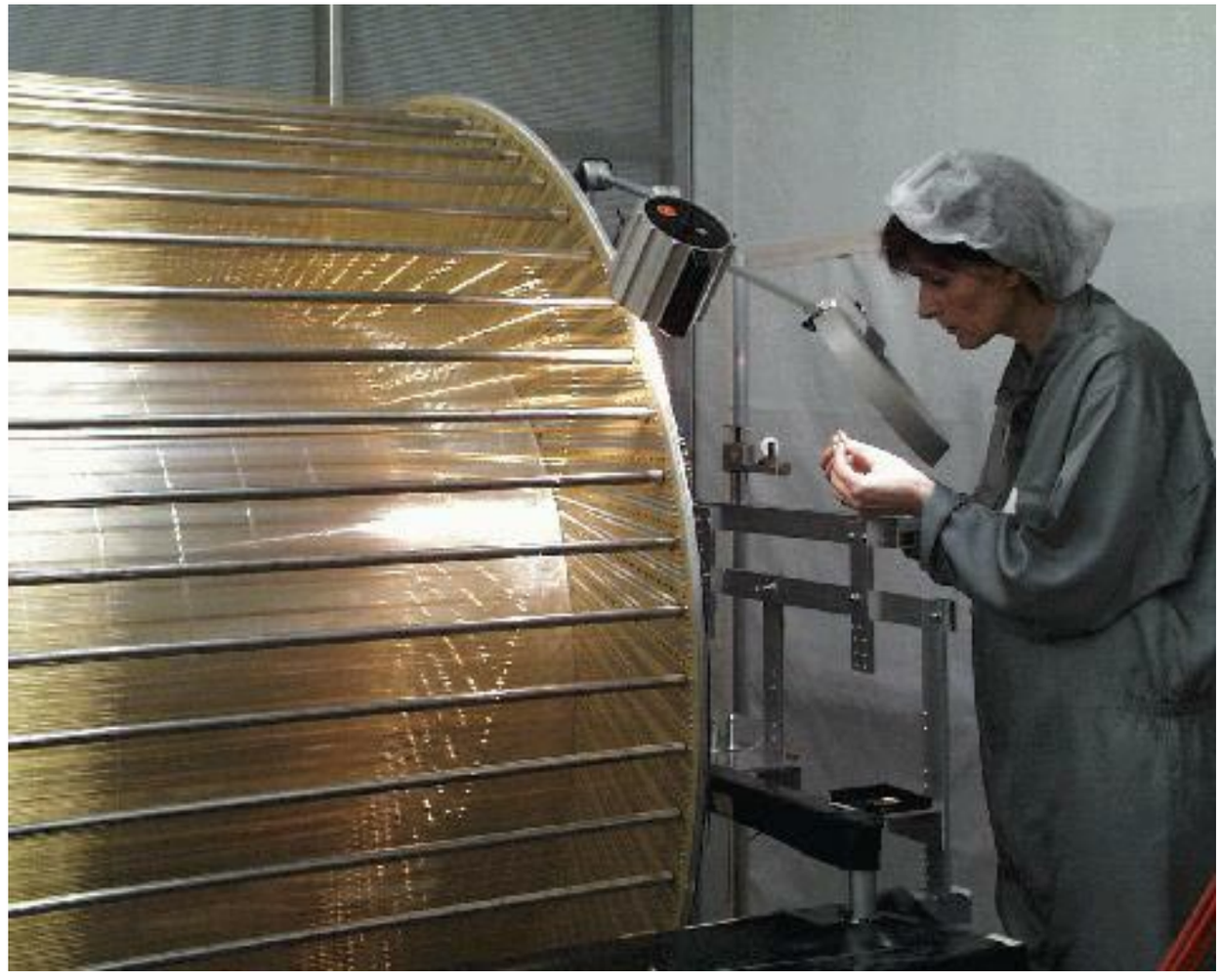

- ≈ 15000 wires
- total force from wire tension ≈ 6 tons

Central Drift Chamber of H1: CJC

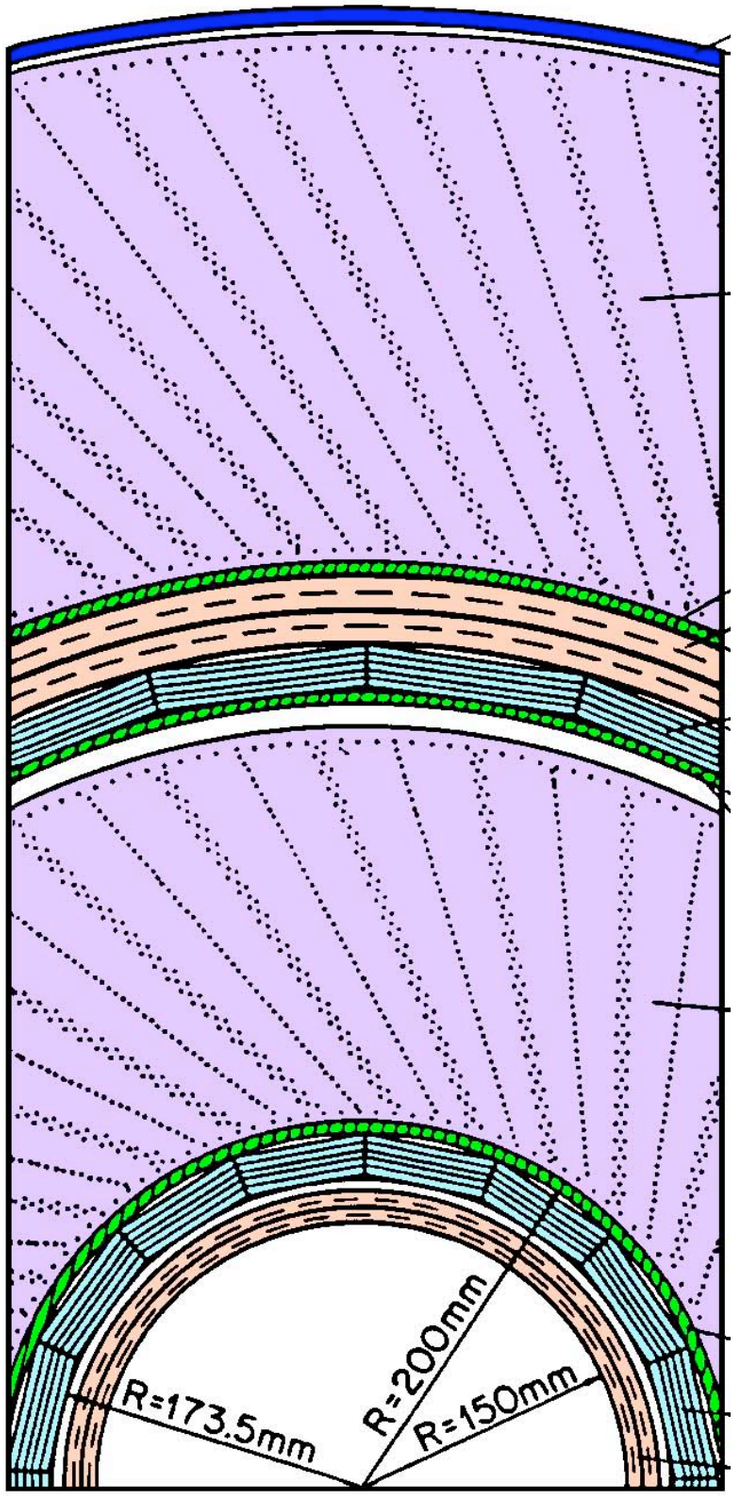

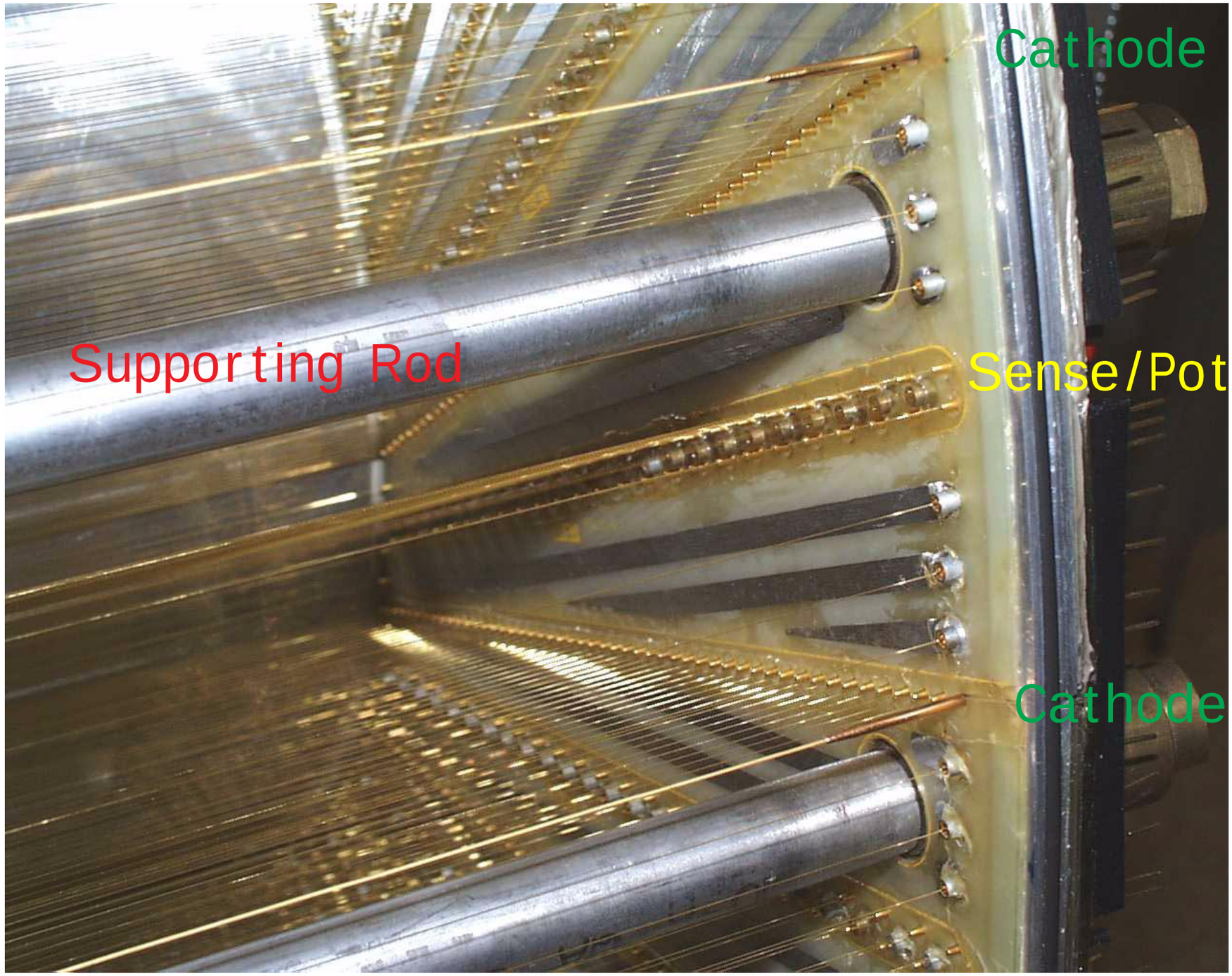

Cells are tilted in order to compensate Lorentzangle

Deviations from the ideal Configuration in CJC2

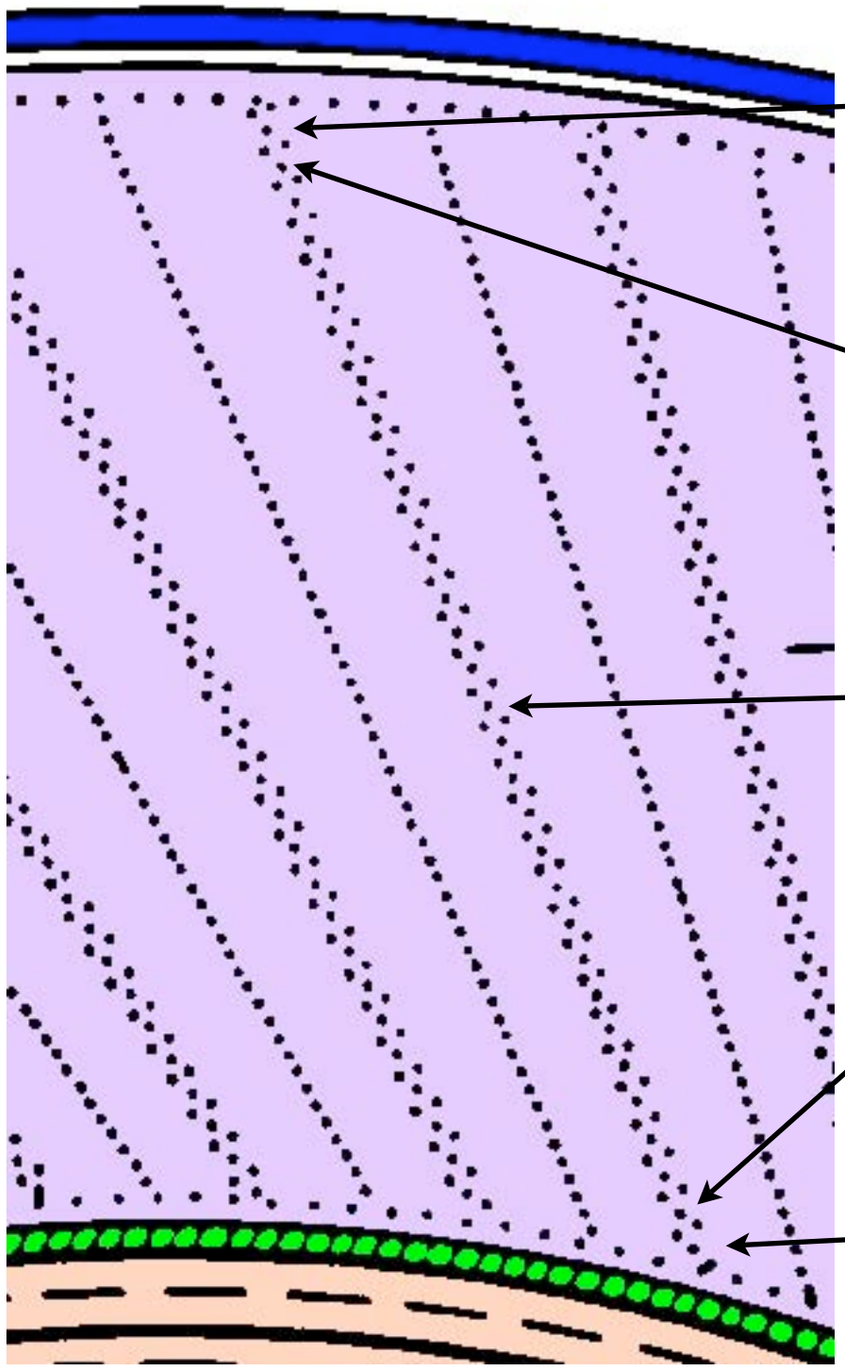

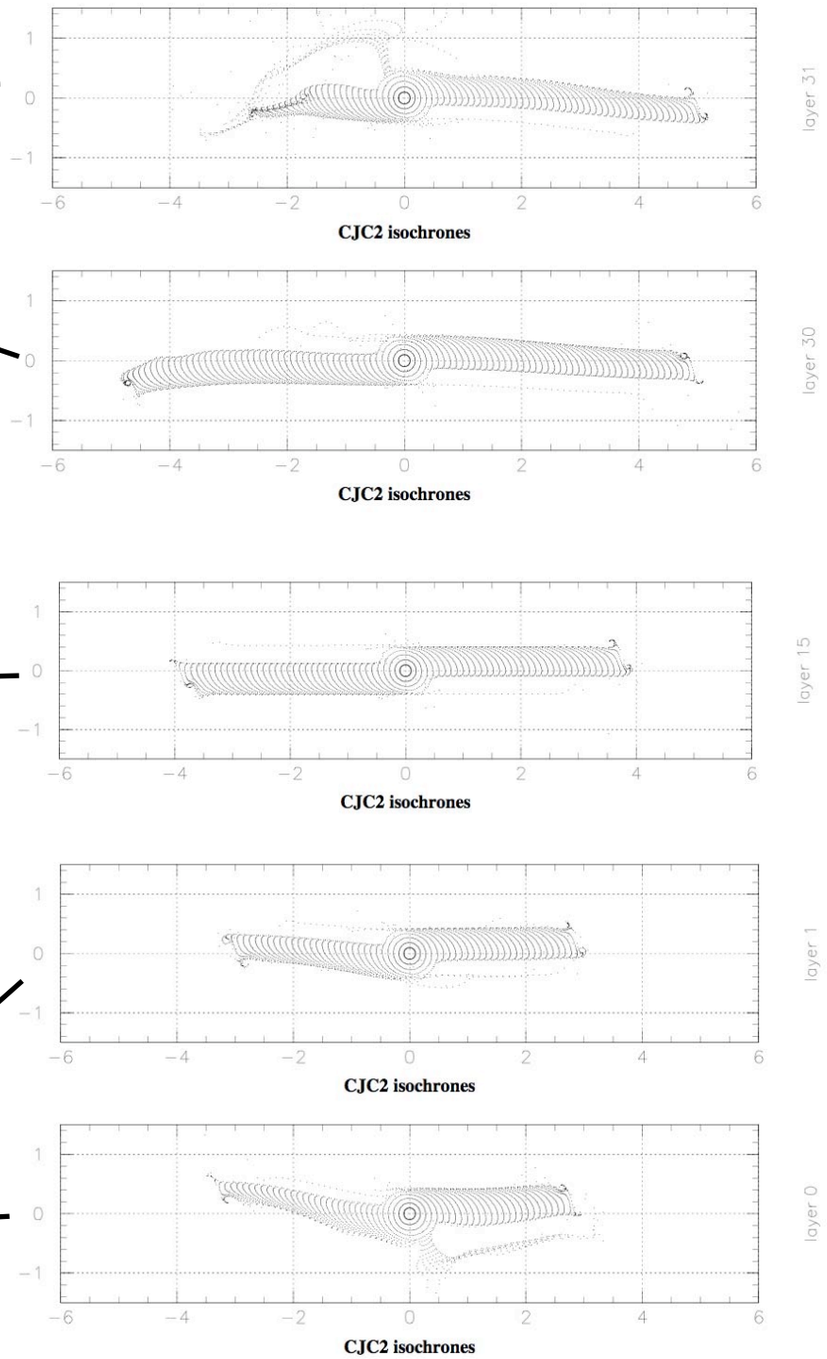

- electrostatic effects at the boundary lead to distortions at small and large radii
- such effects must be taken into account in calibration / reconstruction

Options for Readout of Second Coordinate

Crossed Planes

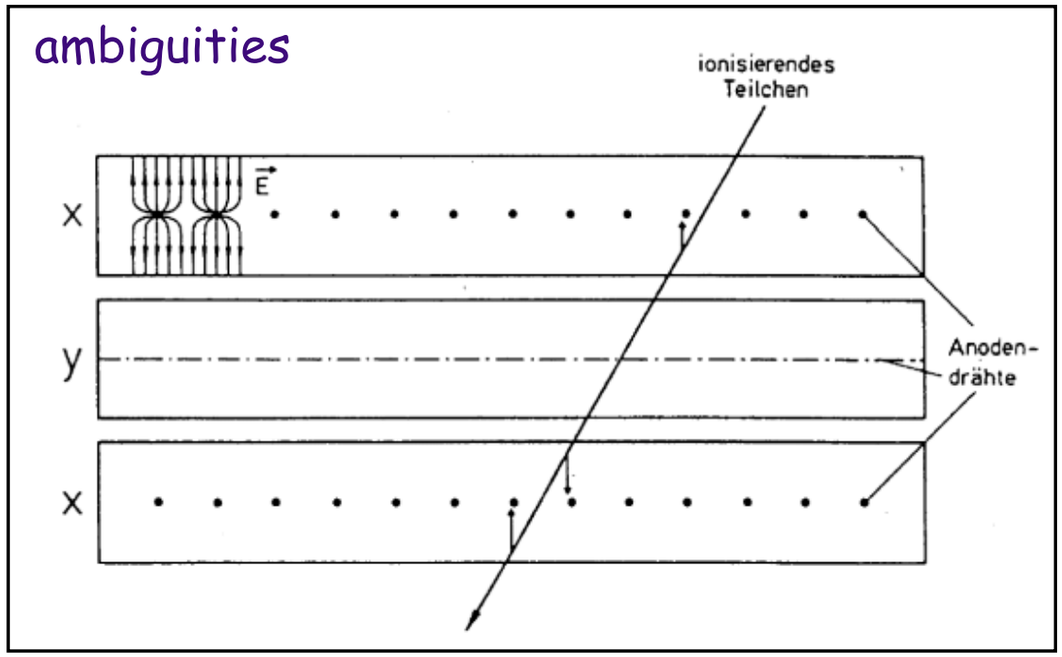

Charge Divison, z-by-timing

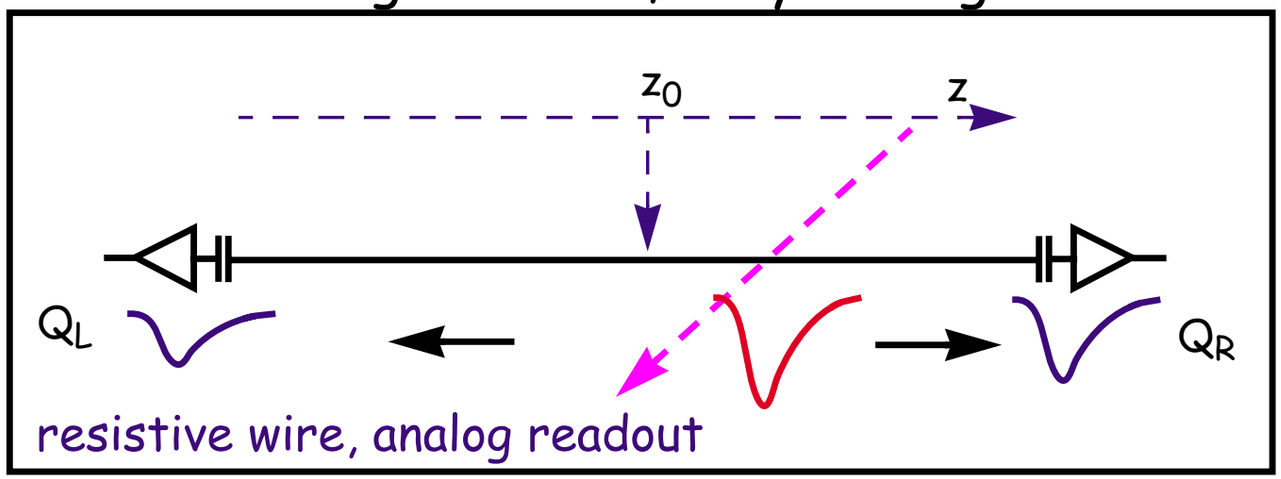

Segmented Cathodes

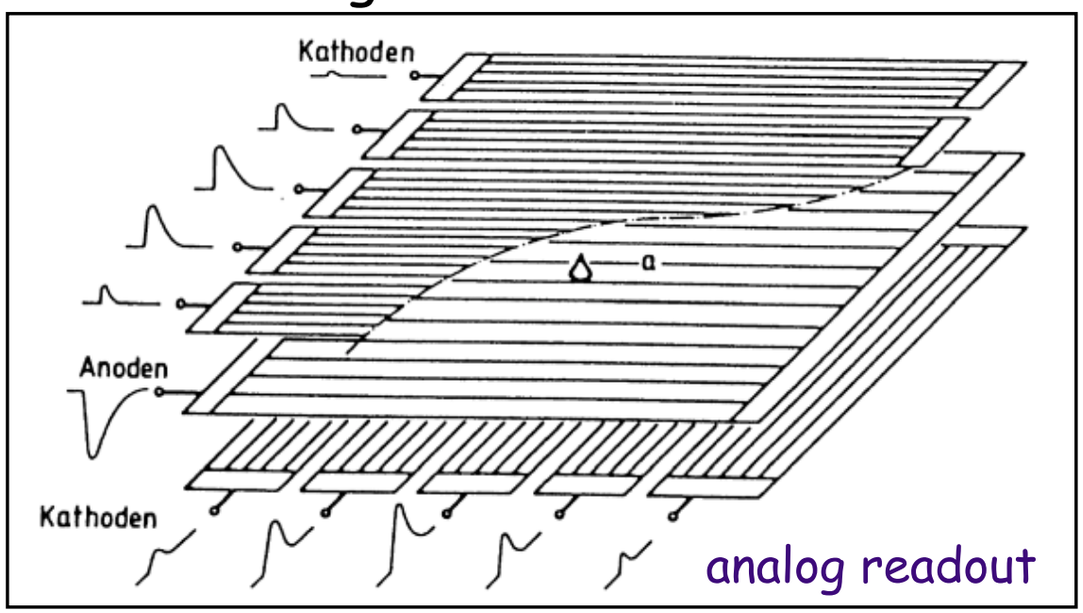

Stereo Wires

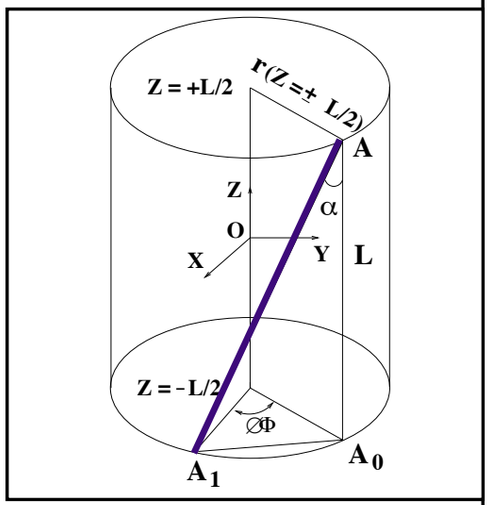

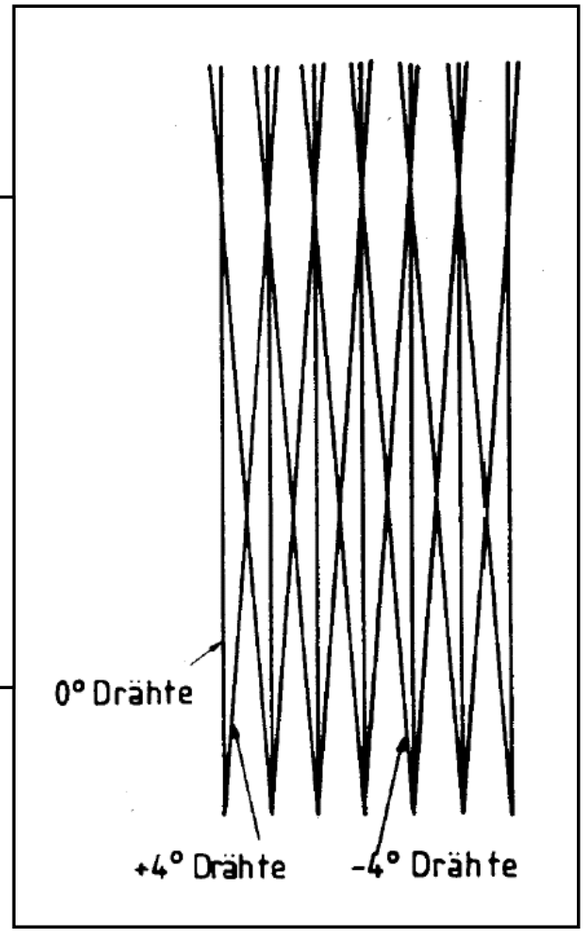

$\rightarrow \sigma_z \approx 0.1$ mm

A simple Case

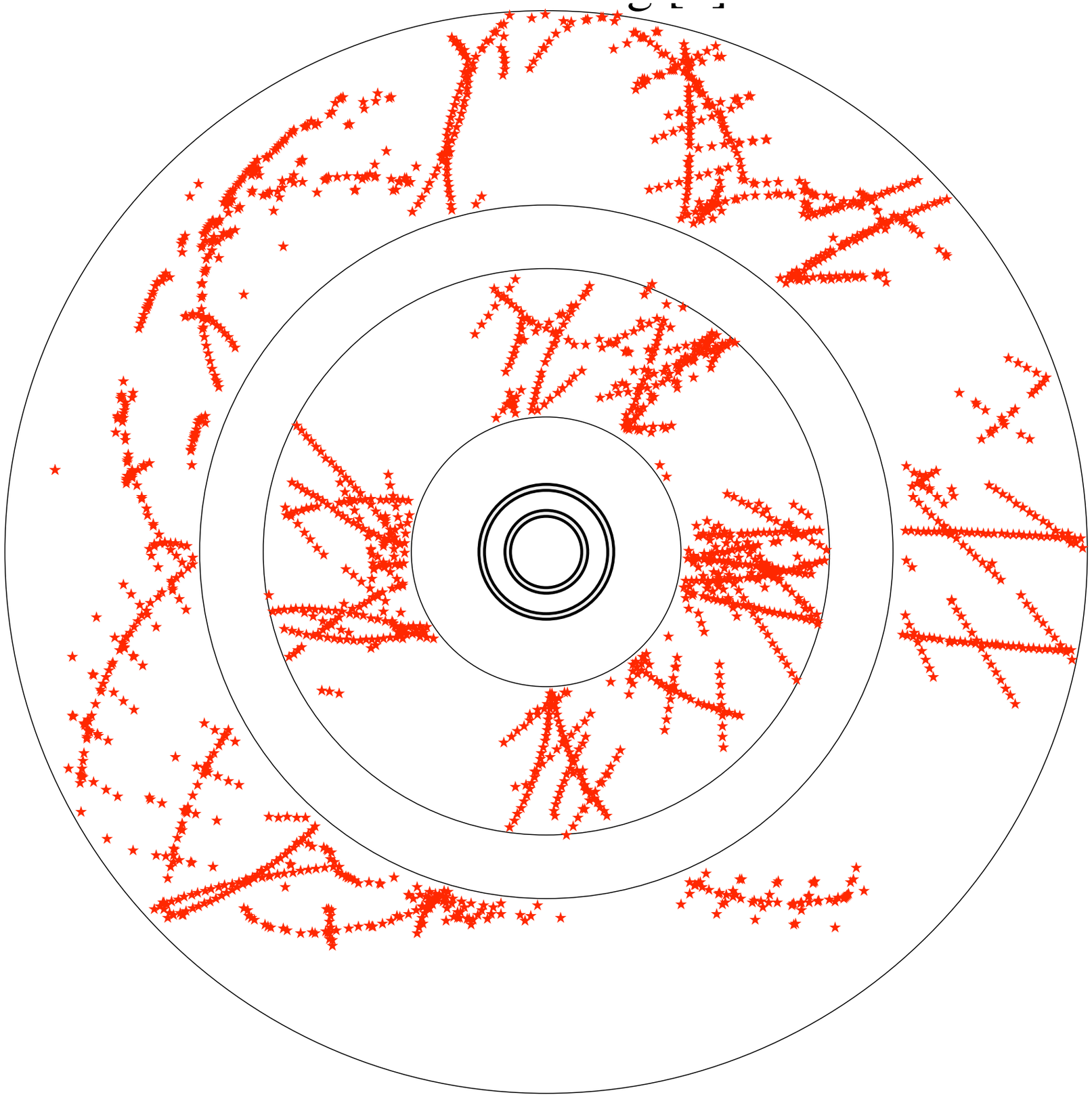

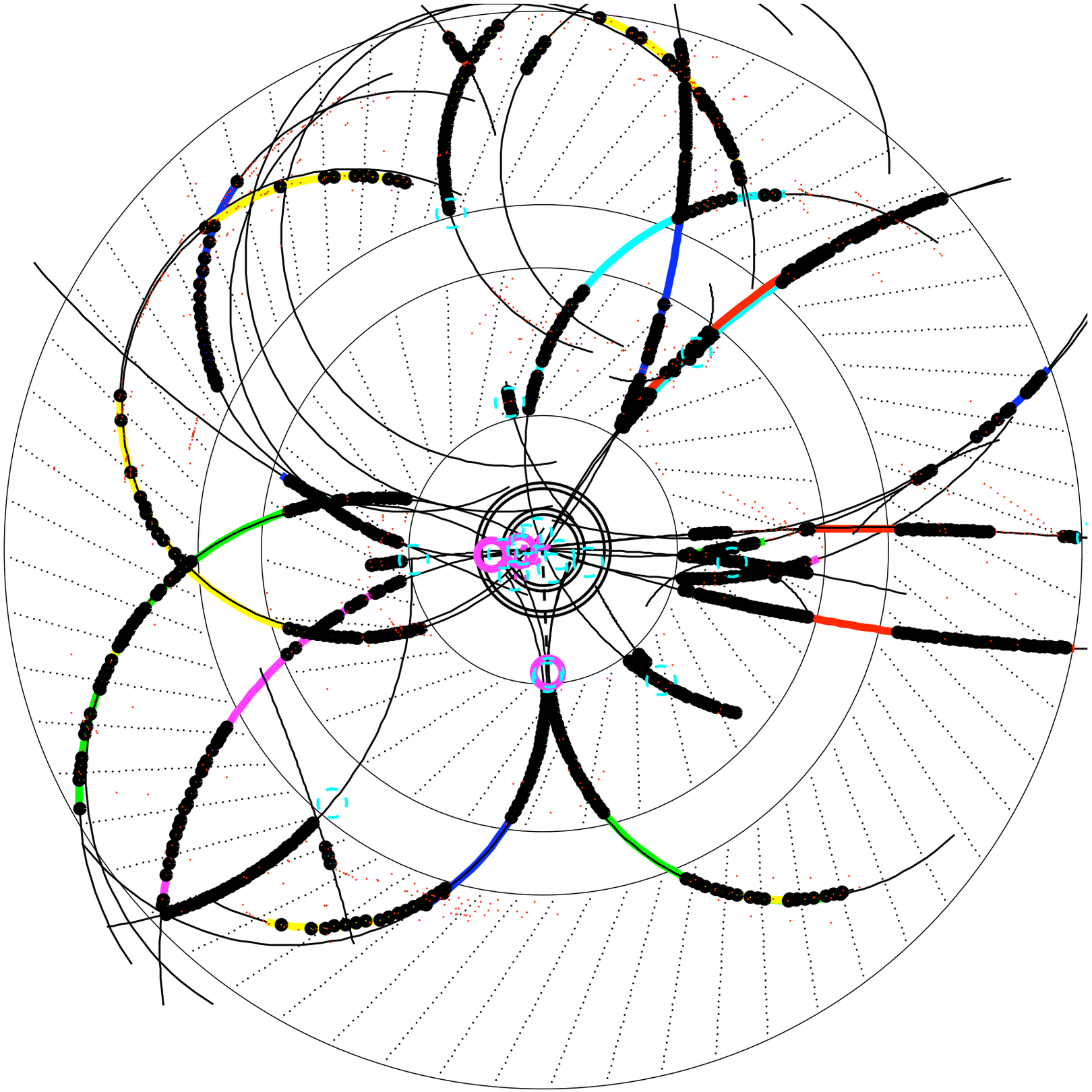

Example taken from V. Blobel Uni HH

Somewhat more busy

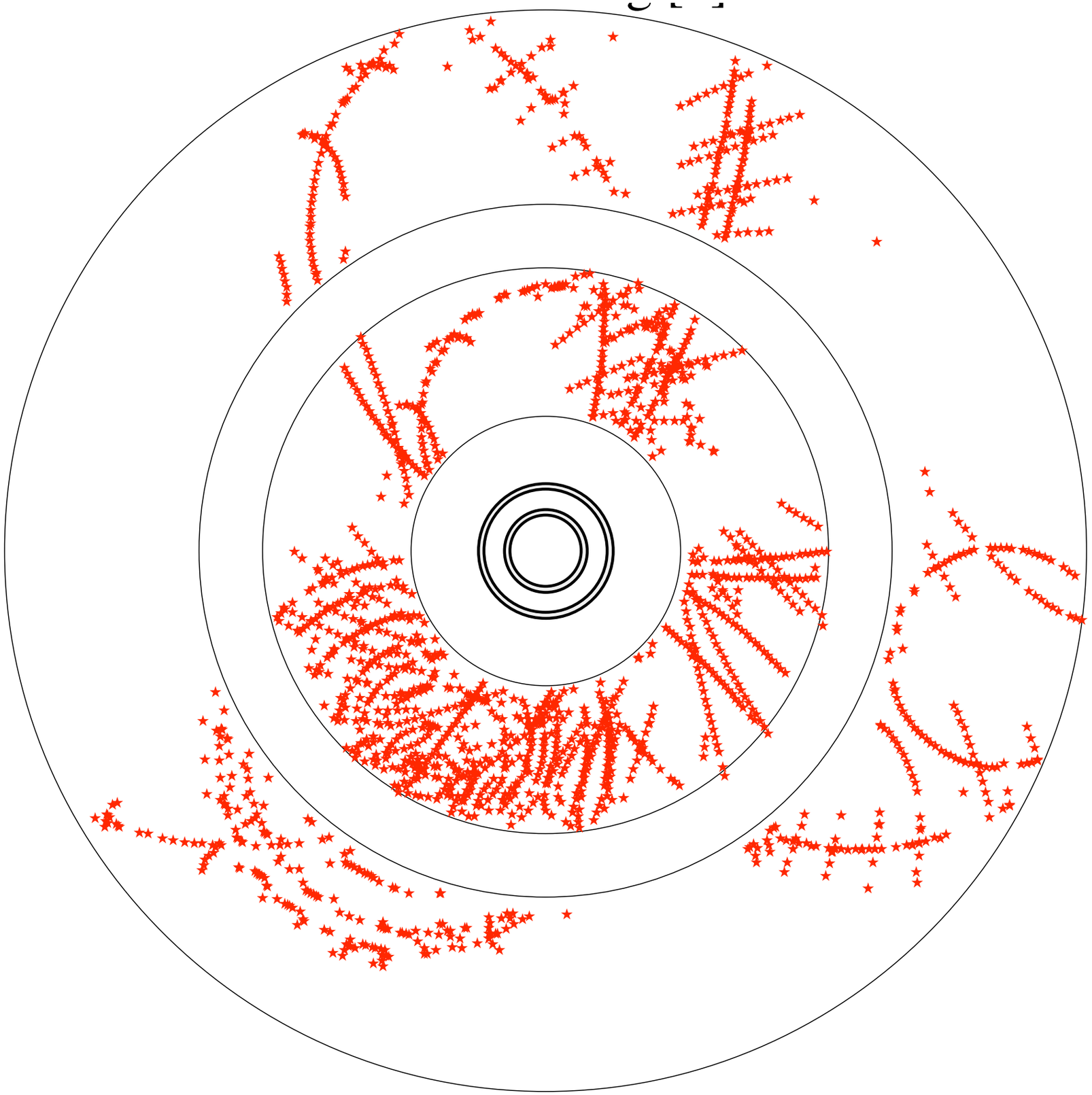

Event with „Looper“

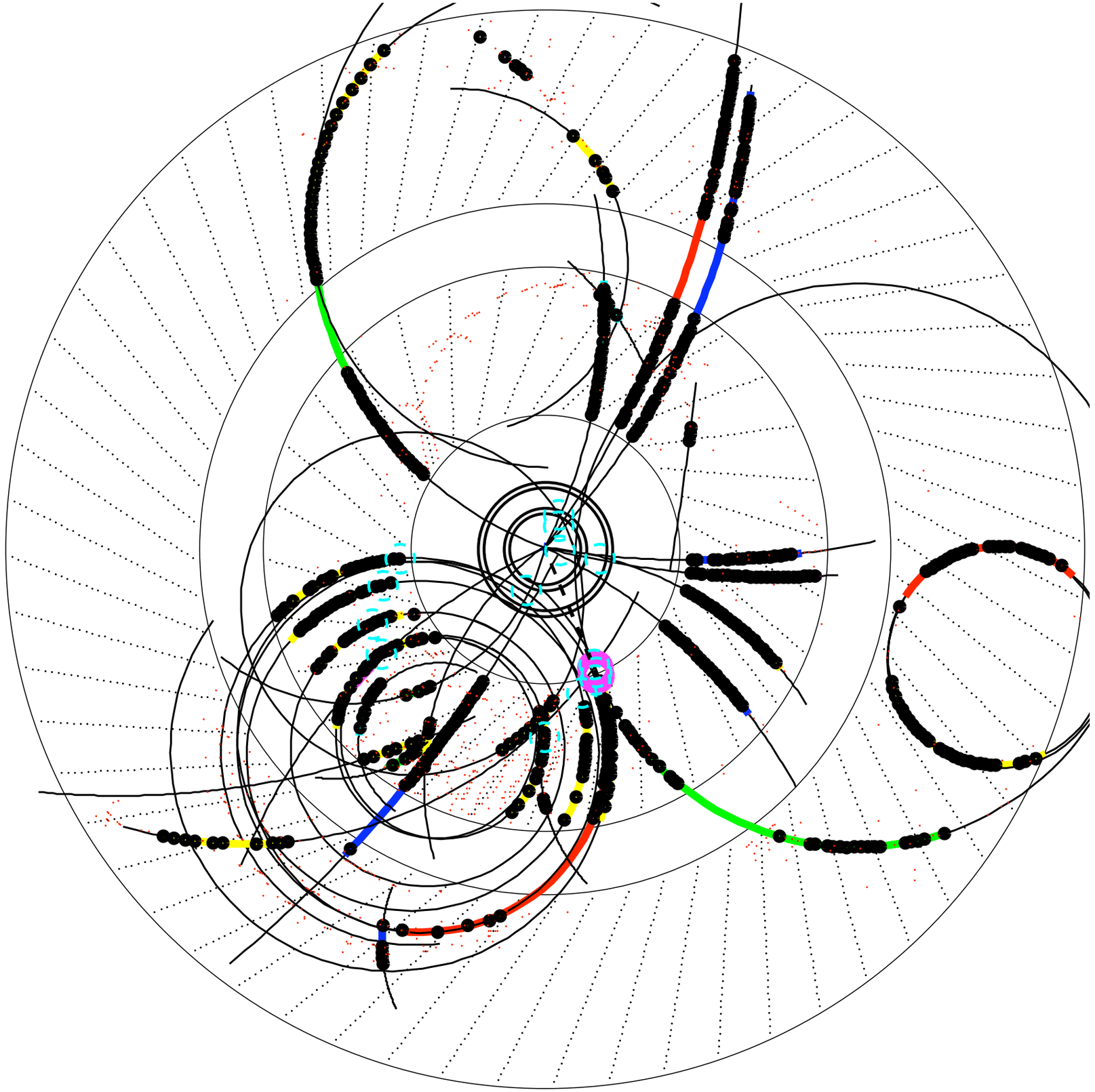

Example taken from V. Blobel Uni HH

carsten.niebuhr@desy.de

Challenging …

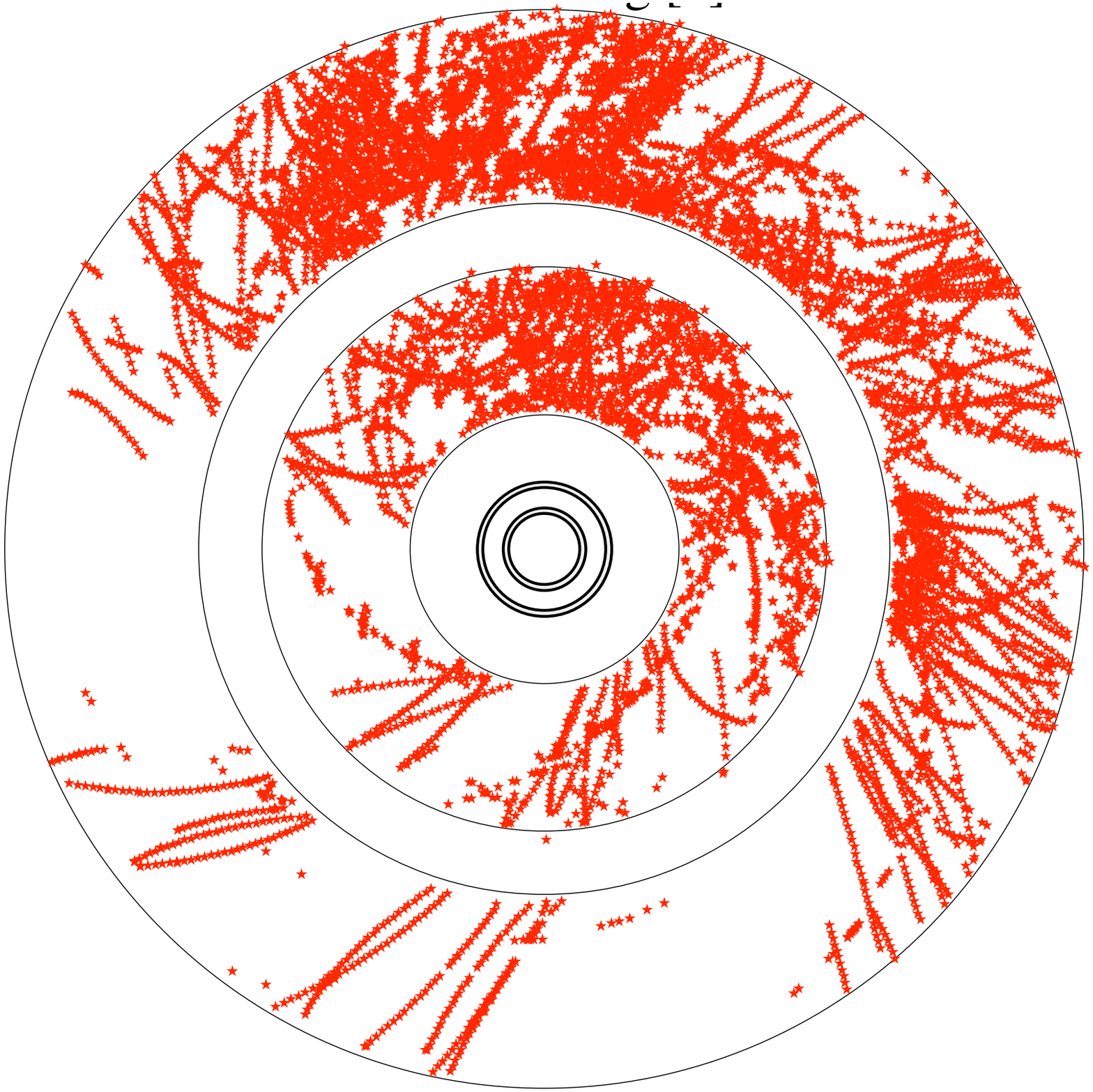

Do you find the missing Track ?

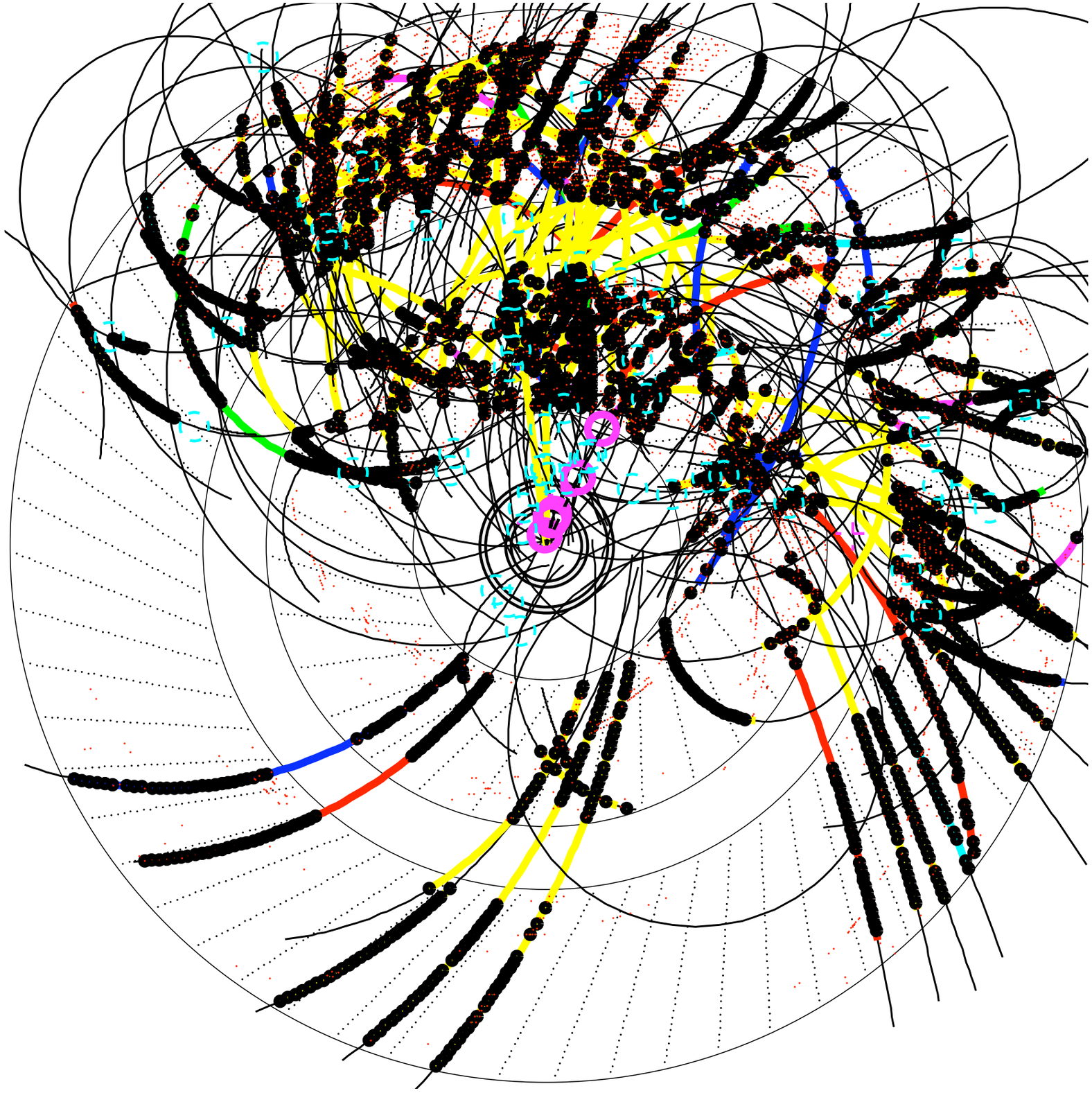

Example taken from V. Blobel Uni HH

carsten.niebuhr@desy.de

Simulated Event in ATLAS

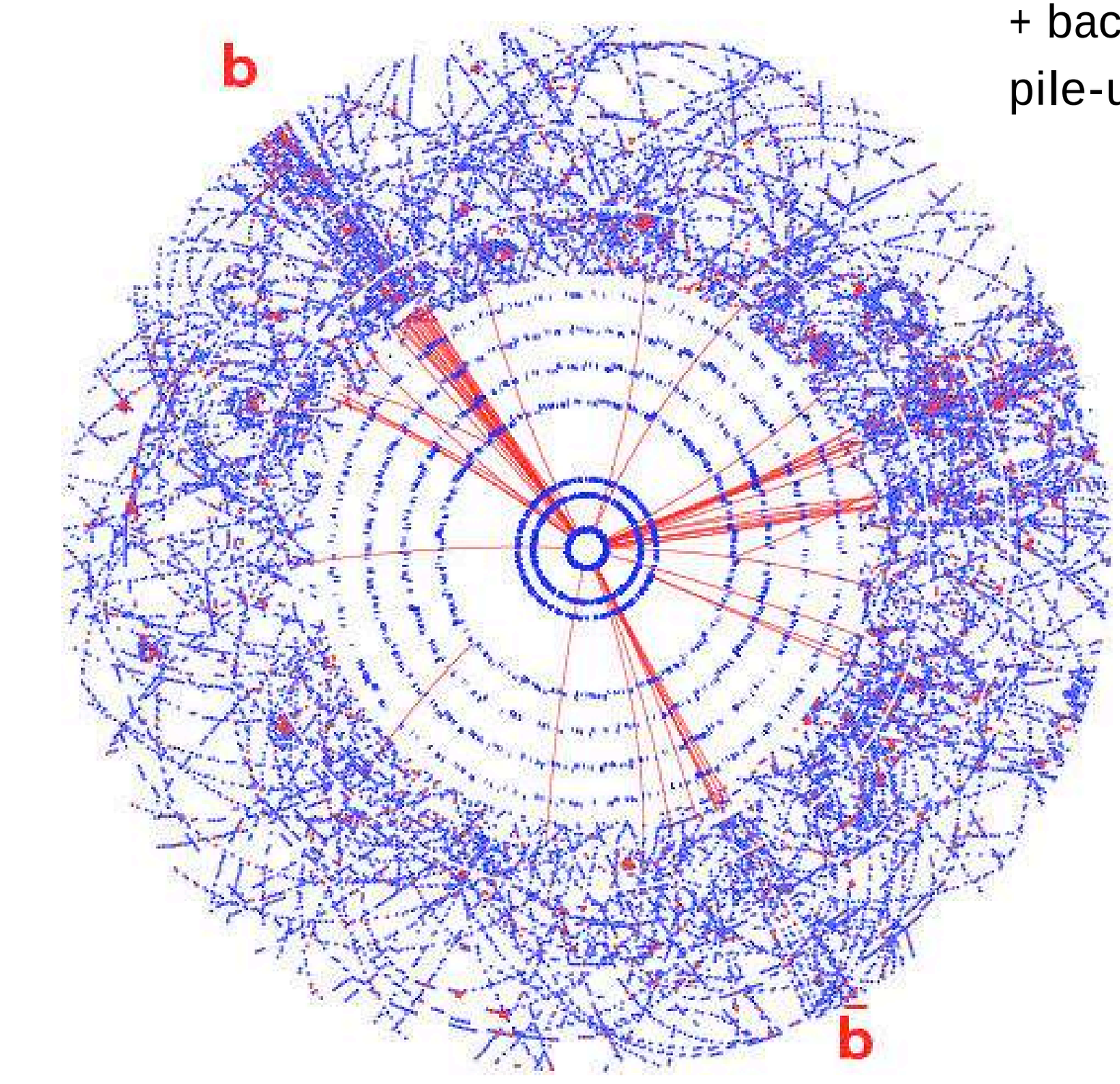

$\mathrm{Higgs} \rightarrow \mathrm{b\bar{b}}$

+ background from pile-up

Methods of Pattern Recognition and Fitting

- Global Methods of Pattern Recognition
  - Template Matching
  - Fuzzy Radon Transform
  - Histogramming Methods
  - Neural Network Techniques
    - Hopfield neuron
    - Denby-Peterson method .
    - Elastic arms and deformable templates
- Local Methods of Pattern Recognition
  - Seeds
  - 2D Versus 3D propagation
  - Naive Track Following
  - Combinatorial Track Following
  - Use of Kalman Filter
  - Arbitration

Track fitting usually is based on minimization of the so called chi^2 function:

$$\chi^2 = \sum_{i=1}^{N} \frac{(m_i - f_{\vec{p}})^2}{\sigma_i^2}$$

- m_i are the individual measurements (hits)
- f_p is an expression describing the trajectory (e.g. helix), which depends on a set of parameters p

Properties: For normally distributed measurements this expression is proportional to the negative logarithm of the corresponding likelihood function. In the linear case the result is unbiased and has smallest variance.